Malaria Control: Insights from Mathematical Models

Malaria Control: Insights from Mathematical Models

Lindsay T Keegan, B. S.

A Thesis

Submitted to the School of Graduate Studies

in Partial Fulfillment of the Requirements

for the Degree

Doctor of Philosophy

McMaster University

DOCTOR OF PHILOSOPHY (2015) McMaster University

(Biology) Hamilton, Ontario

TITLE: Malaria Control: Insights from Mathematical Models

AUTHOR: Lindsay T Keegan, B.S., (University of Florida)

SUPERVISOR: Dr. Jonathan Dushoff

NUMBER OF PAGES: [xv], 136

ABSTRACT

Malaria is one of the most devastating infectious diseases, with nearly half of the worlds population currently at risk of infection [105]. Although mathematical models have made significant contributions towards the control and elimination of malaria, it continues to evade control. This thesis focuses on two aspects of malaria that complicate dynamics, helping it persist.

The basic reproductive number is one of the most important epidemiological quantities as it provides a foundation for control and elimination. Recently, it has been suggested that $\mathcal{R}_0$ should be modified to account for the effects of finite host population on a single disease-generation. In chapter 2, we analytically calculate these finite-population reproductive numbers for both vector-borne and directly transmitted diseases with homogeneous transmission. We find simple, generalizable formula and show that when the population is small, control and elimination may be easier than predicted by $\mathcal{R}_0$.

In chapter 3, we extend the results of chapter 2 and find expressions for the finite-population reproductive numbers for directly transmitted diseases with different types of heterogeneity in transmission. We also outline a framework for discussing the different types of heterogeneity in transmission. We show that although the effects of heterogeneity in a small population are complex, the implications for control are simple: when $\mathcal{R}_0$ is large relative to the size of the population, control or elimination is made easier by heterogeneity.

Another basic question in malaria modeling is the effects of immunity on the population-level dynamics of malaria. In chapter 4, we explore the possibility that clinical immunity can cause bistable malaria dynamics. This has important implications for control: in areas with bistable malaria, if malaria could be eliminated until clinical immunity wanes, it

would not be able to invade. We built a simple, analytically tractable model of malaria transmission and solved it to find a criterion for when we expect bistability to occur. Additionally, we review what is known about about the parameters underlying the model and highlighted key clinical immunity parameters for which little is known. Building on these results, in chapter 5, we fit the model developed in chapter 4 to incidence data from Kericho, Kenya and estimate key clinical immunity parameters to better understand the role clinical immunity plays in malaria transmission.

Finally, in chapter 6, we summarize the key results and discuss the broader implications of these findings on future malaria control.

ACKNOWLEDGEMENTS

I have been afforded a fantastic opportunity at McMaster to work with an incredibly supportive and intellectually stimulating, interdisciplinary group of people. First and foremost, I would like to thank my thesis advisor, Jonathan Dushoff, whose enthusiasm for scientific inquiry is contagious. Working with Jonathan has been challenging, inspiring, and incredibly instructional. His continued guidance has taught me a plethora of invaluable skills, not the least of which has been how to write. I would also like to thank my supervisory committee: Ben Bolker, David Earn, and Mark Loeb. I thank Ben, not only for pointing me to McMaster, but also for continuing to mentor me throughout my time here. David, for his help in building my foundational knowledge of infectious disease modeling and for his mentorship throughout my dissertation. And Mark for ensuring my work was well grounded in biology. I am very grateful for the guidance of Marta Wayne, who has always helped to put things into perspective; whom I consider a mentor and a role model. Many thanks to Chyun Shi who helped to keep us all sane. Away from McMaster, I have benefited greatly from my collaboration with Mercedes Pascual and her group at the University of Michigan.

My time at McMaster has been greatly improved by my friends and colleagues in both the biology and the mathematics departments. Particularly past and present members of the TheoBio lab, including: Audrey Patocs, Jake Cowper Szmosi, Spencer Hunt, David Champredon, Dave Leaman, Chyun Shi, Steve Walker, and Lee Worden. Thanks to Chai Molina, Audrey Patocs, and Spencer Hunt for their help proofreading. I would be remiss if I did not mention: Connie O'Connor, Kerry Regan, Gaby Blohm, Audrey Patocs, Chai Molina, Hermina Ghenu and Spencer Hunt, from whom I have learned a tremendous amount and who were always there for support and coffee.

None of this would have ever been possible without the support of my family. My dad, the original Dr. Keegan, who inspired me to become a biologist at the age of three and who has continued to inspire and encourage me in all of my scientific pursuits; my mom, who always believed in me and has encouraged and supported me along the way; and my siblings, Dan and Caroline Keegan. Of course, my partner, Greg Barltrop who as always been there for me, providing a never ending source of adventure and support. A special thanks to Greg for ensuring I didn't starve in a pile of laundry while writing this thesis. And to my adopted Canadian family. I am eternally grateful for all of the support from my friends, family, and colleagues, this would not have been possible without you.

DECLARATION OF ACADEMIC ACHIEVEMENT

Chapters 2 and 4 of this thesis have been prepared as a separate manuscripts and published. Chapters 3 and 5 are manuscripts in preparation. For each chapter, analysis, programming, and manuscript preparation was primarily an individual effort, with contributions from Jonathan Dushoff and Benjamin Bolker.

TABLE OF CONTENTS

List of Figures

List of Tables

Chapter 1

Introduction

Historically, malaria is one of the most devastating infectious diseases, spreading in the human population for over 4,000 years [51]. Although malaria has been investigated for hundreds of years, the most significant advances in understanding malaria epidemiology were made around the turn of the 20th century: in 1880, Charles Louis Alphonse Laveran discovered parasites in the blood of malaria patients [23, 78] and shortly thereafter, in 1887, Ronald Ross discovered that mosquitoes transmitted malaria [8]. These discoveries, coupled with advances in anti-malarial drugs and the advent of DDT, ushered in a wave of successful elimination efforts. From 1945 to 2010, 79 countries successfully eliminated malaria, of those 75 countries remain malaria free, even in the absence of sustained control efforts [139, 98]. Piggybacking on these successes, the World Health Organization (WHO) announced its goal of global malaria eradication [98]. However, with nearly half of the worlds populations still at risk of malaria, no effective vaccine available, and many older anti-malarial drugs losing efficacy due to evolved resistance, the WHO has since abandoned the goal of eradication and now focuses on rolling back malaria [105]. Currently, the most viable malaria control strategies rely on vector control (e.g. Indoor residual spraying) and

prevention (e.g. bed nets) [105].

Malaria is a vector-borne disease caused by protozoan parasites of the genus *Plasmodium*. In humans, malaria is caused by *Plasmodium falciparum*, *P. vivax*, *P. malariae*, and *P. ovale*. Although there are also human cases of *P. knowlsi*, it primarily affects macaques [105]. Malaria spreads through bites of infected female mosquitoes of the genus *Anopheles* [105]. When an infected mosquito bites a host, it inoculates sporozoites into the human host; those sporozoites then infect liver cells. After initial asexual replication in the liver, parasites move to the red blood cells. There, some differentiate into sexual stages (gametocytes) while others remain sporozoites. The male and female gametocytes are then ingested during a blood meal. Once in the mosquito, the gametocytes invade the wall of the mid-gut where they replicate and develop into sporozoites. The sporozoites move to the salivary glands where they can be transmitted to a new host; and the life cycle repeats. The complex epidemiology of malaria makes it a prime candidate for mathematical modeling.

Mathematical models are an important tool used to understand disease transmission and inform control efforts. The use of epidemiological models date back to 1760, with Daniel Bernoulli, who used differential equations to explore the effect of smallpox inoculation on disease related mortality [29]. Mathematical modeling was first applied to malaria in 1911 by Ronald Ross [8]. Ross showed that not all mosquitoes needed to be eliminated in order to eliminate malaria; rather, their density only needed to be reduced below a critical threshold for successful elimination to occur. Shortly thereafter, in 1927, Kermack and McKendrick showed that this threshold density held true for host populations of directly transmitted diseases [66]. Their formulation of this threshold density has come to be called the basic reproductive number.

The basic reproductive number, $\mathcal{R}_0$, is defined as the average number of secondary infections that can be traced back to a single infectious individual in an otherwise totally

susceptible population [66]. $\mathcal{R}_0$ is one of the most important epidemiological quantities as it provides the epidemic threshold: when $\mathcal{R}_0 > 1$, a disease can invade, whereas when $\mathcal{R}_0 < 1$ the disease will die out. Thus, to eliminate an infectious disease, transmission must be reduced by a factor of $1/\mathcal{R}_0$, rather than all the way to zero [66]. Additionally, $\mathcal{R}_0$ gives the critical vaccination fraction – the proportion of people who must be vaccinated or otherwise made not susceptible to achieve herd immunity [43]. Accurate calculation of $\mathcal{R}_0$ is critical for understanding disease dynamics and planning control efforts.

The first model of malaria, developed by Ross was a simple, single equation model. It divided humans into susceptible and infected individuals. Susceptible individuals get infected at a rate proportional to the fraction infected, times the contact rate (vectoral capacity) [122, 93]. This simple model of malaria yields major insights into malaria dynamics. First and foremost, it was the first to identify that not all mosquitoes needed to be eliminated in order to eliminate malaria. Ross showed that below a critical vectoral capacity, malaria would die out; above that threshold, the relationship was highly non-linear. Ross showed that when the vectoral capacity is close to the critical threshold, small increases in vectoral capacity lead to large increases in malaria prevalence, whereas when the vectoral capacity is large, even large decreases in vectoral capacity have little impact on reducing prevalence. Additionally, Ross showed that a reduction in prevalence of malaria without changing the vectoral capacity is not sustainable, as malaria will eventually return to the pre-reduction prevalence. Although simple, this model of malaria provides critical insights for the control of malaria [73, 93, 131].

Building on the work of Ross, in 1952, George MacDonald extended this model to include susceptible and infected hosts and susceptible, infected, and infectious vectors [73, 93, 131]. Although this model introduces a level of complexity, it still makes some simplifying assumptions, including: no acquired immunity, homogeneous hosts and vec-

tors populations, and that mosquitoes bite randomly. The "Ross-MacDonald" model, as it has come to be known, has formed the foundation for vector-borne modeling. In addition to the insights of Ross, the main contribution of the Ross-MacDonald model was the formulation of $\mathcal{R}_0$ – MacDonald was the first to define "z_0", the "basic reproductive rate" for malaria, what we now call $\mathcal{R}_0$ [85]. Additionally, MacDonald performed a sensitivity analysis of the parameters affecting $\mathcal{R}_0$ [85]. The sensitivity analysis revealed that the most effective way to reduce $\mathcal{R}_0$ is by increasing the adult mosquito mortality rate, suggesting this is where control should be focused.

Incorporating immunity into models of malaria was the next step forward in malaria modeling [93, 28, 6]. The Ross-MacDonald model of malaria assumed that individuals did not develop immunity which lead to unrealistic predictions, meaning that the model predicts that when $\mathcal{R}_0$ is large, nearly the entire population is infected (and infectious), which is not realistic. There were two ways in which immunity was incorporated. The Garki model, a model of *P. falciparum* transmission used in conjunction with a large, control trial in Garki, Nigeria, incorporated partial immunity – characterized by an increased recovery rate and a decrease in interactivity and detection [93, 28]. Other models [6] incorporated full immunity, moving immune individuals into a class where they are neither susceptible nor infectious until immunity is lost. Like the Garki model, immunity in these models was lost without re-exposure. These models incorporated immunity to malaria to explore the effects of immunity on vaccination [6]. Since then, a variety of models have explored immunity to malaria [134, 2, 31, 21, 77] and have shown immunity can have important implications for control.

Another simplifying assumption of the Ross-MacDonald model is the assumption that all hosts are identical and that all hosts are equally attractive to mosquitoes, this has important ramifications when planning control. There is considerable variation among individual

hosts, in disease susceptibility. Dramatic examples include the sickle-cell trait and glucose-6-phosphate dehydrogenase deficiency, both of which cause disease in homozygotes, but reduces malaria parasitemia in heterozygotes [118, 137, 18, 87]. In addition to individual variation in the susceptibility to disease, there is incredible variation in the attractiveness of individual hosts to mosquitoes. It is well known that mosquitoes prefer some hosts over others for a variety of reasons including: pregnancy [82, 5], ABO blood group [130], body size [115], and alcohol use [129], among others. This individual variation can further complicate malaria control.

Although mathematical models of homogeneous populations have provided significant contributions to our understanding of infectious disease dynamics, host heterogeneity has important implications for disease spread and control. In general, models of malaria that incorporate heterogeneity usually look at heterogeneity in the attractiveness of hosts to mosquitoes. This type of heterogeneity has important implications for $\mathcal{R}_0$. Namely, heterogeneity in the biting rate of mosquitoes has been shown to increase $\mathcal{R}_0$ compared to the $\mathcal{R}_0$ calculated from uniform biting [37, 73], making malaria more difficult to control than predicted by the homogeneous $\mathcal{R}_0$.

Despite the many insights into malaria control derived from mathematical models, malaria continues to evade control. This thesis focuses on modeling two aspects of malaria that complicate dynamics, to better inform malaria control programs. In chapters 2 and 3 we explore the effects of finite population on the basic reproductive number for homogeneous populations (in chapter 2) and for diseases with heterogeneity in transmission (in chapter 3). Chapters 4 and 5 are devoted to exploring the effects of clinical immunity on transmission.

Measuring and predicting disease spread is a foundational concept in mathematical epidemiology, dating back to Ross [8] and Kermack and McKendrick [66]. Classical calcula-

tions of $\mathcal{R}_0$ implicitly assume a disease spreading in an infinite population of susceptible hosts. However, for diseases, like malaria, with large reproductive numbers spreading in small populations, it is possible for $\mathcal{R}_0$ to approach or exceed the size of the population, rendering $\mathcal{R}_0$ difficult to interpret. Smith et al. [132] introduced the idea of measuring the reproductive number in a *finite* population. These finite-population reproductive numbers are the average number of secondary infections that can be traced back to a single infected individual in a *finite* population of susceptible hosts. Smith et al. [132] estimated these finite-population reproductive numbers for malaria, tracing malaria through one full cycle of transmission. In addition to Smith et al. [132], Keeling and Grenfell [65] and Ross [121] also estimated these finite-population reproductive numbers, for directly transmitted diseases, using stochastic models. In chapter 2, we take a step towards better understanding these finite-population reproductive numbers by analytically calculating these finite-population reproductive numbers for both directly-transmitted and vector-borne diseases in homogeneous populations.

Despite the usefulness of homogeneous models, host heterogeneity has important implications particularly for the reproductive number. Diekmann et al. [26] first laid out a framework for calculating $\mathcal{R}_0$ for a directly transmitted disease with heterogeneity in both the mixing rate of susceptibles and infected individuals. Dye and Hasibeder [37, 74] calculated $\mathcal{R}_0$ for malaria, with heterogeneity in the attractiveness to mosquitoes. They showed that heterogeneity in the mixing rate increases $\mathcal{R}_0$, making control more difficult than predicted by the homogeneous $\mathcal{R}_0$. Interested in understanding the effect of super-spreaders on disease transmission, Lloyd-Smith et al. [84] explored the effect of heterogeneity in the mixing rate for a directly-transmitted disease. Similarly, they showed that while heterogeneity increased the probability of disease extinction, when an epidemic did occur, it was more likely to be explosive [84].

Although the effects of heterogeneity on $\mathcal{R}_0$ in an infinite population are straightforward, Smith et al. [132] suggested that heterogeneity in finite populations can have complicated effects on the reproductive number. They suggest that although heterogeneity *increases* $\mathcal{R}_0$ in an infinite population, in a finite population, heterogeneity actually *decreases* $\mathcal{R}_0$. This is because individuals who are more attractive to mosquitoes are more likely to get bitten multiple times, absorbing some possible infections, reducing $\mathcal{R}_0$.

In chapter 3 we extend the results from chapter 2 and calculate the reproductive number for diseases spreading in small, heterogeneous populations. We explore the relationship between heterogeneity and $\mathcal{R}_0$ in a *finite* population of susceptible hosts and outline a framework for discussing the different "types" of heterogeneity. In doing so, we highlight the importance of the different types of heterogeneity in terms of the spread and control of infections. We find simple expressions for finite-population reproductive number with different types of heterogeneity and solve them for different distributions of heterogeneity. Chapter 3 sheds further light on the different types of heterogeneity and how they affect the reproductive number in a finite population.

Chapters 4 and 5 concentrate on the other aspect of malaria we model in this thesis: clinical immunity. Clinical immunity to malaria is the acquired immune response that provides protection against the clinical symptoms of malaria, despite the presence of parasites [47, 49]. It is acquired with age and exposure and is lost in the absence of re-exposure [47, 49, 30, 125, 42]. Clinical immunity has long been of interest due to its complicated effects on malaria control. Because clinical immunity can be lost without re-exposure, under certain circumstances a decrease in malaria transmission could *increase* malaria morbidity and mortality, due to a loss of immunity [134, 103, 102]. Although clinical immunity protects individuals from disease, its effects at the population level are complex. Consequently, understanding clinical immunity is a critical part of planning malaria control efforts.

An important aspect of clinical immunity is the possibility that clinically immune individuals are particularly effective at transmitting malaria over the duration of their infection. If clinically immune individuals have a higher reproductive number, in some cases, malaria may be able to spread more effectively in areas where it is already present, all else being equal. That is, under certain circumstances, malaria may be able to persist, if endemic, in areas where it would not be able to invade [2]. This is because for some parameter values, both a stable endemic and a stable disease free equilibrium exist – a phenomenon known as bistability [34]. Aguas et al. [2] suggested that clinical immunity could be a mechanism for bistability in malaria. They also suggested that bistability would have important implications for control – if malaria could be eliminated until clinical immunity waned, it would not be able to re-invade, under current transmission and treatment conditions.

In chapter 4, we build a simple, compartmental model of malaria that includes clinical immunity. Unlike the Ross-Macdonald model, we do not explicitly model mosquitoes. We solve this model and find a criterion for when we expect bistability to occur. Additionally, we review what is known about clinical immunity and highlight key clinical immunity parameters that are not well understood, including the duration of clinically immune infection and the relative susceptibility of clinically immune individuals, two parameters highlighted by the bistability criterion as important for understanding when and whether bistability will occur.

In chapter 5 we attempt to estimate these critical clinical immunity parameters by fitting our simple, compartmental model, outlined in chapter 4, to data from the Kericho region of Kenya. Kericho has been central to the malaria climate change debate for over 10 years [52, 127, 3, 104]. Due to its elevation, malaria transmission in Kericho has largely consisted of imported cases from the holoendemic region surrounding Lake Victoria (defined as having a parasite ratio consistently greater than 75% of infants [90]). However, in 1990, large, mid-

year, seasonal epidemics began. The cause of these explosive epidemics has been debated. We do not set out to add to this debate, rather we work within the existing framework that includes temperature as an important factor in malaria transmission in Kericho, and incorporate temperature into the force of infection of our simple model.

The relatively low prevalence of malaria in Kericho coupled with the rapid increase of cases makes Kericho a good data set to use to explore clinical immunity. This is because we expect to see relatively low levels of immunity prior to the rapid increase of malaria cases, after which we expect to see clinical immunity develop rapidly. This is supported by Shanks et al. [127] who found that the rapid increase of malaria incidence coincides with a drop in the adult-to-child ratio of inpatient malaria cases, suggesting the development of clinical immunity. Using a version of the model in chapter 4, modified to include temperature as a driver of malaria transmission; we fit the model to hospital confirmed malaria cases from Kericho, to better understand the key clinical immunity parameters highlighted in chapter 5. To help elucidate the role clinical immunity plays in malaria transmission in Kericho.

Finally, in chapter 6 we summarize our key results from chapters 2 – 5 and discuss the broader impacts of the findings on future malaria control. It should be noted that overlap may occur between the chapters as they were all prepared for independent publication.

Chapter 2

Analytic calculation of finite-population reproductive numbers for direct- and vector-transmitted diseases with homogeneous mixing.

Keegan LT, Dushoff J, (2014) *Bulletin of Mathematical Biology* 76(5):1143-54.
doi: 10.1007/s11538-014-9950-x

2.1 Abstract

The basic reproductive number, $\mathcal{R}_0$, provides a foundation for evaluating how various factors affect the incidence of infectious diseases. Recently, it has been suggested that, particularly for vector-transmitted diseases, $\mathcal{R}_0$ should be modified to account for the effects of finite host population within a single disease-transmission generation. Here, we use a transmission-factor approach to calculate such "finite-population reproductive numbers", under the assumptions of homogeneous and heterogeneous mixing, for both vector-borne and directly transmitted diseases. In the case of vector-borne diseases, we estimate finite-population reproductive numbers for both host-to-host and vector-to-vector generations,

assuming that the vector population is effectively infinite. We find simple, interpretable formulas for these three quantities. In the direct case, we find that finite-population reproductive numbers diverge from $\mathcal{R}_0$ before $\mathcal{R}_0$ reaches half of the population size. In the vector-transmitted case, we find that the host-to-host number diverges at even lower values of $\mathcal{R}_0$, while the vector-to-vector number diverges very little over realistic parameter ranges.

2.2 Introduction

The basic reproductive number, $\mathcal{R}_0$, measures the expected number of new infections that can be traced back to a single infectious individual in an otherwise totally susceptible population. The concept of $\mathcal{R}_0$ provides a foundation for evaluating when infectious diseases can spread in a population, what factors determine disease incidence, and when interventions can eliminate disease [27, 55]. Its foundations go back over a century [122, 66].

In a study of malaria reproductive numbers, Smith et al. [132] pointed out that classical calculations of $\mathcal{R}_0$ implicitly assume infinite host population sizes, and are hard to interpret when $\mathcal{R}_0$ approaches or exceeds the population size. They introduced the idea of measuring the typical number of new infections per infectious individual for a disease invading *a finite host population*. These finite-population reproductive numbers account for the fact that some individuals get bitten by multiple mosquitoes, at random, and absorb some of the infections. However, like classic calculations of $\mathcal{R}_0$, Smith et al. [132] are only interested in the initial spread of infection; their estimates of these reproductive numbers ignore longer-term depletion of susceptibles. They used simulations to estimate the vector-to-vector and host-to-host reproductive numbers, which they called $\mathcal{Z}_0(H)$ and $\mathcal{R}_0(H)$, respectively, and ask how these reproductive numbers change when vector biting is heterogeneous – where

some hosts are more attractive to mosquitoes than others. They showed that in the case of finite-sized populations, unlike the infinite-population case, the number of vectors infected per vector is not necessarily the same as the number of hosts infected per host, and suggested that measuring $\mathcal{Z}_0(H)$ and $\mathcal{R}_0(H)$ could be informative for understanding the effects of different control measures.

Other studies (Keeling and Grenfell [65] and Ross [121]) have done similar work on directly transmitted diseases using stochastic models, here we use a next-generation framework to explore the impact of finite-population size on both directly-transmitted and vector-borne diseases.

Here we take a step towards better understanding of these "finite-population reproductive numbers" by calculating them analytically for homogeneous mixing between hosts (or hosts and vectors). We consider both directly transmitted and vector-transmitted diseases. For directly transmitted diseases, we calculated the average number of hosts infected by a single infectious host, which we call $\mathcal{R}(N)$. In the latter case, we calculate separate finite-population reproductive numbers for transmission from host species (via the vector) back to the host species, and for the vector species (via the host) back to the vector species which we call $\mathcal{R}(H)$ and $\mathcal{Z}(H)$ respectively.

Our calculations are based on Nåsell's idea of transmission factors, as described by Bailey [8]. Transmission factors are analogous to reproductive numbers for a single "leg" of host-vector transmission (or heterosexual HIV transmission, see [36]). They give the number of new cases of one group that can be attributed to a single infectious individual of another group. In the case of malaria, the transmission factor from hosts to vectors (τ_{hv}) is the average number of vector infections that are caused by a single infectious host, and the transmission factor from vectors to hosts (τ_{vh}) is the average number of host infections that are caused by a single infectious vector. Unlike the reproductive numbers, we use

these transmission factors only in the infinite-population limits. The reproductive number $\mathcal{R}_0$, for a vector-transmitted disease is equal to the product $\tau_{hv}\tau_{vh}$, we call the ratio of the transmission factors $\rho = \tau_{hv}/\tau_{vh}$. For a directly transmitted disease, there is only one "transmission factor", which we call τ, and which is equal to $\mathcal{R}_0$.

Although we consider only homogeneous mixing here, in order to implement a model that takes finite population size into account, we need to account for the fact that each infectious individual will create a discrete number of new infections. Since we assume that each infectious individual will have a constant contact rate over an exponentially distributed infectious period, the number of contacts is geometrically distributed. We then account for the fact that the population-size is finite by allowing some of the potential infections to land on the same host.

2.3 Methods

We calculate finite-population reproductive numbers for directly transmitted diseases, $\mathcal{R}(N)$, in a finite population of size N; and we calculate these finite-population reproductive numbers for vector-borne diseases, for host-to-host $\mathcal{R}(H)$, and vector-to-vector $\mathcal{Z}(H)$ transmission in a finite host population of size H (under the assumption of an effectively infinite vector population). To calculate these finite-population reproductive numbers, we trace infections through one cycle of transmission. For a directly transmitted disease, hosts infect other hosts: we start with one "typical" infected individual and calculate how many individuals are infected by that individual. For a vector-borne disease, we look at cycles of transmission: for $\mathcal{R}(H)$, we start with one typical infected host and calculate how many vectors are infected from that host, and then how many hosts will become infected, on average, from that distribution of vectors; likewise for $\mathcal{Z}(H)$, we start with one infected vector,

calculate how many hosts it infects and then how many vectors those hosts are expected to infect. These three scenarios $\mathcal{R}(N)$, $\mathcal{R}(H)$, and $\mathcal{Z}(H)$ are depicted diagrammatically in Fig. 2.1 for an infinite population, where the dashed arrows depict steps that change in the finite case.

To validate our results, we simulated host-to-host and vector-to-vector transmission under the same assumptions used to calculate the finite-population reproductive numbers. Starting with a single infectious host (or vector), we simulate the number of hosts (or vectors) infected by those infectious individuals. We repeated those simulations 1000 times for a mosquito population of $M = 100,000$, and took the mean of those 1000 simulations for each value of $\mathcal{R}_0$. Results are plotted in Fig. 2.2, Fig. 2.4 (for direct- and vector-borne transmission, respectively). We explore the effects of smaller vector-population sizes in 2.A.

2.3.1 Assumptions

For directly transmitted diseases, we assume a finite population of size N. Each infected host produces an average of τ potential new infections, using the geometric distribution, as discussed above; this is equivalent to assuming that the infection and recovery processes are Markovian. We assume that all hosts behave identically and independently. Since the host population is finite, some of these *potential* infections may fall at random on the same susceptible host, so the average number of *realized* infections in general, will be smaller.

In the case of vector-borne transmission, we assume that the host population is finite, of size H, and that the vector population is effectively infinite (i.e., much larger than the host population; we relax this assumption in the 2.A) since mosquitoes are not the limiting factor. Thus, a single infected host produces a geometrically distributed number of new infections,

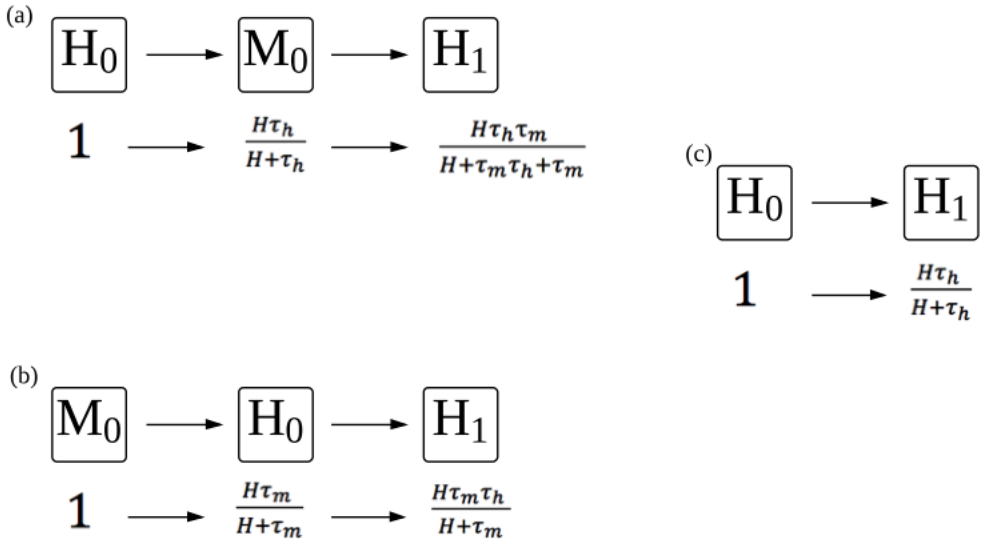

Figure 2.1: Schematic of one generation of disease transmission for (a,b) vector-borne and (c) directly transmitted diseases. The compartmental depiction represents transmission for both the infinite and the finite case. The dashed arrows indicate places where we change the calculation to take account of finite host populations. The depiction using transmission factors describes transmission only in the infinite case. (a) Transmission beginning with a single infectious host (H_0). That host goes on to produce τ_{hv} infected vectors (M_0) who each produce τ_{vh} new infected hosts resulting in $\tau_{hv}\tau_{vh}$ new infected hosts (H_1) from a single infectious host. (b) Transmission beginning with a single infectious vector (M_0) who on average, infects τ_{vh} hosts (H_0). Each of those infectious hosts goes on to produce τ_{hv} new infected vectors, resulting in $\tau_{hv}\tau_{vh}$ new infected vectors (M_1). (c) Direct transmission beginning with one infected individual (H_0) who infects an average of τ new individuals (H_1).

with mean τ_{hv}, in a susceptible vector population. We assume that all hosts and all vectors are identical and independent, as in the case of directly transmitted diseases. A single infected vector produces a geometrically distributed number of potential infectious events (we call these infectious *bites*) in the host population, with mean τ_{vh}, however, because the host population is finite, some of these bites may fall at random on the same host, so the average number of new *infections* will be smaller.

2.3.2 Calculation framework

If we know that a generation of infected vectors produces a potentially infectious bites on the finite host population, the probability that any individual host *escapes* infection is $\left(1-\frac{1}{H}\right)^a$. Thus, the expected number of new infections is $H\left(1-\left(1-\frac{1}{H}\right)^a\right)$.

To calculate expectations, we use probability distributions over numbers of potentially infectious events $p(a)$, and corresponding generating functions, $\phi(x)=\sum_a p(a)x^a$. In particular, the generating function that corresponds to a geometric distribution with probability P is:

$$\phi(x)=\sum_{a=0}^{\infty}(1-P)P^a x^a=\frac{1-P}{1-Px}. \tag{2.1}$$

Since $\tau=\frac{P}{1-P}$ is the mean number of events, we can solve for P to get $P=\tau/(\tau+1)$ and substitute to write $\phi(x)=\frac{1}{1+\tau(1-x)}$.

In particular, if $\phi_a(x)$ corresponds to the distribution of infectious bites on the host population $p(a)$, then we have that the expected number of infections, I, is:

$$I = \sum_{a=0}^{\infty} H(1-(1-1/H)^a)p(a) \tag{2.2a}$$

$$= H\left(\sum_{a=0}^{\infty} p(a) - \sum_{a=0}^{\infty}(1-1/H)^a p(a)\right) \tag{2.2b}$$

$$= H(1-\phi_a(1-1/H)) \tag{2.2c}$$

2.4 Results

2.4.1 Calculation framework

We use generating functions to calculate finite-population reproductive numbers for both directly transmitted and vector-borne diseases.

Since we assume that the number of infectious bites that land on a host is geometrically distributed, the generating function for the expected number of *bites* from one infectious vector is:

$$\phi_{v1}(x) = \frac{1-P_{vh}}{1-P_{vh}x}, \tag{2.3}$$

where $P_{vh} = \tau_{vh}/(\tau_{vh}+1)$ is the probability that an infected vector bites a host.

If we substitute equation (2.3) into equation (2.2c), we have that the expected number of *infections* from one infectious vector is $I_1 = H - \phi_{v1}(1-1/H)$. Solving yields:

$$I_1 = \frac{H\tau_{vh}}{H+\tau_{vh}}. \tag{2.4}$$

Equation (2.3) gives the generating function for the number of infectious bites from one

infectious vector, from this we can calculate the generating function for the number of infectious bites by m infectious vectors is:

$$\phi_{vm}(x) = \left(\frac{1 - P_{vh}}{1 - P_{vh}x}\right)^m \tag{2.5}$$

Plugging in to (2.2), with mean $P_{vh} = \tau_{vh}/(\tau_{vh} + 1)$, the distinct number of hosts infected by m vectors is:

$$I_m = H\left(1 - \left(\frac{H}{H + \tau_{vh}}\right)\right)^m \tag{2.6}$$

2.4.2 Direct Transmission, $\mathcal{R}(N)$

The expected number of infections that can be traced back to a single infected host is analogous to the expected number of bites from a single infectious vector in a finite population, above (for a vector-borne disease). Thus, by analogy with (2.4), the expected number of new infections from a single infectious host is:

$$I_1 = \frac{N\tau}{N + \tau}. \tag{2.7}$$

Since $\mathcal{R}_0$ is exactly τ, the expected number of infections from a single host is:

$$\mathcal{R}(N) = \frac{N\tau}{N + \tau} = \frac{N\mathcal{R}_0}{N + \mathcal{R}_0} \tag{2.8}$$

Fig. 2.2 shows how our analytic calculation and simulations of $\mathcal{R}(N)$ increase with the basic reproductive number, for a fixed value of $H = 1000$. $\mathcal{R}(N)$ diverges from $\mathcal{R}_0$ as

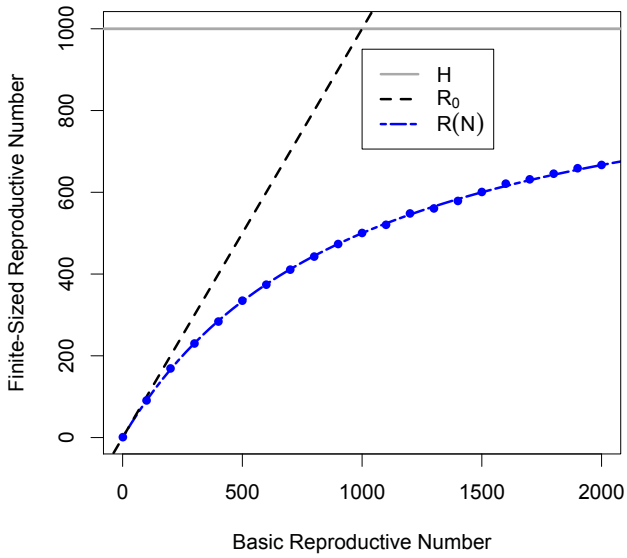

Figure 2.2: The finite-population reproductive number $\mathcal{R}(N)$ versus the basic reproductive number, $\mathcal{R}_0$ for directly transmitted diseases. Host population size is $N = 1000$. The blue points represent the average of 1000 simulations each.

the basic reproductive number approaches the population size – around $\mathcal{R}_0 = 1/2H$, and approaches the population size for very large values of $\mathcal{R}_0$. Simulated results match the analytically calculated results, as expected. Fig. 2.3 shows how $\mathcal{R}(N)$ varies with H for fixed $\mathcal{R}_0 = 1000$; $\mathcal{R}(N)$ converges on $\mathcal{R}_0$ as the population size increases relative to the basic reproductive number.

2.4.3 Vector-borne disease transmission

Vector-to-vector transmission, $\mathcal{Z}(H)$

To calculate the vector reproductive number, $\mathcal{Z}(H)$, we start with a single infectious vector, calculate the expected number of hosts infected by that single infectious vector and then

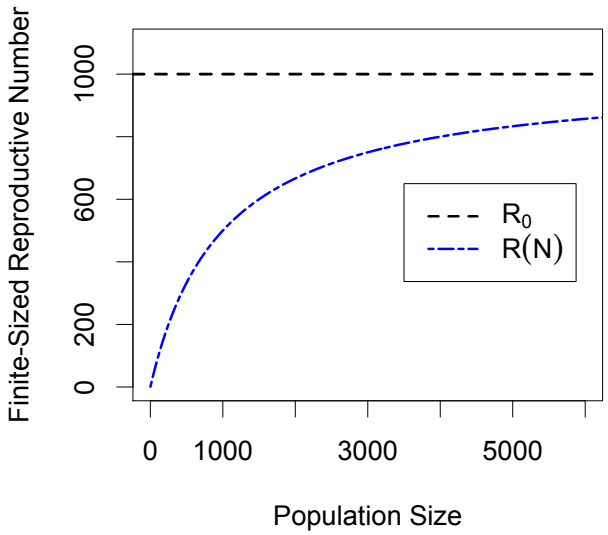

Figure 2.3: The finite-population reproductive number $\mathcal{R}(N)$ versus the population size, N, for directly transmitted diseases. The basic reproductive number is $\mathcal{R}_0 = 1000$.

calculate the expected number of vectors infected by those infectious hosts.

Since we assume that the vector population is effectively infinite (from equation (2.3)), we know that the number of hosts infected by a single infectious vector is:

$$I_1 = \frac{H\tau_{vh}}{H + \tau_{vh}}. \tag{2.9}$$

Those I_1 infected hosts go on to infect τ_{hv} vectors. Thus, the finite-population reproductive number for vectors is:

$$\mathcal{Z}(H) = \frac{H\tau_{vh}\tau_{hv}}{H + \tau_{vh}} = \frac{H}{H + \tau_{vh}}\mathcal{R}_0 \tag{2.10}$$

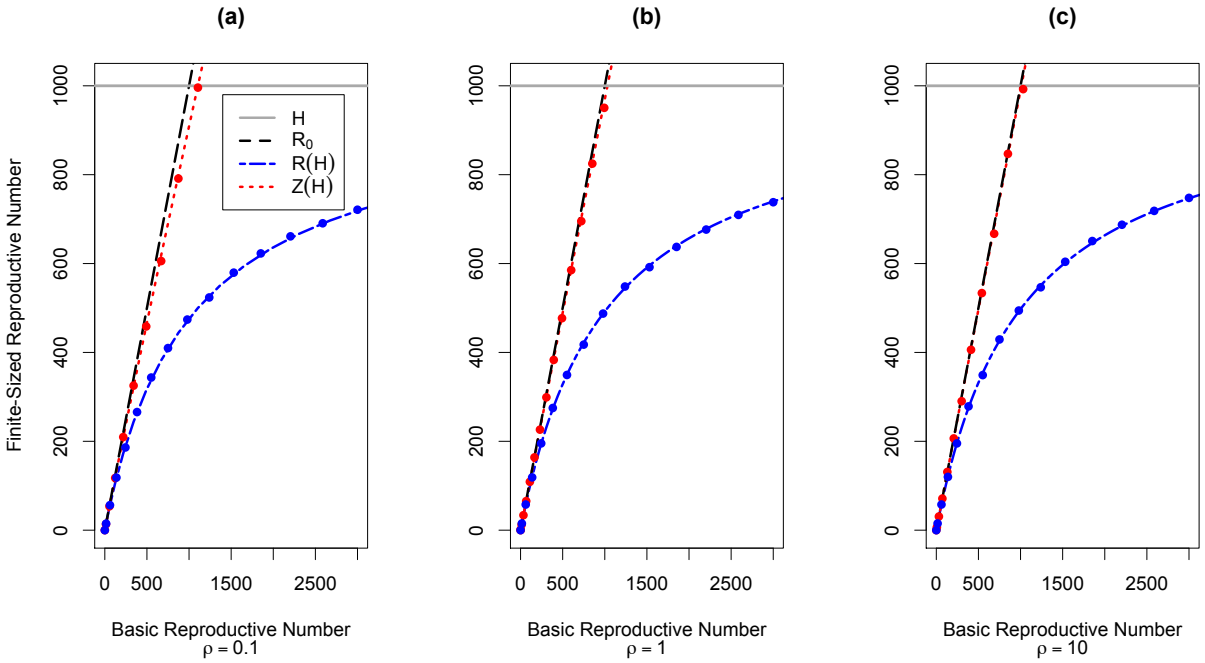

Figure 2.4: Plot of the basic reproductive number, $\mathcal{R}_0$ (black), versus the finite sized reproductive numbers $\mathcal{R}(H)$ (blue) and $\mathcal{Z}(H)$ (red), for three values of ρ, for vector-borne diseases. The host population size, $H = 1000$ (gray). We simulated the host-to-host reproductive number (blue points) and the vector-to-vector reproductive number (red points). For the simulations, the vector population size is $M = 100,000$.
(a) ρ= 0.1 (b) ρ= 1 (c) ρ= 10.

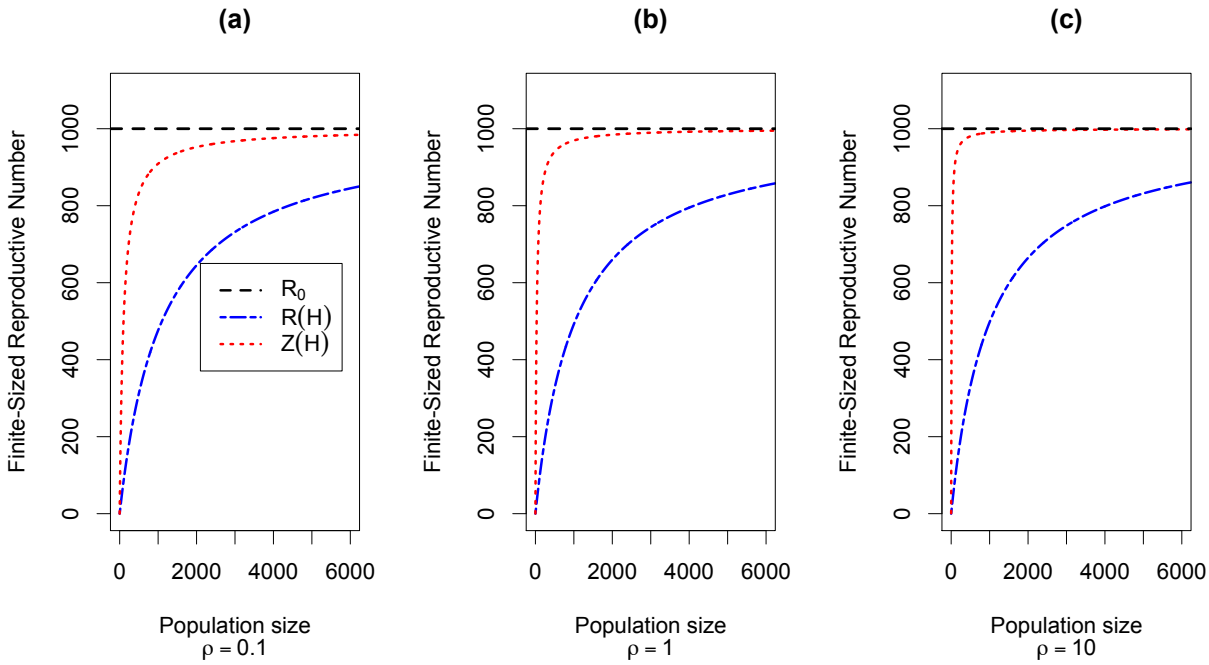

Figure 2.5: Plot of the population size H versus the finite-population reproductive number, $\mathcal{R}(H)$ (blue) and $\mathcal{Z}(H)$ (red), for three values of ρ. The basic reproductive number, $\mathcal{R}_0 = 1000$ (black). (a) ρ= 0.1 (b) ρ= 1 (c) ρ= 10.

Host-to-host transmission, $\mathcal{R}(H)$

To calculate the host reproductive capacity, $\mathcal{R}(H)$, we start with a single infectious host, calculate the expected number of vectors infected by that one host; then we calculate the expected number of hosts infected by infected vectors.

Starting from a single infected host we calculate the expected number of vectors infected by that host. The number of infected vectors is distributed geometrically with mean $P_{hv} = \tau_{hv}/(\tau_{hv}+1)$ where P_{hv} is the probability that an infectious host infects a vector. Thus, the distribution of infected vectors (from a single infectious host) is:

$$p(m) = (1 - P_{hv})P_{hv}^{m} \tag{2.11}$$

From equation (2.6) we know that the number of hosts infected by m vectors is $I_m = H(1-(\frac{H}{H+\tau_{vh}})^m)$. The finite-population reproductive number for is $\mathcal{R}(H) = \sum_m p(m)I_m$. We calculate the finite-population reproductive number for hosts to be:

$$\mathcal{R}(H) = \frac{\tau_{hv}\tau_m H}{H + \tau_{vh}\tau_{hv} + \tau_{vh}} = \frac{\mathcal{R}_0 H}{\mathcal{R}_0 + H + \tau_{vh}} \tag{2.12}$$

The relationship between $\mathcal{R}(H)$, $\mathcal{Z}(H)$, and $\mathcal{R}_0$ are shown in Fig. 2.4, Fig. 2.5, and the results are compared in Table 2.1. Fig. 2.4 is a plot of the finite-population reproductive numbers ($\mathcal{R}(H)$ and $\mathcal{Z}(H)$) compared to $\mathcal{R}_0$ for a fixed population of size H. We varied τ_{hv} for three fixed values of ρ. It highlights the divergence of the host-to-host and vector-to-vector finite-population reproductive numbers and $\mathcal{R}_0$ as the reproductive numbers approach the size of the host population, H; which occurs at about $\mathcal{R}_0 = H/3$. It also highlights the effect of ρ on the divergence of $\mathcal{Z}(H)$ from $\mathcal{R}_0$, an effect better shown in

Finite-sized Reproductive Numbers			Basic Reproductive numbers	
Direct	Vector-borne		Direct	Vector-borne
R(N)	R(H)	Z(H)	R_0	R_0
$\frac{N\tau}{N+\tau}$	$\frac{\tau_{hv}\tau_{vh}H}{\tau_{hv}\tau_{vh}+H+\tau_{vh}}$	$\frac{\tau_{hv}\tau_{vh}H}{H+\tau_{vh}}$	τ	$\tau_{hv}\tau_{vh}$

Table 2.1: Finite-population reproductive number for direct- and vector-borne diseases compared with the basic reproductive number (for infinite population sizes).

Fig. 2.5.

In addition, Fig. 2.4 shows the results of our simulations of vector-borne transmission in a finite-population. We simulated vector-to-vector and host-to-host transmission and plotted the resulting reproductive numbers. We see that our simulations match the analytically calculated results.

Fig. 2.5 displays the relationship between the finite-sized reproductive numbers ($\mathcal{R}(H)$ and $\mathcal{Z}(H)$) and the infinite-population reproductive number, $\mathcal{R}_0$, for a fixed value of $\mathcal{R}_0$, varying the host population size, H, for three values of ρ. It shows $\mathcal{R}(H)$ and $\mathcal{Z}(H)$ converging on $\mathcal{R}_0$ as the size of the population increases and highlights the importance of ρ in the convergence of $\mathcal{Z}(H)$ on $\mathcal{R}_0$. When hosts infect few vectors (relative to vectors infecting hosts), that is, when ρ is small, Fig. A1a, $\mathcal{Z}(H)$ converges on $\mathcal{R}_0$ slower compared to when ρ is large, Fig. A1c. ρ has much less of an effect on the convergence of $\mathcal{R}(H)$.

2.5 Discussion

Accurate calculation of the basic reproductive number, $\mathcal{R}_0$, is crucial for designing and implementing control and elimination programs. Smith et al. [132] suggested that when $\mathcal{R}_0$ is large relative to the size of the population, as can happen with malaria, $\mathcal{R}_0$ does

not accurately reflect the disease dynamics. They introduced the idea of finite-population reproductive numbers for both host and vectors, for malaria, and used simulations to estimate both $\mathcal{R}_0$ and the finite-population reproductive numbers ($\mathcal{Z}_0(H)$ and $\mathcal{R}_0(H)$), while allowing for heterogeneous biting, transmission-blocking immunity, and sampling issues.

Here, we consider the simpler case of homogeneous mixing, where all hosts are equally attractive to mosquitoes, and we are able to derive analytic formulas for those finite-population reproductive numbers for both vector-borne ($\mathcal{Z}(H)$ and $\mathcal{R}(H)$) and for directly transmitted diseases ($\mathcal{R}(N)$). We find simple formulas for these quantities in terms of transmission factors (τ_{hv}, τ_{vh}, and τ) [8] (Table 2.1), and show that the finite-population reproductive numbers, particularly $\mathcal{R}(N)$ and $\mathcal{R}(H)$, diverge from $\mathcal{R}_0$ when $\mathcal{R}_0$ approaches the population size. We then simulated our results in a finite population of hosts to validate our analytic calculations (Fig. 2.2, Fig. 2.4).

Since we assume a finite population size in the direct-transmission case, and a finite host population size in the vector-borne case (with an infinite vector population size), the reproductive numbers $\mathcal{R}(N)$ and $\mathcal{R}(H)$ are necessarily smaller than the size of the population, however, for vector-borne transmission, $\mathcal{Z}(H)$ can exceed the host population size as the vector population is infinite (Fig. 2.4, Fig. 2.5). However, unlike $\mathcal{R}_0$, $\mathcal{Z}(H)$ does decrease as it approaches the population size, but not as quickly as $\mathcal{R}(H)$ does (Fig. 2.4, Fig. 2.5). Our results show that $\mathcal{Z}(H)$ is very similar to $\mathcal{R}_0$ when τ_{hv} is large relative to τ_{vh} (large ρ) (Fig. 2.4c, Fig. 2.5c), and somewhat smaller (though still larger than $\mathcal{R}(H)$) when τ_{hv} is small relative to τ_{vh} (small ρ) (Fig. 2.4a, Fig. 2.5a). In other words, the number of vectors infected by a single infectious vector is more strongly affected by the host population size when the number of *hosts* infected by a single vector is large compared to the number of *vectors* infected by a single host.

If we were to relax the assumption of infinite vector population size, both $\mathcal{R}(H)$ and

$\mathcal{Z}(H)$ would be limited by M in an analogous way to how they are limited by H: $\mathcal{R}(H)$ would decrease if M was small relative to the reproductive number (in the same way that $\mathcal{Z}(H)$ decreases as a result of H) but it would not be limited by M; and $\mathcal{Z}(H)$ would be bounded by M (just as $\mathcal{R}(H)$ is bounded by H).

Since $\mathcal{R}(N)$ and $\mathcal{R}(H)$ are bounded by the population size and $\mathcal{R}_0$ is not, they diverge. In the case of directly transmitted diseases, $\mathcal{R}(N)$ diverges from $\mathcal{R}_0$ near $\mathcal{R}_0 = N/2$ (Fig. 2.2). Similarly, for vector-borne diseases, $\mathcal{R}(H)$ diverges much sooner than $\mathcal{R}(N)$ (for directly transmitted diseases). Our results show that when $\mathcal{R}_0$ is near the size of the host population size, $\mathcal{R}_0$ overestimates the actual dynamics, making control and elimination seem more difficult then they actually are.

It is well known that malaria-transmitting mosquitoes prefer some hosts over others for a variety of reasons (for example [72, 96]). This heterogeneity has complicated effects: in simple models, it increases the reproductive number [143, 37], but it can decrease finite-population reproductive numbers [132]. Extending the work here to gain analytic insight into finite-population reproductive numbers in the presence of heterogeneity in host attractiveness to mosquitoes would be a valuable contribution to understanding diseases spreading in small populations.

2.A Finite vector population

We assume, for the calculations of $\mathcal{R}(H)$ and $\mathcal{Z}(H)$, that the population of vectors is effectively infinite. In our simulations of finite-sized reproductive numbers, we chose a population of vectors to be very large relative to the host population size. However, here we explore how finite vector population size affects the simulations of the finite-population reproductive numbers.

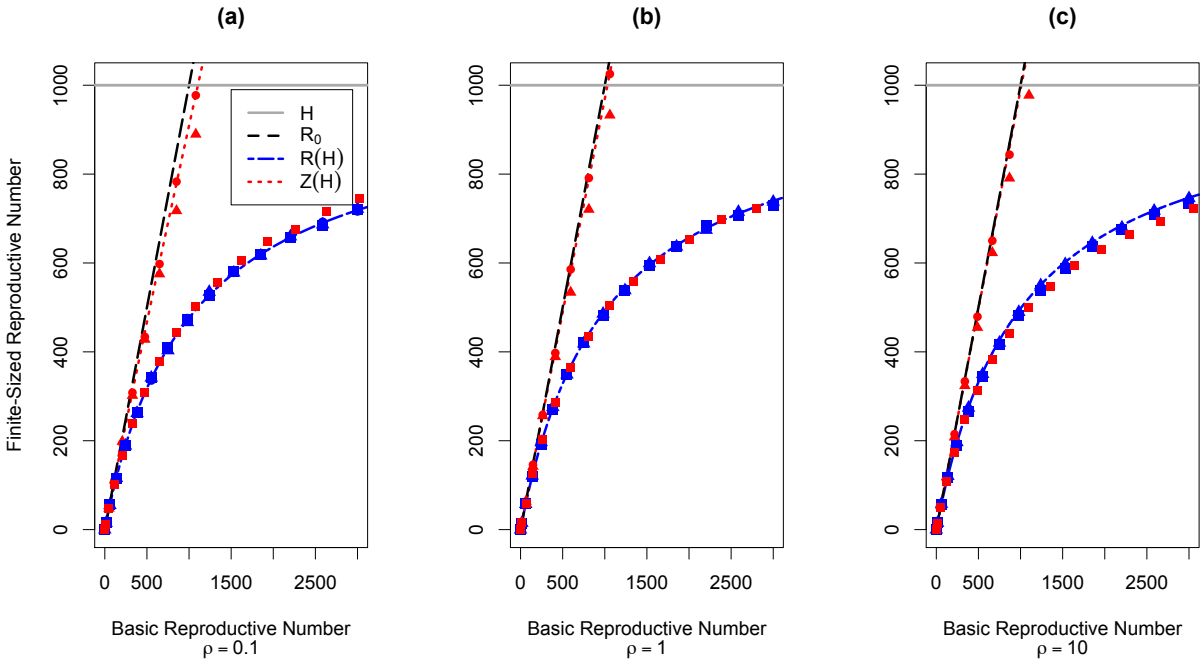

Figure A1: The basic reproductive number, $\mathcal{R}_0$ (black), versus the finite sized reproductive numbers $\mathcal{R}(H)$ (blue) and $\mathcal{Z}(H)$ (red), for three values of ρ, for vector-borne diseases. The host population size, $H = 1000$ (gray). Points represent the average of 1000 simulations. We vary the vector population size, from $M = 100,000$ (closed circles) to $M = 10,000$ (triangles), to 1000 (Squares). (a) ρ= 0.1 (b) ρ= 1 (c) ρ= 10.

We find that the vector-population size, M, does not significantly affect the finite-sized reproductive numbers unless M is small relative to the host-population size, H. We also see that when M is small relative to H, ρ has the opposite effect on $\mathcal{Z}(H)$ than when the vector population size is infinite: when ρ is small, for the same value of M, $\mathcal{Z}(H)$

diverges from $\mathcal{R}_0$ slower than when ρ is large. That is, when hosts are better at transmitting to vectors (than vectors are at transmitting to hosts) the effect of small vector-population size is smaller than when the vectors are better at transmitting to hosts (relative to hosts transmitting to vectors).

Chapter 3

Estimating Finite-Population Reproductive Numbers in Heterogeneous Populations.

Keegan LT, Dushoff J, (2014) *Journal of Theoretical Biology* [Submited]

3.1 Introduction

The effect of heterogeneity on disease dynamics is a foundational question in infectious disease modeling. Recently, renewed attention has been given to the impact of heterogeneity on the basic reproductive number, $\mathcal{R}_0$ [84, 132, 110]. $\mathcal{R}_0$ is the average number of secondary infections from a single infectious individual in an otherwise totally susceptible population. Kermack and McKendrick [66] formulated $\mathcal{R}_0$ assuming a disease spreading in a large, homogeneous population; this construction of $\mathcal{R}_0$ has since dominated epidemic theory.

Despite the common, convenient assumption that diseases are spread in well mixed homogeneous populations, there is a great deal of evidence that population heterogeneity is an

important determinant of disease spread. Woolhouse [144] argued that heterogeneity in disease spread is pervasive, and often characterized by the '20/80 rule' – i.e., 20% of infected individuals cause 80% of cases. Perhaps the most famous example of disease heterogeneity is typhoid Mary, who is estimated to have have caused over 50 new cases, despite typhoid having an $\mathcal{R}_0$ of 2.8 [113, 16]. Other examples include: vector-borne diseases, including malaria [126], dengue fever [25] and West Nile Virus [69]; sexually transmitted infections (STI), including HIV [45] and gonorrhea [101, 56]; and other directly transmitted diseases such as severe acute respiratory syndrome (SARS) [84], tuberculosis (TB) [71], and small pox [84]. Individual variation has important implications for disease dynamics, including emergence, spread, and control.

The effect of population heterogeneity on the basic reproductive number, $\mathcal{R}_0$, has been well studied [38, 84, 110, 132, 26, 88]. May and Anderson explored the effects of heterogeneity on $\mathcal{R}_0$ for directly transmitted diseases and showed that heterogeneity increases $\mathcal{R}_0$, making eradication harder under a homogeneously applied immunization program [88]. Diekmann et al. [26] defined and calculated $\mathcal{R}_0$ for heterogeneous populations of directly-transmitted diseases. They calculated $\mathcal{R}_0$ in terms of the next-generation operator, which maps generations of infected individuals to each other. Like other calculations of $\mathcal{R}_0$, it assumes one infected individual in an otherwise very large population of susceptible hosts. Hasibeder and Dye [38] showed that for vector-borne diseases, heterogeneity in the mosquito biting rate *increases* $\mathcal{R}_0$, which suggests that heterogeneity makes invasion likely and elimination more difficult than would be predicted by a standard calculation of $\mathcal{R}_0$ based on parameters. Lloyd-Smith et al. [84] showed that for directly transmitted diseases with heterogeneous transmission, like SARS, both the probability that an epidemic will occur and the subsequent size of the epidemic will be affected: heterogeneity made extinction more likely than predicted by the standard calculation of $\mathcal{R}_0$, but if an epidemic

did occur, it was more likely to be explosive.

While heterogeneity increases $\mathcal{R}_0$ in infinite populations, Smith et al. [132] suggest that heterogeneity actually decreases $\mathcal{R}_0$ in finite populations. They introduced the idea of calculating the expected number of secondary infections from a single infectious individual in a finite population of susceptible hosts. Motivated by malaria, a disease with a large $\mathcal{R}_0$, where $\mathcal{R}_0$ can easily approach or exceed the size of the population, they simulated these finite-population reproductive numbers and show that in a finite population, heterogeneity actually *decreases* $\mathcal{R}_0$; this is because in a finite population, individuals who are more susceptible are more likely to get infected multiple times, absorbing some possible infections. Keegan and Dushoff [63] calculated these finite-population reproductive numbers for both vector-borne and directly-transmitted diseases assuming a well mixed host population.

Building on this previous work we calculate finite-population reproductive numbers for directly transmitted diseases under different assumptions of heterogeneity in transmission. We also discuss a framework for discussing different "types of heterogeneity" (Fig. 3.1) and their importance in terms of disease control and intervention.

3.1.1 Heterogeneity Framework

In general, heterogeneity in transmission can be broken into two categories: structural heterogeneity where individuals are separated into groups, either by age or by spatial structure; and heterogeneity in individual level parameters in which individuals exhibit different disease-related behaviors [84, 35]. Here, we outline the different types of heterogeneity in individual level parameters.

Although a great deal of work has been done in understanding how heterogeneity affects the spread and control of infectious diseases (eg. [84, 35, 26]), we have found little

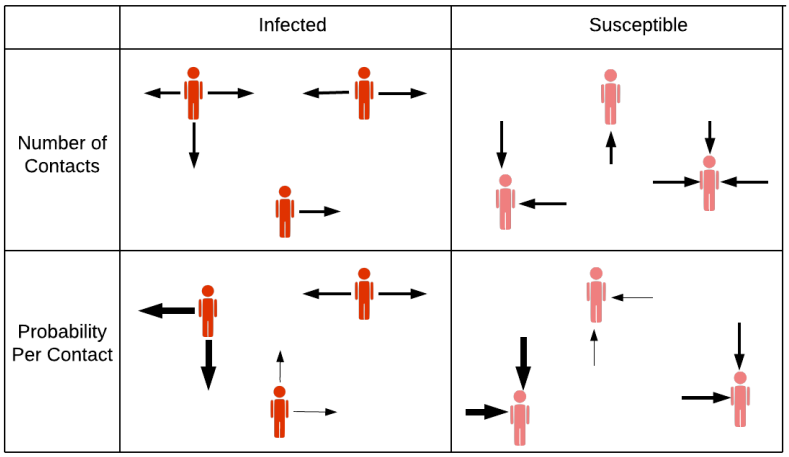

Figure 3.1: Schematic of the different types of heterogeneity in individual level parameters. The red people are infected and the pink people are susceptible. Each arrow represents a contact and the weight of the arrow represents the probability that contact will result in infection.

detailed discussion of different types of heterogeneity in transmission and their effects. Often, heterogeneity is discussed in terms of presence/absence: a population is assumed to be homogeneous or it is not. Less attention is given to the type or types of heterogeneity in disease spread. When heterogeneity is discussed in more detail, it tends to be discussed in terms of heterogeneity in infected individuals, ie "super-spreaders" [45, 84, 135] and "super-shedders" [50, 136, 19], likely because heterogeneity in susceptible individuals is harder to measure. However, clearly identifying and understanding the different types of heterogeneity and how they affect disease dynamics provides new opportunities for control. Here, we outline a framework for discussing heterogeneity in individual-level parameters.

Mixing rate

The mixing rate, also called "contact rate" describes the number of contacts that an individual has that could result in an infection. Mixing rates vary by modes of transmission

and by disease. The contact rate for a vector-borne disease depends on hosts being bitten by vectors and consequently, it is dependent both on host-related and vector-related factors. The mixing rate for an STI is the number of potentially infectious sexual contacts an individual has. This can be affected by a multitude of factors including condom use, etc. For other directly transmitted diseases, the mixing rate may be harder to quantify and depend on specific disease-related factors such as how long infectious particles remain in the air or stay alive on surfaces, and environmental factors such as humidity[50, 11, 62, 92, 61].

Heterogeneity affects mixing rates in a multitude of ways. For a vector-borne disease, such as malaria, heterogeneity in the mixing rate is often a result of host-related factors, such as differential attractiveness to mosquitoes (eg. [115, 130, 82]) or the use of bed nets [81]. Heterogeneity in the mixing rate for sexually transmitted infections can be affected by including rate of sexual partner change, sexual practices [7], and access to condoms [20, 86, 10, 112]. For directly transmitted diseases, contacts are often harder to define, and heterogeneity arises from a mixture of host, pathogen, and environmental factors. Heterogeneity in the mixing rate can be further broken down into the mixing rate of *infected* individuals and the mixing rate of *susceptible* individuals. Here, we assume that individuals have an intrinsic mixing rate that does not change with infection status.

Heterogeneity in infected mixing – The mixing rate of infected individuals is the number of contacts that an infected individual has that could result in an infection, during the course of infection. This type of heterogeneity is the most widely discussed and is often discussed in terms of infected individuals with large numbers of contacts, or super-spreaders [84, 45].

Malaria is a well known example of a disease with heterogeneity in the mixing rate: some hosts are more attractive to mosquitoes for a variety of reasons, including body size [115], blood type [130], pregnancy [82, 5], and alcohol consumption [129, 80], among

others. An example of a directly transmitted disease with heterogeneity in the mixing rate of infected individuals is SARS. During the 2002-2003 SARS epidemic, renewed attention was given to the role of super-spreading events in the epidemic; particularly in the context of control. In a model of SARS transmission, Lloyd-Smith et al. [84] showed that targeted control was up to three times more effective than random control.

Heterogeneity in susceptible mixing – The mixing rate of susceptible individuals is the number of contacts that a susceptible individual has that could result in an infection. The susceptible mixing rate may or may not be closely related to the infected mixing rate, depending on whether contacts are symmetric, and whether behavior is changed by the disease. For example, vector-borne and sexually transmitted diseases involve symmetric contact (both the susceptible and infected individual need to be bitten by a vector, or to have sexual intercourse to transmit disease), whereas food-borne illnesses often involve asymmetric contact (food workers infect food consumers, but not the other way around). Ebola virus disease is an example where behavior is changed by disease: effective mixing rates of well people depend on how likely they are to be involved in care-giving, and likely vary less than the effective mixing rates of infectious people. Sick individuals may also voluntarily attempt to reduce risk [57, 44].

Probability per contact

The probability of infection per contact describes the probability of successful transmission per potentially infectious contact. A “potentially infectious contact" is defined as one which would succeed in transmitting if both the probability of transmitting and the probability of contracting an infection are 1. The probability of successful transmission is the product of an infectiousness probability and a susceptibility probability.

Heterogeneity in infectiousness – The infectiousness of an individual is the probability of transmitting an infection per potentially infectious contact, assuming the susceptibility probability is 1. This type of heterogeneity is often discussed in terms of individuals who shed a lot of virus, or super-shedders [50, 136, 19].

Influenza and tuberculosis are examples of directly transmitted diseases with heterogeneity in infectiousness. For influenza, viral shedding influences the per contact infectiousness, there is a large variation in the number aerosolized respiratory secretions, making some individuals more infectious than others [50]. Additionally, external factors such as taking antipyretics may also increase the per-contact probability of transmission by increasing both the rate and duration of viral shedding [40]. For TB, access to health care interventions and proper nutrition may reduce the probability of transmitting per contact, by reducing the risk of pulmonary TB [71].

HIV is an example of an STI with heterogeneity in infectiousness. For HIV, the infectiousness per contact varies for a variety of reasons: individuals who are co-infected with another STI have been shown to be more infectious per contact [46, 1], while individuals on antiretroviral treatment are less infectious per contact [141].

Heterogeneity in susceptibility – The susceptibility of an individual is the probability of contracting an infection per potentially infectious contact, assuming the infectiousness probability is 1. This is the least talked about as it is likely the hardest to measure and probably depends on the interaction between host, pathogen, and environment.

An example of a disease with heterogeneity in susceptibility is HIV. There are a multitude of factors that can cause susceptibility to vary including gender and circumcision. It has been suggested that women are physiologically more susceptible to HIV than men [48, 116] and that male circumcision has a protective effect against the per contact trans-

mission of HIV [142, 9].

3.2 Methods

We calculate finite-population reproductive numbers for directly transmitted diseases under three heterogeneity assumptions: heterogeneity in intrinsic mixing rate (assumed to be independent of disease status), $\mathcal{R}_m(N)$; heterogeneity in mixing rate when infected, $\mathcal{R}_{t_m}(N)$; and heterogeneity in the probability of contracting an infection per contact, $\mathcal{R}_{s_p}(N)$. Two other assumptions: heterogeneity in the probability of transmitting an infection per contact, $\mathcal{R}_{t_p}(N)$and heterogeneity in mixing rate when susceptible, $\mathcal{R}_{s_m}(N)$, are shown in the appendix.

We numerically calculate each of these finite-population reproductive numbers using two different distributions to underlie the heterogeneity: the gamma and log-normal distributions for $\mathcal{R}_{t_m}(N)$, $\mathcal{R}_{s_m}(N)$, and $\mathcal{R}_m(N)$ and the beta and logit-normal distributions for $\mathcal{R}_{t_p}(N)$ and $\mathcal{R}_{s_p}(N)$.

3.2.1 Assumptions

We assume a finite population of size N. We talk about transmission, $t = t_m t_p$, as the product of the mixing rate of infected individuals, t_m, and the probability of transmitting an infection per infectious contact, t_p. Similarly, we talk about susceptibility, $s = s_m s_p$, as the product of the mixing rate of susceptible individuals, s_m, and the probability of contracting and infection per contact, s_p.

We assume that an infected individual of type y produces a geometric distribution of new infections with mean of $t(y)$. This is equivalent to assuming that the infection and

recovery processes are Markovian [63]. We assume that all hosts behave independently. Since the host population is finite, some of the *possible* infections may fall on the same susceptible host, so the average number of *realized* infections, in general, will be smaller.

3.2.2 Calculation framework

We start with a known infectious individual of type y. We know that this infected individual produces a geometric distribution of potentially successful challenges (contacts) with mean $t(y)$ (where $t(y) = t_m(y)t_p(y)$). For each challenge, the risk to a particular susceptible individual of type x, is $\frac{s(x)}{\bar{s}_m N}$, where $\bar{s}_m$ is the mean susceptible mixing rate.

The probability of escaping a challenges from an infected individual is $\left(1 - \frac{s(x)}{\bar{s}_m N}\right)^a$. The risk of being infected by at least one of those contacts is $\left(1 - \left(1 - \frac{s(x)}{\bar{s}_m N}\right)^a\right)$. Using the generating function method detailed in [63], we find the risk to a susceptible individual of type x from a single infected individual of type y is:

$$\frac{s(x)t(y)}{s(x)t(y) + \bar{s}_m N} \tag{3.1}$$

The expected number of infections from the known infectious individual is

$$\left\langle \frac{s(x)t(y)}{s(x)t(y) + \bar{s}_m N} \right\rangle_x N \tag{3.2}$$

We then average over the distribution of "typical" individuals [26], $s(y)/\bar{s}$, and find:

$$R(N) = \left\langle \frac{s(y)}{\bar{s}} \left\langle \frac{s(x)t(y)N}{s(x)t(y) + \bar{s}_m N} \right\rangle_x \right\rangle_y \tag{3.3}$$

Which is equivalent to

$$R(N) = \int \frac{s(y)}{\bar{s}} \int \frac{s(x)t(y)N}{s(x)t(y) + \bar{s}_m N} f(x)f(y)dxdy \tag{3.4}$$

Where $f(x)$ is the distribution of susceptible individuals and $f(y)$ is the distribution of infected individuals. Here, we always choose the same distribution for $f(x)$ and $f(y)$ however, we allow the mean of the distributions to vary (s, t, and m).

Heterogeneity in mixing rate, $\mathcal{R}_m(N)$

We calculate the finite-population reproductive number for the case where we allow only heterogeneity in the mixing rates of infected and susceptible individuals.

Because individuals need to contact each other we want s to be proportional to τ, so we write $\tau = m$ and $s = m/\bar{m}$.

We find the expected number of new infections from our known infectious individual is

$$\left\langle \frac{m(x)m(y)N}{m(x)m(y) + \bar{m}N} \right\rangle_x \tag{3.5}$$

We then account for the distribution of typical individuals, $m(y)/\bar{m}$ and find

$$\mathcal{R}_m(N) = \left\langle \frac{m(y)}{\bar{m}} \left\langle \frac{m(x)m(y)N}{m(x)m(y) + \bar{m}N} \right\rangle_x \right\rangle_y \tag{3.6}$$

3.3 Results

3.3.1 Heterogeneity in mixing rate, $\mathcal{R}_m(N)$

The finite-population reproductive number is

$$\mathcal{R}_m(N) = \left\langle \frac{m(y)}{\bar{m}} \left\langle \frac{m(x)m(y)N}{m(x)m(y) + \bar{m}N} \right\rangle_x \right\rangle_y \tag{3.7}$$

We solve for $\mathcal{R}_m(N)$ numerically for two distributions of mixing rates, gamma-distributed heterogeneity (Fig. 3.2) and log-normally distributed heterogeneity (Fig. A1). Fig. 3.2a and Fig. A1a show how the finite-population reproductive numbers increase with $\mathcal{R}_0$ for a fixed population size. The finite-population reproductive numbers diverge from their corresponding infinite population reproductive number as $\mathcal{R}_0$ approaches the size of the population. Where they diverge depends on the coefficient of variation – the finite-population reproductive number with $CV = 3$ diverges around $1/5N$ whereas the homogeneous finite-population reproductive number diverges around $1/2N$. Further, the heterogeneous finite-population reproductive numbers are larger than the homogeneous finite-population reproductive number when $\mathcal{R}_0$ is large relative to the size of the population and the heterogeneous finite-population reproductive numbers are smaller than the homogeneous finite-population reproductive number when $\mathcal{R}_0$ is small relative to the size of the population. For gamma distributed heterogeneity, this occurs between $1/3N$ and $3/4N$ (Fig. 3.2a) and at around N for log-normally distributed heterogeneity (Fig. A1).

Fig. 3.2b and Fig. A1b show how the finite-population reproductive numbers vary with the size of the population for fixed $\mathcal{R}_0 = 100$. It shows the finite-population reproductive numbers converging on their corresponding infinite population reproductive number; with

finite-population reproductive numbers with large coefficient of variation converging slower than finite-population reproductive numbers with small coefficient of variation.

Fig. 3.3 shows the relationship between gamma distributed and log-normally distributed heterogeneity. Although the results are fairly robust to the distribution, the finite-population reproductive numbers with log-normally distributed heterogeneity is larger than the finite-population reproductive numbers with gamma distributed heterogeneity for the biologically relevant parameter range.

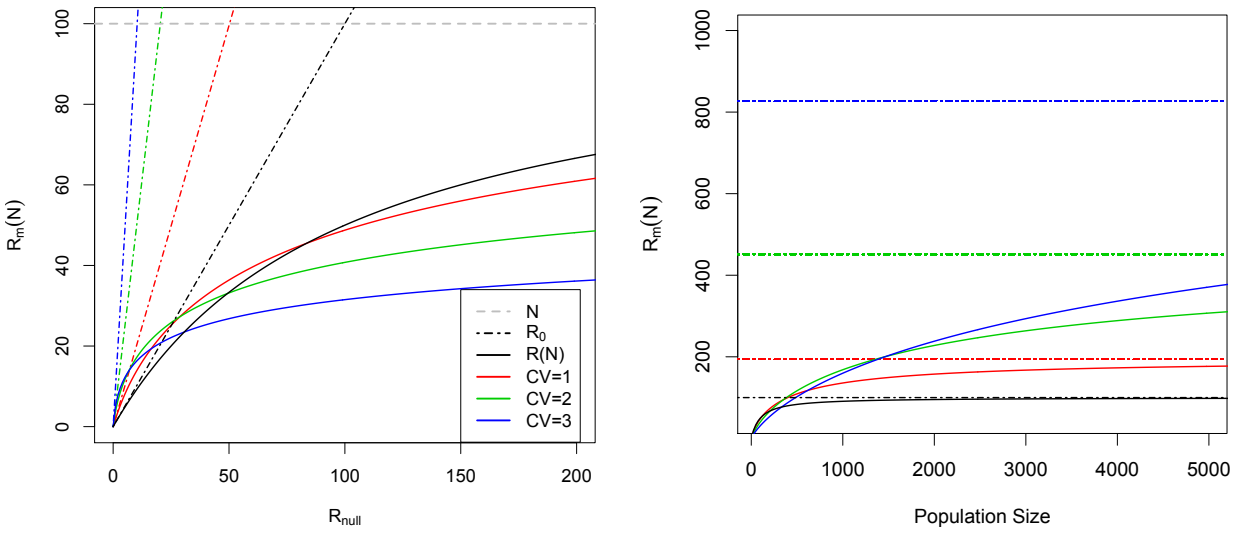

(a) Fixed Population Size

(b) Fixed $\mathcal{R}_0$

Figure 3.2: The finite-population reproductive number, $\mathcal{R}_m(N)$, for gamma distributed heterogeneity. The solid lines are the finite-population reproductive numbers with different coefficients of variation and the dot-dashed lines represent the infinite reproductive numbers with corresponding coefficients of variation. (a) the finite-population reproductive numbers versus the null reproductive numbers, $\mathcal{R}_{null}$ with a fixed population of size $N = 100$ (dashed line) and (b) the finite-population reproductive numbers versus the population size for fixed $\mathcal{R}_0 = 100$ (dot-dashed line).

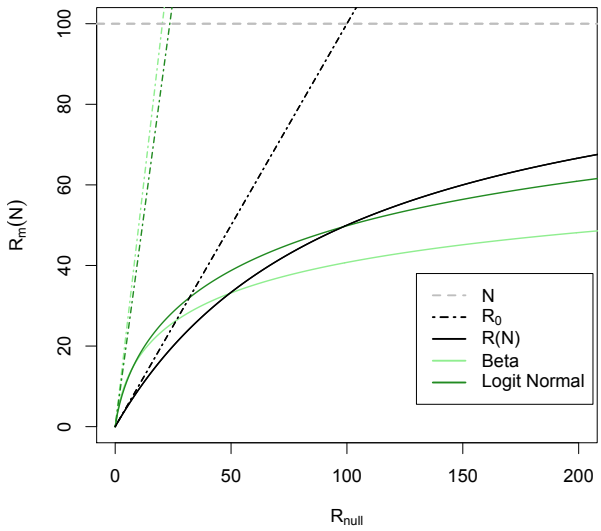

Figure 3.3: The finite-population reproductive numbers, $\mathcal{R}_m(N)$, versus the homogeneous basic reproductive number, $\mathcal{R}_0$ for gamma distributed (light green) and log-normally distributed (forest green) heterogeneity for CV=2. The population size is $N = 500$, the homogeneous $\mathcal{R}_0$ is the solid black line and the heterogeneous reproductive numbers are the solid green lines, the homogeneous finite-population reproductive number, $\mathcal{R}(N)$, is the dotted black line, and the dot-dashed lines represent heterogeneous finite-population reproductive numbers with different coefficients of variation.

3.3.2 Heterogeneity in transmission mixing $\mathcal{R}_{t_m}(N)$

The finite-population reproductive number is

$$\mathcal{R}_{t_m}(N) = \left\langle \frac{\bar{s}t(y)N}{\bar{s}t(y) + \bar{s}_m N} \right\rangle_y \tag{3.8}$$

We solve for $\mathcal{R}_{t_m}(N)$ numerically for two distributions of mixing rates, gamma-distributed heterogeneity (Fig. 3.4) and log-normally distributed heterogeneity (Fig. A2). Fig. 3.4a and Fig. A2a show how the finite-population reproductive numbers increase with $\mathcal{R}_0$ for a fixed population size. The finite-population reproductive numbers diverge from their correspond-

ing infinite population reproductive number as $\mathcal{R}_0$ approaches the size of the population. Where they diverge depends on the coefficient of variation – the finite-population reproductive number with $CV = 3$ diverges around $1/5N$ whereas the homogeneous finite-population reproductive number diverges around $1/2N$. Unlike intrinsic mixing, the finite-population reproductive numbers with heterogeneity in transmission mixing are always smaller than the homogeneous finite-population reproductive number.

Fig. 3.4b and Fig. A2b show how the finite-population reproductive numbers vary with the size of the population for fixed $\mathcal{R}_0 = 100$. It shows the finite-population reproductive numbers converging on their corresponding infinite population reproductive number; with finite-population reproductive numbers with large coefficient of variation converging slower than finite-population reproductive numbers with small coefficient of variation.

Fig. 3.5 shows the relationship between gamma distributed and log-normally distributed heterogeneity. Although the results are fairly robust to the distribution, the finite-population reproductive numbers with log-normally distributed heterogeneity is larger than the finite-population reproductive numbers with gamma distributed heterogeneity for the biologically relevant parameter range.

3.3.3 Heterogeneity in transmission probability $\mathcal{R}_{t_p}(N)$

The finite-population reproductive number is

$$\mathcal{R}_{t_p}(N) = \left\langle \frac{t(y)\bar{s}N}{t(y)\bar{s} + \bar{s}_m N} \right\rangle_y \tag{3.9}$$

We solve for $\mathcal{R}_{t_p}(N)$ numerically for two distributions of mixing rates, beta-distributed heterogeneity (Fig. **??**) and logit-normally distributed heterogeneity (Fig. A2). Fig. 3.6a

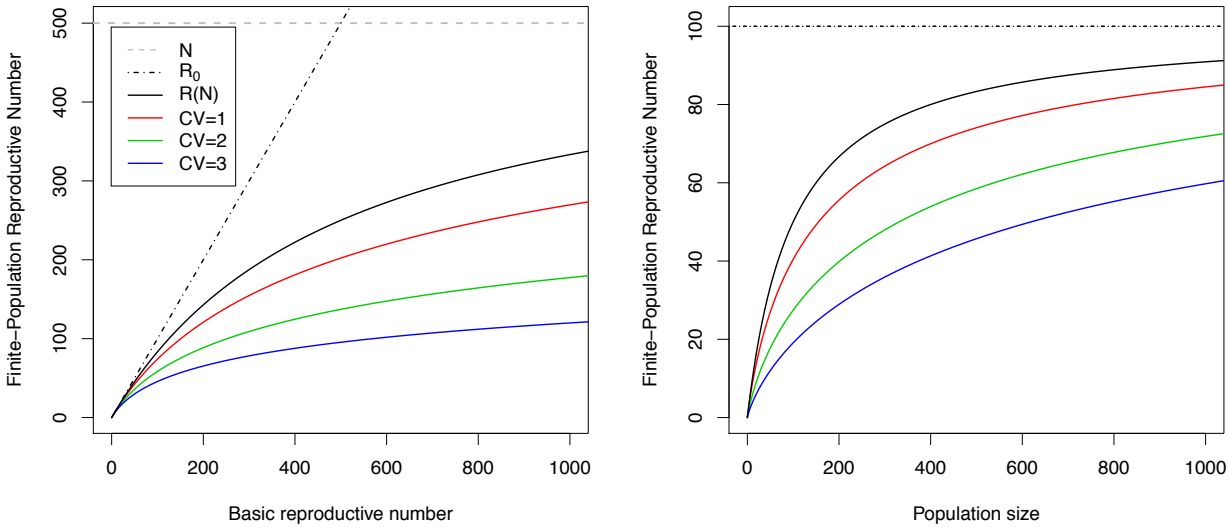

(a) Fixed Population Size

(b) Fixed $\mathcal{R}_0$

Figure 3.4: The finite-population reproductive number, $\mathcal{R}_{t_m}(N)$, for gamma distributed heterogeneity. The solid lines are the finite-population reproductive numbers with different coefficients of variation and the dot-dashed lines represent the infinite reproductive numbers with corresponding coefficients of variation. (a) the finite-population reproductive numbers versus the null reproductive numbers, $\mathcal{R}_{null}$ with a fixed population of size $N = 100$ (dashed line) and (b) the finite-population reproductive numbers versus the population size for fixed $\mathcal{R}_0 = 100$ (dot-dashed line).

and Fig. A2c show how the finite-population reproductive numbers increase with $\mathcal{R}_0$ for a fixed population size. The finite-population reproductive numbers diverge from their corresponding infinite population reproductive number as $\mathcal{R}_0$ approaches the size of the population. Where they diverge depends on the coefficient of variation – the finite-population reproductive number with $CV = 3$ diverges around $1/5N$ whereas the homogeneous finite-population reproductive number diverges around $1/2N$. Unlike intrinsic mixing, the finite-population reproductive numbers with heterogeneity in transmission probability are always smaller than the homogeneous finite-population reproductive number.

Fig. 3.6b and Fig. A2d show how the finite-population reproductive numbers vary with

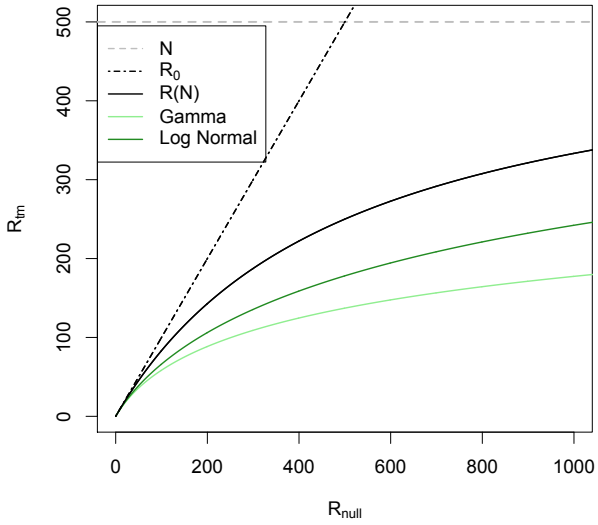

Figure 3.5: The finite-population reproductive numbers, $\mathcal{R}_{t_m}(N)$, versus the basic reproductive number, $\mathcal{R}_0$ for gamma distributed (light green) and log-normally distributed (forest green) heterogeneity for CV=2. The population size is $N = 500$, $\mathcal{R}_0$ is the solid black line, the homogeneous finite-population reproductive number, $\mathcal{R}(N)$, is the dotted black line, and the dot-dashed lines represent heterogeneous finite-population reproductive numbers with different coefficients of variation.

the size of the population for fixed $\mathcal{R}_0 = 100$. It shows the finite-population reproductive numbers converging on their corresponding infinite population reproductive number; with finite-population reproductive numbers with large coefficient of variation converging slower than finite-population reproductive numbers with small coefficient of variation.

Fig. 3.7 shows the relationship between beta distributed and logit-normally distributed heterogeneity. Although the results are fairly robust to the distribution, the finite-population reproductive numbers with logit-normally distributed heterogeneity is larger than the finite-population reproductive numbers with beta distributed heterogeneity for the biologically relevant parameter range.

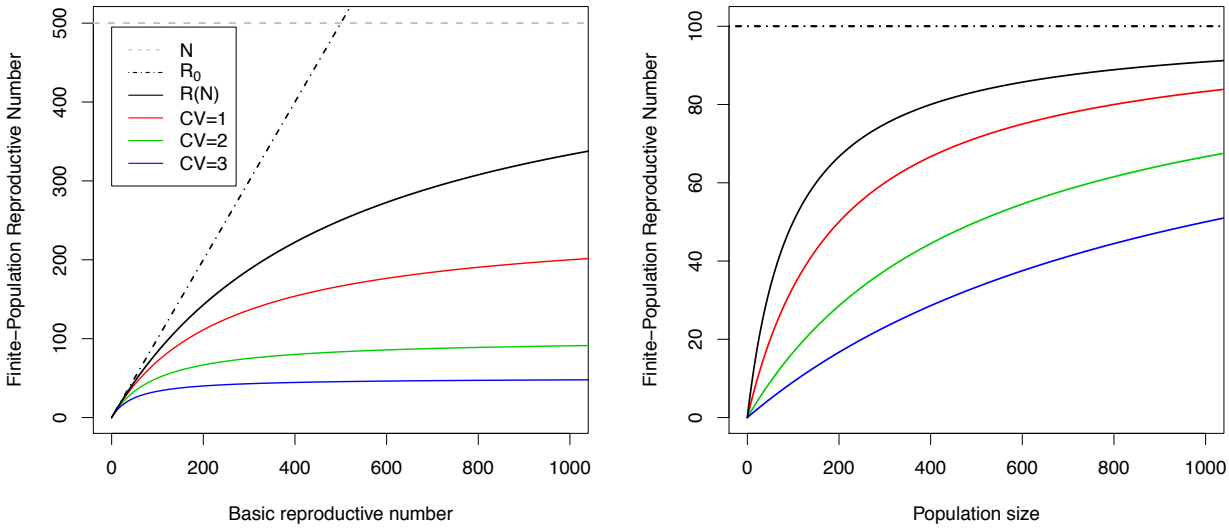

(a) Fixed Population Size

(b) Fixed $\mathcal{R}_0$

Figure 3.6: The finite-population reproductive number, $\mathcal{R}_{t_p}(N)$, for beta distributed heterogeneity. The solid lines are the finite-population reproductive numbers with different coefficients of variation and the dot-dashed lines represent the infinite reproductive numbers with corresponding coefficients of variation. (a) the finite-population reproductive numbers versus the null reproductive numbers, $\mathcal{R}_{null}$ with a fixed population of size $N = 100$ (dashed line) and (b) the finite-population reproductive numbers versus the population size for fixed $\mathcal{R}_0 = 100$ (dot-dashed line).

3.3.4 Heterogeneity in susceptible mixing, $\mathcal{R}_{s_m}(N)$

The finite-population reproductive number is

$$\mathcal{R}_{s_m}(N) = \left\langle \frac{s(y)}{\bar{s}} \left\langle \frac{s(x)\bar{t}N}{s(x)\bar{t} + \bar{s}_m N} \right\rangle_x \right\rangle_y \tag{3.10}$$

$$= \left\langle \frac{s(x)\bar{t}N}{s(x)\bar{t} + \bar{s}_m N} \right\rangle_x \tag{3.11}$$

We solve for $\mathcal{R}_{s_m}(N)$ numerically for two distributions of mixing rates, gamma-distributed

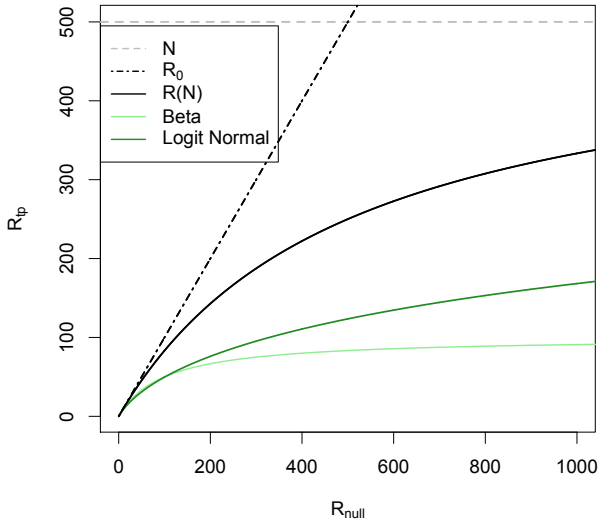

Figure 3.7: The finite-population reproductive numbers, $\mathcal{R}_{t_p}(N)$, versus the basic reproductive number, $\mathcal{R}_0$ for beta distributed (light green) and logit-normally distributed (forest green) heterogeneity for CV=2. The population size is $N = 500$, $\mathcal{R}_0$ is the solid black line, the homogeneous finite-population reproductive number, $\mathcal{R}(N)$, is the dotted black line, and the dot-dashed lines represent heterogeneous finite-population reproductive numbers with different coefficients of variation.

heterogeneity (Fig. 3.8) and log-normally distributed heterogeneity (Fig. A2). Fig. 3.8a and Fig. A2e show how the finite-population reproductive numbers increase with $\mathcal{R}_0$ for a fixed population size. The finite-population reproductive numbers diverge from their corresponding infinite population reproductive number as $\mathcal{R}_0$ approaches the size of the population. Where they diverge depends on the coefficient of variation – the finite-population reproductive number with $CV = 3$ diverges around $1/5N$ whereas the homogeneous finite-population reproductive number diverges around $1/2N$. Unlike intrinsic mixing, the finite-population reproductive numbers with heterogeneity in susceptible mixing are always smaller than the homogeneous finite-population reproductive number.

Fig. 3.8b and Fig. A2f show how the finite-population reproductive numbers vary with

the size of the population for fixed $\mathcal{R}_0 = 100$. It shows the finite-population reproductive numbers converging on their corresponding infinite population reproductive number; with finite-population reproductive numbers with large coefficient of variation converging slower than finite-population reproductive numbers with small coefficient of variation.

Fig. 3.9 shows the relationship between gamma distributed and log-normally distributed heterogeneity. Although the results are fairly robust to the distribution, the finite-population reproductive numbers with log-normally distributed heterogeneity is larger than the finite-population reproductive numbers with gamma distributed heterogeneity for the biologically relevant parameter range.

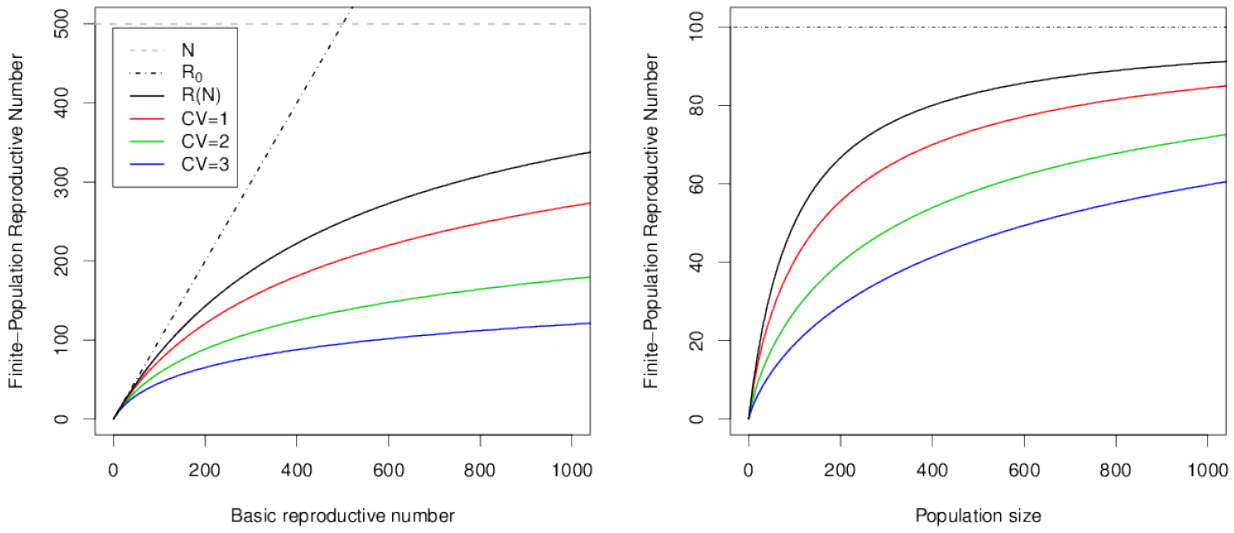

(a) Fixed Population Size

(b) Fixed $\mathcal{R}_0$

Figure 3.8: The finite-population reproductive number, $\mathcal{R}_{s_m}(N)$, for gamma distributed heterogeneity. The solid lines are the finite-population reproductive numbers with different coefficients of variation and the dot-dashed lines represent the infinite reproductive numbers with corresponding coefficients of variation. (a) the finite-population reproductive numbers versus the null reproductive numbers, $\mathcal{R}_{null}$ with a fixed population of size $N = 100$ (dashed line) and (b) the finite-population reproductive numbers versus the population size for fixed $\mathcal{R}_0 = 100$ (dot-dashed line).

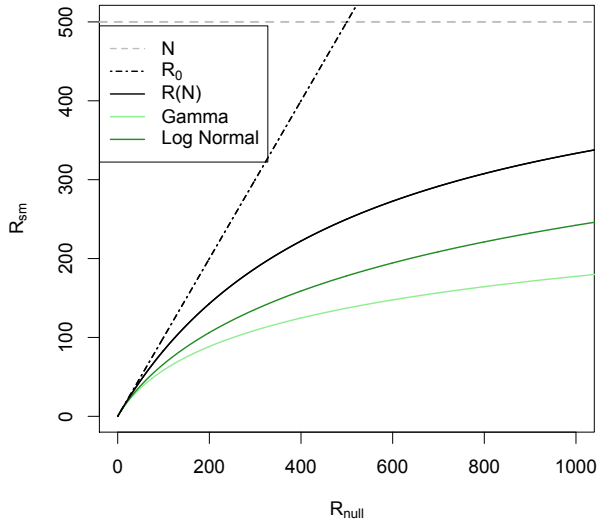

Figure 3.9: The finite-population reproductive numbers, $\mathcal{R}_{s_m}(N)$, versus the basic reproductive number, $\mathcal{R}_0$ for gamma distributed (light green) and log-normally distributed (forest green) heterogeneity for CV=2. The population size is $N = 500$, $\mathcal{R}_0$ is the solid black line, the homogeneous finite-population reproductive number, $\mathcal{R}(N)$, is the dotted black line, and the dot-dashed lines represent heterogeneous finite-population reproductive numbers with different coefficients of variation.

3.3.5 Heterogeneity in susceptibility probability $\mathcal{R}_{s_p}(N)$

The finite-population reproductive number is

$$\mathcal{R}_{s_p}(N) = \left\langle \frac{s(y)}{\bar{s}} \left\langle \frac{s(x)\bar{t}N}{s(x)\bar{t} + \bar{s}_m N} \right\rangle_x \right\rangle_y \tag{3.12}$$

$$= \left\langle \frac{s(x)\bar{t}N}{s(x)\bar{t} + \bar{s}_m N} \right\rangle_x \tag{3.13}$$

We solve for $\mathcal{R}_{s_p}(N)$ numerically for two distributions of mixing rates, beta-distributed heterogeneity (Fig. **??**) and logit-normally distributed heterogeneity (Fig. A2). Fig. 3.10a

and Fig. A2g show how the finite-population reproductive numbers increase with $\mathcal{R}_0$ for a fixed population size. The finite-population reproductive numbers diverge from their corresponding infinite population reproductive number as $\mathcal{R}_0$ approaches the size of the population. Where they diverge depends on the coefficient of variation – the finite-population reproductive number with $CV = 3$ diverges around $1/5N$ whereas the homogeneous finite-population reproductive number diverges around $1/2N$. Unlike intrinsic mixing, the finite-population reproductive numbers with heterogeneity in susceptible mixing are always smaller than the homogeneous finite-population reproductive number.

Fig. 3.10b and Fig. A2h show how the finite-population reproductive numbers vary with the size of the population for fixed $\mathcal{R}_0 = 100$. It shows the finite-population reproductive numbers converging on their corresponding infinite population reproductive number; with finite-population reproductive numbers with large coefficient of variation converging slower than finite-population reproductive numbers with small coefficient of variation.

Fig. 3.11 shows the relationship between beta distributed and logit-normally distributed heterogeneity. Although the results are fairly robust to the distribution, the finite-population reproductive numbers with logit-normally distributed heterogeneity is larger than the finite-population reproductive numbers with beta distributed heterogeneity for the biologically relevant parameter range.

3.4 Discussion

Host heterogeneity has been shown to have a significant effect on disease dynamics [38, 84, 110, 132, 26]. Of particular interest is the effect of heterogeneity in transmission on $\mathcal{R}_0$ [38, 84, 110, 132]. In an infinite population of susceptible hosts, heterogeneity has been shown to *increase* $\mathcal{R}_0$, whereas in a finite population, we show that heterogeneity has a

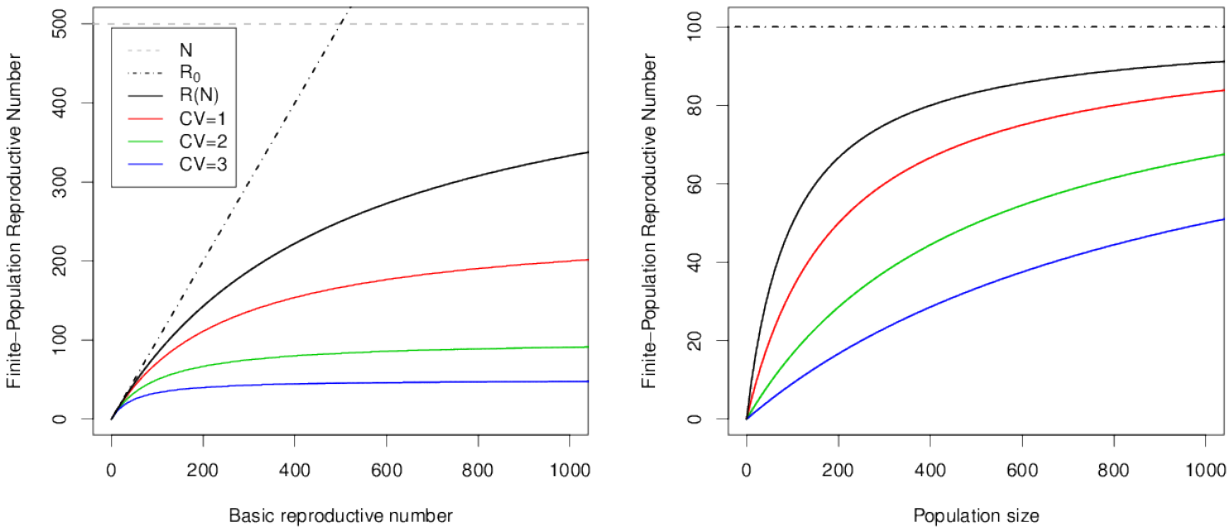

(a) Fixed Population Size

(b) Fixed $\mathcal{R}_0$

Figure 3.10: The finite-population reproductive number, $\mathcal{R}_{s_p}(N)$, for beta distributed heterogeneity. The solid lines are the finite-population reproductive numbers with different coefficients of variation and the dot-dashed lines represent the infinite reproductive numbers with corresponding coefficients of variation. (a) the finite-population reproductive numbers versus the null reproductive numbers, $\mathcal{R}_{null}$ with a fixed population of size $N = 100$ (dashed line) and (b) the finite-population reproductive numbers versus the population size for fixed $\mathcal{R}_0 = 100$ (dot-dashed line).

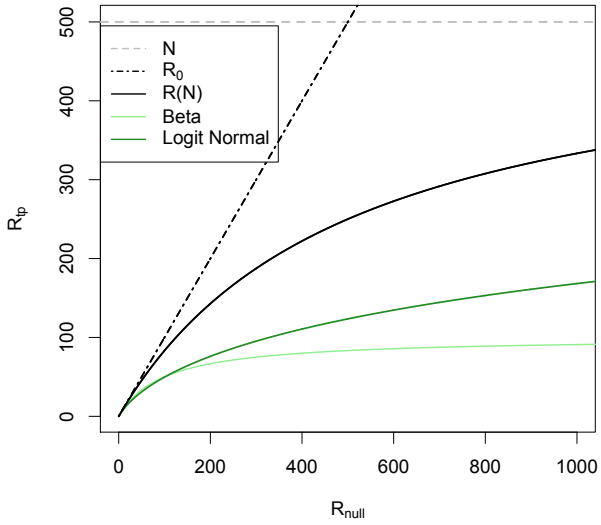

Figure 3.11: The finite-population reproductive numbers, $\mathcal{R}_{t_p}(N)$, versus the basic reproductive number, $\mathcal{R}_0$ for beta distributed (light green) and log-normally distributed (forest green) heterogeneity for CV=2. The population size is $N = 500$, $\mathcal{R}_0$ is the solid black line, the homogeneous finite-population reproductive number, $\mathcal{R}(N)$, is the dotted black line, and the dot-dashed lines represent heterogeneous finite-population reproductive numbers with different coefficients of variation.

more complicated effect on the reproductive number.

Smith et al. [132] found that in a finite population, heterogeneity in the attractiveness to mosquitoes *decreases* the reproductive number; our results for simple heterogeneity (ie. heterogeneity either mixing or probability for only susceptible or infected) support this Fig. 3.4, **??**, 3.8, 3.10, Fig. A2. However, for heterogeneity in the mixing rate of both infected and susceptible individuals, we find that when the population is large compared to the homogeneous $\mathcal{R}_0$, heterogeneity *increases* $\mathcal{R}_m(N)$ compared to the homogeneous $\mathcal{R}_0$; and when the population is small relative to $\mathcal{R}_0$, heterogeneity *decreases* $\mathcal{R}_m(N)$ compared to the homogeneous $\mathcal{R}_0$ Fig. 3.2 and Fig. **??**.

Compared to the heterogeneous $\mathcal{R}_0$, the effect of small population *decreases* the re-

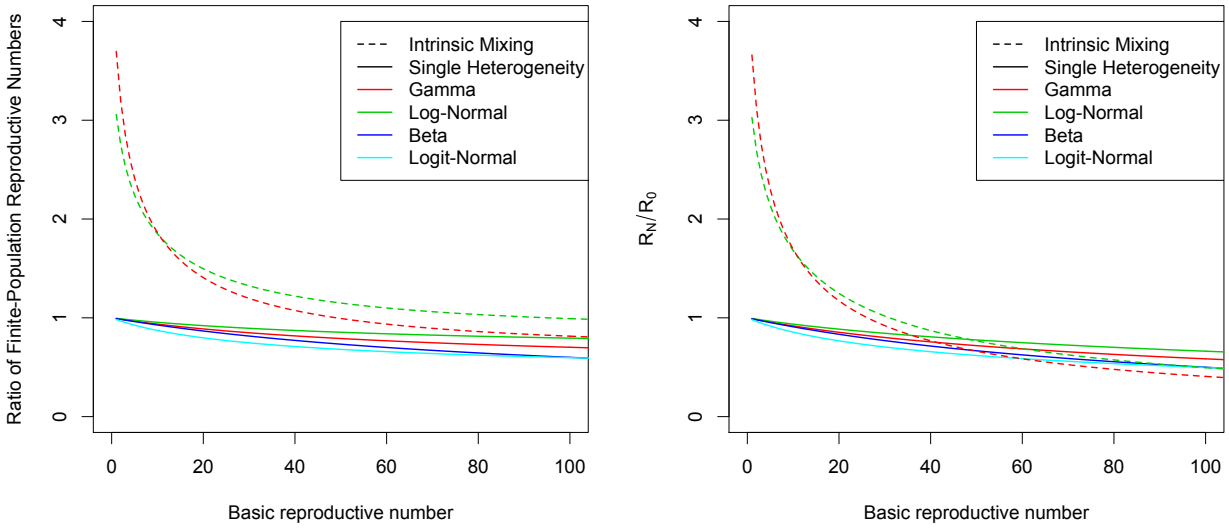

(a) Heterogeneous/Homogeneous

(b) Heterogeneous/$\mathcal{R}_0$

Figure 3.12: Plot comparing the different distributions. (a) Plot of the ratio of the heterogeneous finite-population reproductive numbers to the homogeneous finite-population reproductive number versus $\mathcal{R}_0$; for each of the four distributions of heterogeneity and for both intrinsic mixing (dashed lines) and simple heterogeneity (solid lines). (a) Plot of the ratio of the heterogeneous finite-population reproductive numbers to $\mathcal{R}_0$ versus $\mathcal{R}_0$; for each of the four distributions of heterogeneity and for both intrinsic mixing (dashed lines) and simple heterogeneity (solid lines)

productive number. In general heterogeneity increases the effective mixing rate, because the most susceptible individuals are also the most infectious individuals. This has complex effects in the finite population, when the size of the population is large relative to $\mathcal{R}_0$, few people are contacted multiple times, so increasing the mixing rate increases the reproductive number. However, when the size of the population is small relative to $\mathcal{R}_0$, many more people are contacted multiple times, absorbing some possible infections, reducing $\mathcal{R}_m(N)$ Fig. 3.2 and Fig. **??**.

Smith et al. [132] considered only heterogeneity in attractiveness to mosquitoes. Here, we consider five different types of heterogeneity: the four simple types outlined in the section 3.1.1 and heterogeneity in the mixing rate of both susceptible and infected individuals (the last corresponds to Smith's assumptions). We find simple expressions for each of the five finite-population reproductive numbers in terms of the distribution of heterogeneity and the size of the population.

We show that $\mathcal{R}_0$ is affected by both the choice of the family of distributions of the heterogeneity (e.g., gamma, log normal, etc.) and the specific CV of its distribution. Fig. 3.3, 3.7, 3.9, 3.5, 3.7 show the effect of the distribution on the the finite-population reproductive numbers for a fixed coefficient of variation (CV=2). While the distribution of heterogeneity for a fixed CV affects the finite-population reproductive numbers, the CV has a larger effect on how much the finite-population reproductive number is changed due to heterogeneity. Fig. 3.2 Fig. 3.4, **??**, 3.8, 3.10, Fig. **??**, and Fig. A2 show the effect of the coefficient of variation on the finite-population reproductive numbers. For very small values of the CV, the finite-population reproductive numbers converge on the homogeneous finite-population reproductive number; as CV increases, so does the effect of heterogeneity.

For simple heterogeneity ($\mathcal{R}_{t_m}(N)$, $\mathcal{R}_{s_m}(N)$, $\mathcal{R}_{t_p}(N)$, and $\mathcal{R}_{s_p}(N)$), in which heterogeneity always decreases the finite-population reproductive numbers, classical calculations

of $\mathcal{R}_0$ are over-estimating the diseases actual reproductive number. And although heterogeneity in the mixing rate has a more complicated effect on the finite-population reproductive number, it has the same implications for control: it suggests that for a disease with a large $\mathcal{R}_0$ spreading in a small heterogeneous population, the actual reproductive number may be lower than the standard calculation of $\mathcal{R}_0$, making control easier than predicted.

3.5 Contributions

LK and JD conceived and analyzed the model, drafted the manuscript, and both authors have read and approved the manuscript.

3.6 Acknowledgments

The authors thank David Earn, and Ben Bolker for useful comments and suggestions. We also thank Juliet Pulliam for helpful discussions about framing the research project.

3.A Appendix: Calculation Framework

3.A.1 Heterogeneity in transmission mixing $\mathcal{R}_{t_m}(N)$

We calculate the finite-population reproductive number for the case where we allow only transmission mixing rates, t_m, to vary. We find the expected number of infections from our known infectious individual is

$$= \left\langle \frac{\bar{s}t(y)N}{\bar{s}t(y) + \bar{s}_m N} \right\rangle_x \tag{3.14}$$

$$= \frac{\bar{s}t(y)N}{\bar{s}t(y) + \bar{s}_m N} \tag{3.15}$$

3.A.2 Heterogeneity in transmission probability $\mathcal{R}_{t_p}(N)$

We calculate the finite-population reproductive number for the case where we allow only probability of transmitting an infection per contact, t_p, to vary.

We find the expected number of infections from the known infectious individual is

$$\left\langle \frac{t(y)\bar{s}N}{t(y)\bar{s} + \bar{s}_m N} \right\rangle_x \tag{3.16}$$

$$\frac{t(y)\bar{s}N}{t(y)\bar{s} + \bar{s}_m N} \tag{3.17}$$

3.A.3 Heterogeneity in susceptible mixing, $\mathcal{R}_{s_m}(N)$

We calculate the finite-population reproductive number for the case where we allow only susceptible mixing rates, s_m, to vary. We find the expected number of new infections is

$$\left\langle \frac{s(x)\bar{t}N}{s(x)\bar{t} + \bar{s}_m N} \right\rangle_x \tag{3.18}$$

3.A.4 Heterogeneity in susceptibility probability $\mathcal{R}_{s_p}(N)$

We calculate the finite-population reproductive number for the case where we allow only heterogeneity in the probability contracting an infection per contact, s_p.

We find the expected number of new infections from a single infected individual of type y is:

$$\left\langle \frac{s(x)\bar{t}N}{s(x)\bar{t} + \bar{s}_m N} \right\rangle_x \tag{3.19}$$

3.B Appendix: Results

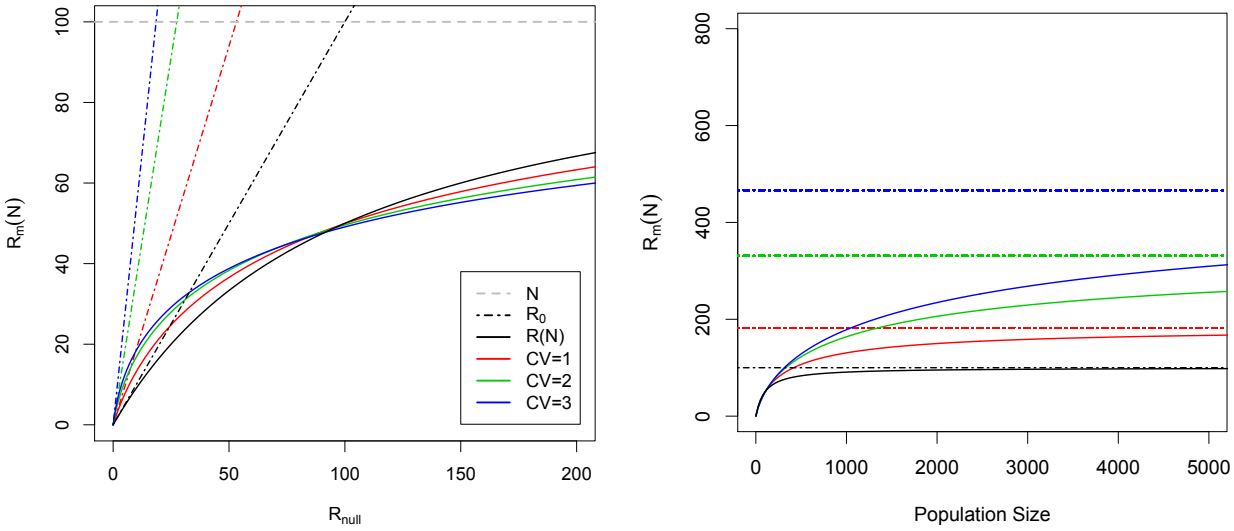

(a) Fixed Population Size

(b) Fixed $\mathcal{R}_0$

Figure A1: The finite-population reproductive number, $\mathcal{R}_m(N)$, for log-normally distributed heterogeneity. The solid lines are the finite-population reproductive numbers with different coefficients of variation and the dot-dashed lines represent the infinite reproductive numbers with corresponding coefficients of variation. (a) the finite-population reproductive numbers versus the null reproductive numbers, $\mathcal{R}_{null}$ with a fixed population of size $N = 100$ (dashed line) and (b) the finite-population reproductive numbers versus the population size for fixed $\mathcal{R}_0 = 100$ (dot-dashed line).

3.B.1 Appendix: Additional figures

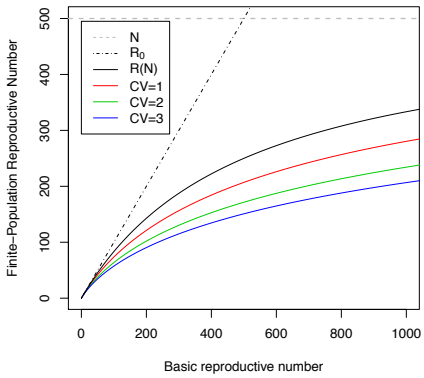

(a) $\mathcal{R}_{t_m}(N)$: Fixed Population Size

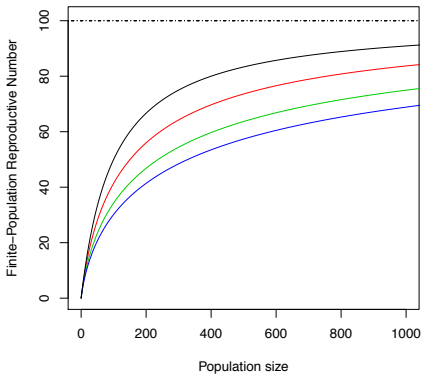

(b) $\mathcal{R}_{t_m}(N)$: Fixed $\mathcal{R}_0$

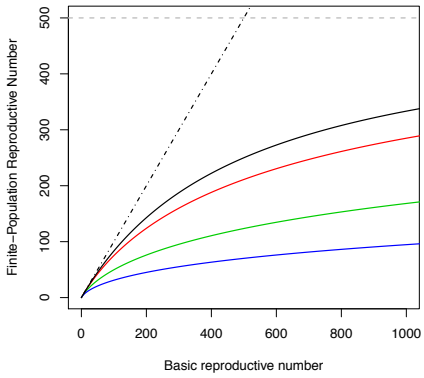

(c) $\mathcal{R}_{t_p}(N)$: Fixed Population Size

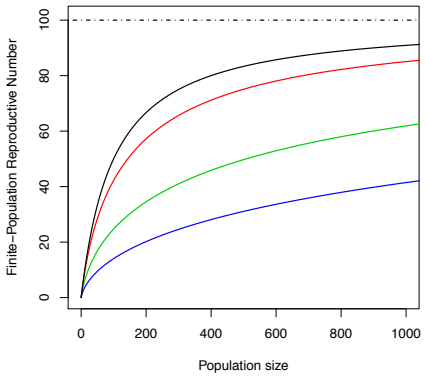

(d) $\mathcal{R}_{t_p}(N)$: Fixed $\mathcal{R}_0$

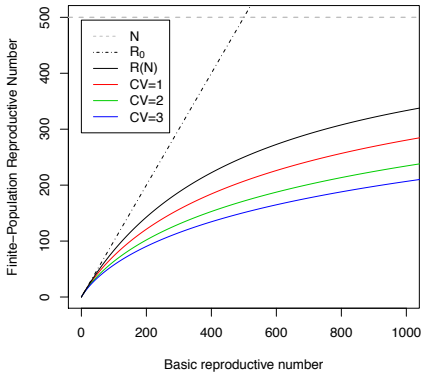

(e) $\mathcal{R}_{s_m}(N)$: Fixed Population Size

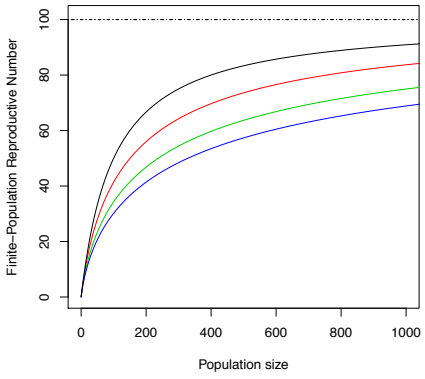

(f) $\mathcal{R}_{s_m}(N)$: Fixed $\mathcal{R}_0$

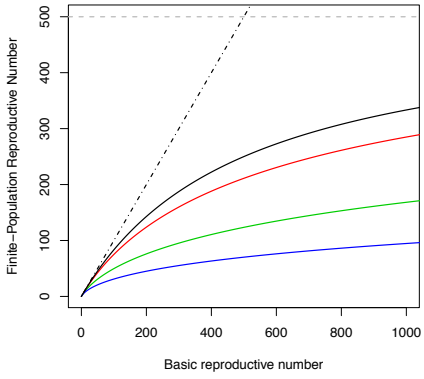

(g) $\mathcal{R}_{s_p}(N)$: Fixed Population Size

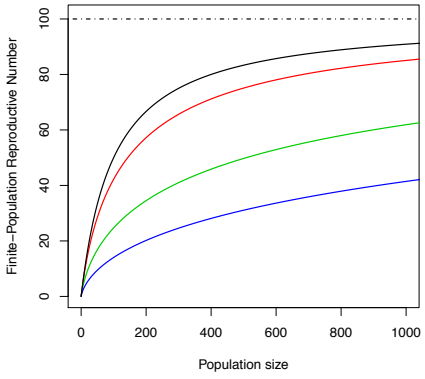

(h) $\mathcal{R}_{s_p}(N)$: Fixed $\mathcal{R}_0$

Figure A2: (Previous page.) Plot of the finite-population reproductive numbers, for log-normally distributed heterogeneity The solid lines are the finite-population reproductive numbers with different coefficients of variation and the dot-dashed lines represent the infinite reproductive numbers with corresponding coefficients of variation. (a,c,e,g) the finite-population reproductive numbers versus the null reproductive numbers, $\mathcal{R}_{null}$ with a fixed population of size $N = 100$ (dashed line) and (b,d,f,h) the finite-population reproductive numbers versus the population size for fixed $\mathcal{R}_0 = 100$ (dot-dashed line). (a,b) $\mathcal{R}_{t_m}(N)$ (c,d) $\mathcal{R}_{t_p}(N)$ (e,f) and (g,h)

Chapter 4

Population-Level Effects of Clinical Immunity to Malaria

Keegan LT, Dushoff J, (2013) *BMC Infectious Diseases* 13:428.
doi: 10.1186/1471-2334-13-428

4.1 Abstract

Background

Despite a resurgence in control efforts, malaria remains a serious public-health problem, causing millions of deaths each year. One factor that complicates malaria-control efforts is clinical immunity, the acquired immune response that protects individuals from symptoms despite the presence of parasites. Clinical immunity protects individuals against disease, but its effects at the population level are complex. It has been previously suggested that under certain circumstances, malaria is *bistable*: it can persist, if established, in areas where it would not be able to invade. This phenomenon has important implications for control: in areas where malaria is bistable, if malaria could be eliminated until immunity wanes, it

would not be able to re-invade.

Methods

Here, we formulate an analytically tractable, dynamical model of malaria transmission to explore the possibility that clinical immunity can lead to bistable malaria dynamics. We summarize what is known and unknown about the parameters underlying this simple model, and solve the model to find a criterion that determines under which conditions we expect bistability to occur.

Results

We show that bistability can only occur when clinically immune individuals are more “effective" at transmitting malaria than naive individuals are. We show how this “effectiveness" includes susceptibility, ability to transmit, and duration of infectiousness. We also show that the amount of extra effectiveness necessary depends on the ratio between the duration of infectiousness and the time scale at which immunity is lost. Thus, if the duration of immunity is long, even a small amount of extra transmission effectiveness by clinically immune individuals could lead to bistability.

Conclusions

We demonstrate a simple, plausible mechanism by which clinical immunity may be causing bistability in human malaria transmission. We suggest that simple summary parameters – in particular, the relative transmission effectiveness of clinically immune individuals and the time scale at which clinical immunity is lost – are key to determining where and whether

bistability is happening. We hope these findings will guide future efforts to measure transmission parameters and to guide malaria control efforts.

4.2 Background

Despite extensive efforts to eradicate it, malaria caused by *Plasmodium falciparum* remains a significant problem resulting in millions of cases and 660,000 deaths in 2010 [106]. A characteristic of *falciparum* malaria disease that complicates control efforts is clinical immunity – an immune response that develops with exposure to parasites and provides protection against the clinical symptoms of malaria, despite the presence of parasites [125]. Although clinical immunity protects individuals against disease, its effects at the population level are complex.

Malaria is highly variable from region to region, further complicating analysis. Geographic variation in average disease burden (endemicity) leads to variation in acquired immunity [42]. Malaria endemicity ranges from “holoendemic" (defined as having a parasite ratio (PR, the percentage of subjects with parasites found in the blood) consistently greater than 75% of infants [90]) through “hyperendemic" and “mesoendemic" to “hypoendemic", defined as having a PR of less than 10% of children age 2–9 [90]. This results in variation in the acquisition of clinical immunity. This variation in endemicity and clinical immunity complicates malaria epidemiology and control.

Clinical immunity to malaria develops after exposure to parasites and varies as endemicity varies [47, 49]. In holoendemic regions, exposure to parasitemia is high enough that clinical immunity develops rapidly, and most adults and older children are clinically immune, whereas in hypoendemic regions, most people are not re-infected often enough to develop clinical immunity [49]. Even after it develops, clinical immunity can be lost in

3-5 years without re-exposure [30, 49, 47, 125, 42]. When individuals first develop clinical immunity, they are only immune to severe symptoms. If re-exposure continues, however, clinical immunity can result in asymptomatic or nearly asymptomatic disease. Full clinical immunity develops slowly and tends to correlate with the onset of puberty [75, 49].

An important aspect of clinical immunity is the possibility that clinically immune individuals are particularly effective at transmitting malaria over the duration of their infections. This phenomenon could arise if clinically immune individuals are more infectious to mosquitoes per unit time, or if they stay infectious for longer (perhaps because they are less likely to seek medical treatment), or both. If clinically immune individuals have a higher reproductive rate, this has potential implications at the population level – in some cases, malaria may be spread more effectively in areas where it is already present, all else being equal.

As transmission of malaria decreases, the proportion of the population protected by clinical immunity decreases as well, since clinical immunity is lost. As a result, decreases in transmission can, under some circumstances, lead to an *increase* in morbidity and mortality, because fewer people are protected against the symptoms of malaria. [134, 103, 102].

Aguas et al. [2] have shown that under certain circumstances when clinically immune individuals are more infectious over the duration of their infection, than naive cases, malaria can persist, if established, in areas where it would not be able to invade. In other words, for some sets of parameters, both an endemic equilibrium and a disease-free equilibrium are stable – a phenomenon known as bistability. Bistability would have important implications for malaria control: in particular, it would imply that there are some areas where, if malaria could be eliminated until clinical immunity wanes, it would not be able to re-invade. Here we use a model of malaria transmission to explore under which conditions we would expect bistability to occur, indicating possible opportunities for malaria elimination.

Malaria elimination has been surprisingly effective in many countries: 75 of the 79 countries that successfully eliminated malaria between 1945 and 2010 remain malaria free, even though many have not sustained control efforts [139]. A recent paper by Chiyaka et al [21] presents six hypotheses for this phenomenon, and argues that $\mathcal{R}_0$ may be reduced either by external factors, like demographic and hydrological changes, or by factors driven by malaria elimination itself, for example economic development catalyzed by reduced disease burden, or bistability due to treatment seeking. They argue that, to the extent that malaria elimination reduces $\mathcal{R}_0$, incentives to aggressively pursue control are increased, since on-going active control efforts will not be required once malaria is eliminated.

In this paper, we first review what is known about infectiousness and susceptibility to infection of clinically immune individuals. We then build a simple transmission model designed to elucidate what factors make bistability likely, and what measurements could shed light on when and whether bistability is likely to be an important phenomenon in malaria dynamics and control. We derive a simple mathematical criterion for how “effective" transmission by clinically immune individuals must be for bistabilty to occur.

4.2.1 Effects of clinical immunity on disease transmission

The overall infectiousness of an infected individual is the product of duration of infection, and mean infectiousness. Below, we review what is known about the effects of clinical immunity on these components.

The duration of a malaria infection is highly variable, and treatment-seeking behavior is an important determinant. In a review of population-level studies done on malaria treatment-seeking behavior, McCombie [89] found that treatment rates were correlated with severity of symptoms, and that in Africa, 64–95% of individuals who sought treatment re-

ceived at least one form of treatment; with the majority of studies reviewed reporting over 90% treatment rate.

It is well known that many clinically immune infections are not even recognized by the individual as malaria. Individuals in hyper- and holo-endemic areas who do not think they have malaria, have been found to test positive at high rates, for example in Ghana [89, 107], Senegal [114], and Kenya [14]. Thus, it seems reasonable to suppose that most clinically immune infections are untreated, and last longer than treated clinical infections because of treatment-seeking behavior. Various studies have been done to estimate the duration of untreated malaria infection. Earle et al. [39] observed the duration of infection in children age 5-15 years old and found all of them had cleared the infection within a year. However, most of what is known about duration of infection comes from malariotherapy data. These studies infected naive adults infected with neurosyphilis with *P. falciparum* strains with low clinical virulence and found the mean duration of infection to be 200 days[123]. A recent study in a highly endemic region found a similar mean duration of infection to that of the malariotherapy data, however, they found a larger variance in duration of infection with many more infections with shorter duration then found in the malariotherapy data [15]. And in an extreme case, an infection was found 8 years after last known exposure to parasites [138]. However, it's not clear how the duration of untreated clinically immune infections compares to untreated symptomatic cases. Bruce et al. [17] found that "episodes" of parasitemia lasted longer in children than in adults and suggest that this may be due to clinical immunity[17]. Unfortunately, it is not straightforward to relate their measured episodes to infection clearance (partly because infected individuals may be "super-infected" by other strains).

While clinically immune cases are frequently asymptomatic or of low clinical virulence, data from malariotherapy studies suggest naive cases may also have a wide range of clinical

virulence ranging from high virulence to asymptomatic [94]. Other studies, suggest that asymptomatic malaria is not limited to areas of high transmission where exposure-related immunity is expected to develop [12, 4, 76]. Thus, not all naive cases may be terminated with treatment.

Another key component to the population-level effects of clinical immunity is the infectiousness per transmission event of infected individuals. Although malaria transmission is much studied, it remains unclear how parasitemia, gametocytemia, and other factors interact to affect malaria transmission. Gametocyte quantity alone is not sufficient to ensure successful transmission; mosquito uptake of gametocytes depends on a wide variety of factors, including transmission-blocking immunity (TBI) [124, 100, 31] and cytokine tumor necrosis factor (TNF) [99, 41].

Transmission-blocking immunity (TBI) is a human immune reaction to sexual stages of malaria. TBI develops with exposure to gametocytes and, through a variety of mechanisms, reduces successful transmission of new infections. TBI increases with gametocyte density; consequently, TBI tends to be negatively correlated with clinical immunity [31], but the importance of TBI to population-level transmission is not clear. In one study, transmission-blocking immunity was found to reduce transmission by up to 90%, with higher immunity in the younger age groups [31]. Two other studies, which did not include the youngest age group, failed to find correlations between age and TBI [97, 13]; the latter of these found that only 15% of urban and 29% of rural gametocyte carriers had reduced transmission. A model of human infectiousness to mosquitoes found that patterns of EIR across Africa and Papua New Guinea could be explained without invoking TBI [67].

Cytokine TNF is another factor that affects gametocyte success. It is present in the blood serum taken during the crisis of a malaria infection [99, 41]. Cytokine TNF is responsible for the loss of infectiousness during peak parasitemia by killing the gametocytes.

Gametocytes present during malaria crisis were found dead before entering the mosquito; as well, gametocytes from crisis serum failed to infect mosquitoes even when washed and re-suspended in normal serum [99].

Although there is immunity against gametocytes at peak parasitemia in non-immune individuals, clinically immune infections often have lower gametocytemia as a result of having anti-parasite immunity, conferring protection against high-density parasitemia [30]. There is also evidence that clinically immune individuals are less infectious per bite but because clinically immune individuals are less likely to seek treatment, they are consistently infectious at low levels for long periods of time and therefore result in producing a large number of new infections over the course of a single clinically immune infectious period [120, 111].

As we will see below, susceptibility to infection in clinically immune individuals is also important to the population-level dynamics of malaria. Although a great deal is known about susceptibility to clinical illness, parasitemia or gametocytemia [91, 32], much less is known about susceptibility to new infection. Individual susceptibility to new infections is complex, and known to be influenced by genotype, parasite virulence, and specific immunity [91]. Though there is evidence to believe that clinically immune individuals are about as susceptible to disease as non-immune individuals [68]

4.2.2 Population-level effects

We investigate the factors underlying bistability with a simple transmission model that accounts for clinical immunity (see Methods). We assume that individuals infected when they are naive have a probability of becoming clinically immune when they recover from infection, and that clinically immune susceptible individuals lose immunity at some rate if

not infected again, meaning that clinical immunity will be maintained when the force of infection is high, and will often wane if the force of infection is low.

To explore the effects that clinically immune individuals have on the population-level disease dynamics, we compare the life-cycle transmission effectiveness of naive and clinically immune individuals, using subgroup reproductive numbers. These are defined as the average number of secondary infections from a single infectious individual in an otherwise totally susceptible population. We define the reproductive number for naive cases, $\mathcal{R}_{NN}$, as the average number of secondary infections generated by a single naively infectious individual in an otherwise totally naively susceptible population. We define the reproductive number for clinically immune cases, $\mathcal{R}_{CC}$, as the average number of secondary infections given by a single clinically immune infectious individual in an otherwise totally clinically immune population.

Because we assume that all individuals are naive in the absence of infection, the basic reproductive number of our system $\mathcal{R}_0 = \mathcal{R}_{NN}$. We stress that this is the basic reproductive number, in the presence of baseline control efforts – in particular, we assume that treatment is always available to those who seek it. This $\mathcal{R}_0$ will typically differ from the $\mathcal{R}_0$ that would be calculated in the absence of control [21].

The reproductive numbers determine malaria disease dynamics. When $\mathcal{R}_{NN} > 1$ the disease will always persist. When $\mathcal{R}_{NN} \leq 1$ the disease cannot invade. However, there is evidence that under certain circumstances when $\mathcal{R}_{CC} > 1 > \mathcal{R}_{NN}$, clinically immune individuals can act as a reservoir and allow malaria to remain endemic, even though $\mathcal{R}_{NN}$ drops below one. In this case, both the disease-free equilibrium and an endemic equilibrium are stable, this is an example of “bistability".

Bistability is typically associated with “backwards bifurcations". In general, as a dis-

ease invades, it reduces its reproductive number $\mathcal{R}$, primarily by reducing the number of susceptibles in the population. In such "forward bifurcations", we expect the disease to go extinct from any starting conditions when $\mathcal{R}_0 \leq 1$, and to reach a small equilibrium, when $\mathcal{R}_0$ is just above 1 [34]. When a disease *increases* its reproductive number as it invades, backwards bifurcations occur. In a backwards bifurcation, the disease invades to a non-zero level even when $\mathcal{R}_0 = 1$, and will be able to persist above a certain threshold when $\mathcal{R}_0$ is just below 1 [34].

4.3 Methods

To explore the dynamics of malaria and determine the conditions in which bistability can occur, we evaluated the following simple transmission model (Fig. 4.1):

$$\frac{dS_N}{dt} = -\Lambda S_N + \alpha S_C - \mu S_N + \mu T + \gamma_{NN} I_N \tag{4.1a}$$

$$\frac{dI_N}{dt} = \Lambda S_N - (\gamma_{NN} + \gamma_{NC}) I_N - \mu I_N \tag{4.1b}$$

$$\frac{dS_C}{dt} = -\sigma\Lambda S_C - \alpha S_C + \gamma_{NC} I_N + \gamma_C I_C - \mu S_C \tag{4.1c}$$

$$\frac{dI_C}{dt} = \sigma\Lambda S_C - \gamma_C I_C - \mu I_C \tag{4.1d}$$

S_N represents naive susceptible individuals, individuals who have never been infected with malaria, those who have been infected but have not developed clinical immunity, or who have lost all immunity. When infected with malaria, they move to the clinically infected class (I_N). Recovered individuals become immediately susceptible again, but with immunity to clinical symptoms (S_C). When non-naive susceptibles get infected, they ac-

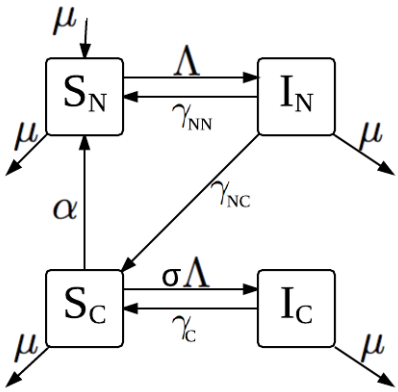

Figure 4.1: **Compartmental diagram of our transmission model** Each compartment in the diagram represents a different epidemiological class. Individuals begin in the susceptible naive class (S_N), return there after losing clinical immunity, at a rate α, and are born into this class, at a rate μ. Individuals in S_N who get infected move to the infected naive class (I_N), at a rate Λ. From I_N, individuals recover from illness to either the susceptible naive class (S_N), at a rate γ_{NN}, if immunity was not conferred, or to the susceptible clinically immune class (S_C), at a rate γ_{NC} if clinical immunity developed. Individuals who are susceptible clinically immune can either lose immunity at a rate α and return to the susceptible naive class, or they can get infected, at a rate $\sigma\Lambda$, and become infected clinically immune (I_C). Infected clinically immune individuals recover to the susceptible clinically immune class, at a rate γ_C. Individuals can die from any of the epidemiological classes and do so at a rate μ not proportional to the level of malaria in the population. Individuals are born and die at the same rate, thus keeping the population size closed.

quire clinically immune infections (I_C). Each class represents a portion of the population. τ_N and τ_C are the transmission rates of naive and clinically immune cases, respectively. γ_{NN} is the recovery rate of naive individuals, γ_{NC} is the rate of acquiring clinically immunity, and γ_C is the recovery rate for clinically immune individuals. α is the rate at which clinical immunity is lost σ is the relative susceptibility to new infection of clinically immune individuals. $\Lambda = \frac{\tau_N I_N + \tau_C I_C}{T}$ is the force of infection. Both types of susceptibles (naive or clinically immune) can be infected by either type of infectious individual (naive or clinically immune). The total population size is $T = S_N + I_N + S_C + I_C$. For this model, $\mathcal{R}_0 = \mathcal{R}_{NN} = \frac{\tau_N}{\gamma_{NN}+\gamma_{NC}+\mu}$, and $\mathcal{R}_{CC} = \frac{\sigma\tau_C}{\gamma_C+\mu}$. We define ρ to be the ratio of

the clinically immune reproductive number to the naive reproductive number ($\mathcal{R}_{CC}/\mathcal{R}_{NN}$). And $\pi = \frac{\gamma_{NC}}{\gamma_{NN}+\gamma_{NC}}$ is the proportion of naive infections that recover to become clinically immune.

We used the statistical package R [117] to simulate our model. We held the average durations of infectiousness for naive and immune individuals ($1/\gamma_{NN}$ and $1/\gamma_C$) constant at 50 and 200 days respectively. We chose $\pi = \frac{\gamma_{NC}}{\gamma_{NC}+\gamma_{NN}}$ to be 0.5, assuming an equal chance of getting clinical immunity and remaining non-immune after each naive infection. Transmission coefficients τ_N and τ_C were calculated from $\mathcal{R}_{NN}$ and $\mathcal{R}_{CN}$ which varied as described in the Results section. We chose duration of immunity $1/\alpha$ to be 1282 days (about 3.5 years), and lifespan $1/\mu$ to be 25,550 days (about 70 years). The relative susceptibility of clinically immune individuals was chosen to be $\sigma = 0.7$ since clinically immune individuals are about as susceptible as naive cases; we also tested other values.

R code and Maxima code to replicate all of our results will be made available upon publication.

In building a simple transmission model, we have lumped a variety of biological mechanisms into the parameters. For example, transmission parameters τ_C and τ_N include transmission blocking immunity and the reduction of parasites in clinically immune individuals. The duration of infection parameters γ_{NN}, γ_{NC}, and γ_C take into account treatment seeking behavior (naive individuals are likely to seek treatment quickly whereas clinically immune individuals are less likely to seek treatment or they wait longer to seek treatment).

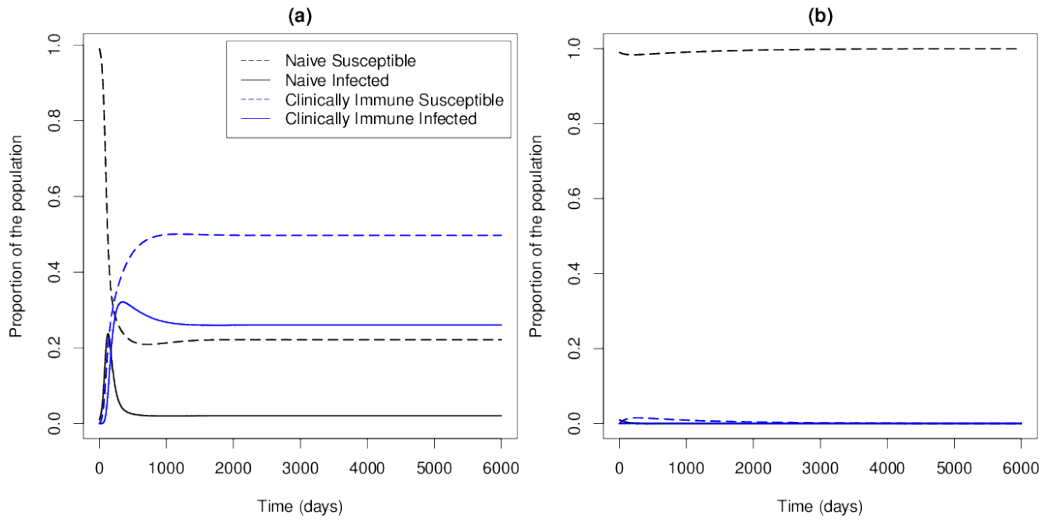

(a) $\mathcal{R}_{NN} > 1 > \mathcal{R}_{CC}$ (b) $1 > \mathcal{R}_{NN} > \mathcal{R}_{CC}$

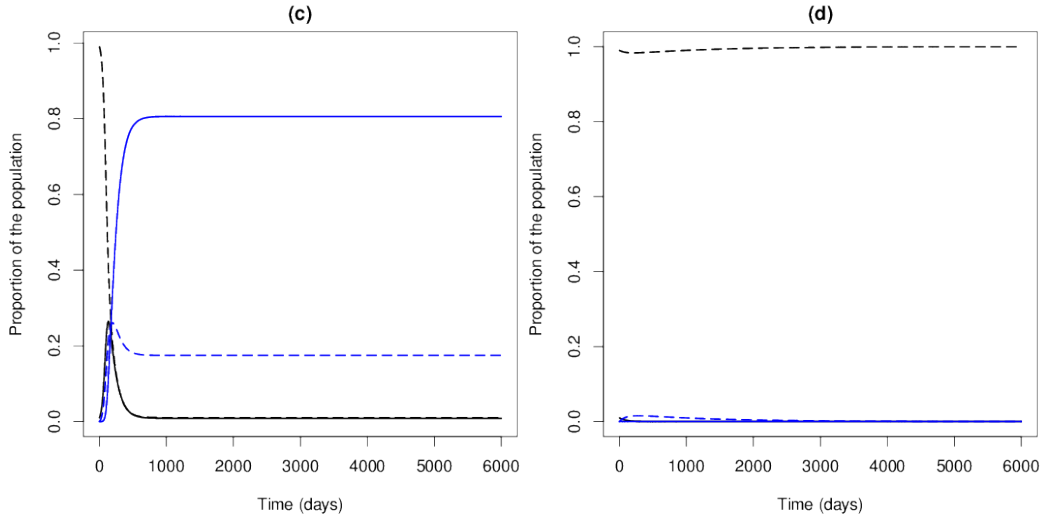

(c) $\mathcal{R}_{CC} > \mathcal{R}_{NN} > 1$ (d) $\mathcal{R}_{CC} > 1 > \mathcal{R}_{NN}$

Figure 4.2: **Simulation of Malaria transmission in a naive population.** We simulated malaria transmission in a population with 95% naive susceptible and 5% naive infectious individuals ($S_N = 0.95, I_N = 0.05, S_C = 0, I_C = 0, N = 1$, $\alpha = 0.001$, $\gamma_{NN} = 0.02$, $\gamma_{NC} = 0.02$, $\gamma_C = 0.005$, $\mu = 0.000039$, and $\sigma = 0.7$) under two assumptions of ρ. Panels a and b show $\rho = 0.5$ and panels c and d show $\rho = 3.5$ (a) $\mathcal{R}_{NN} = 2 > 1 > \mathcal{R}_{CC} = 1$. (b) $1 > \mathcal{R}_{NN} = 0.75 > \mathcal{R}_{CC} > 0.375$. (c) $\mathcal{R}_{CC} = 7 > \mathcal{R}_{NN} = 2 > 1$. (d) $\mathcal{R}_{CC} = 2.625 > 1 > \mathcal{R}_{NN} = 0.75$.

4.4 Results

We simulated our malaria transmission model under two scenarios of infectiousness: overall infectiousness of clinically immune cases was either low ($\rho \equiv \mathcal{R}_{CC}/\mathcal{R}_{NN} = 0.8$, panels 4.2a and 4.2b) or high ($\rho = 4$, panels 4.2c and 4.2d). For each scenario, we simulated two different values of $\mathcal{R}_0 \equiv \mathcal{R}_{NN}$. Disease-invasion results are shown in Fig. 4.2. When we start near the disease-free equilibrium, the qualitative behavior is determined by $\mathcal{R}_0$: when $\mathcal{R}_0 > 1$ (panels 4.2a and 4.2c), the disease invades and reaches an endemic equilibrium; when $\mathcal{R}_0 < 1$, (panels 4.2b and 4.2d), the disease does not invade.

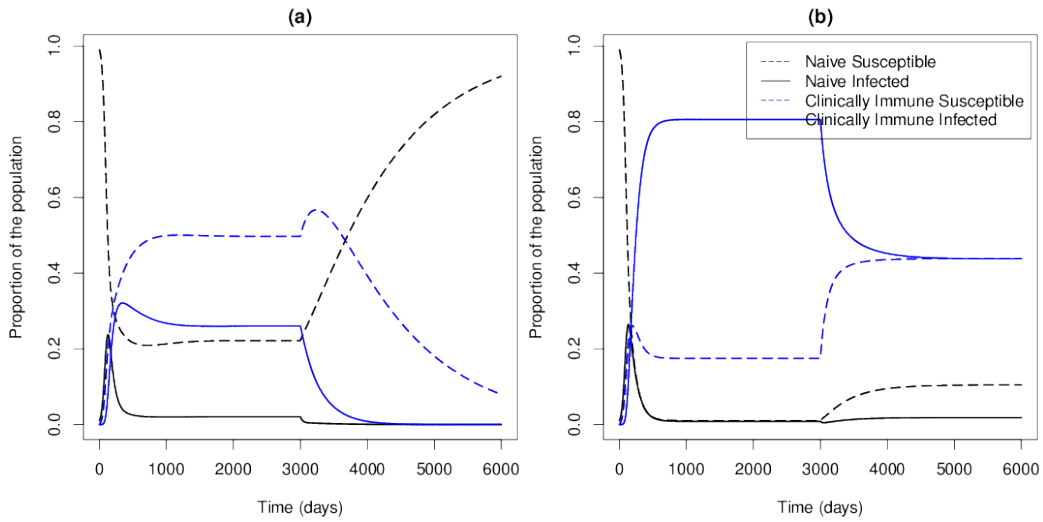

(a) $\mathcal{R}_{NN} > \mathcal{R}_{CC}$ (b) $\mathcal{R}_{CC} > \mathcal{R}_{NN}$

Figure 4.3: **Malaria transmission with changing parameters.** Here we simulated malaria using the parameters from the first column of Fig. 4.2 until they reached equilibrium at which point we changed the parameters to those in the second column and allowed malaria to reach equilibrium again. (a) We used the parameters from Fig. 4.2a from 0 to 3000 and the parameters from Fig. 4.2b from 3000 to 6000. (b) We used the parameters from Fig. 4.2c from 0 to 3000 and from Fig. 4.2d from 3000 to 6000.

In the case where underlying parameters can change over time, however, there are striking differences between the scenarios with low and high relative transmission from immune individuals. Fig. 4.3 shows what would happen in a population with endemic malaria if

control efforts moved transmission from the first column of Fig. 4.2 to those shown in the second column. Panel 4.3a behaves as we would expect: when we change the parameters at day 3000, the system moves to the disease-free equilibrium. Panel 4.3b, however, exhibits bistability. Although the parameters in the latter part of the simulation are consistent with disease extinction, the disease does not go extinct from the equilibrium reached under high transmission, but instead finds a lower endemic equilibrium. Whether or not malaria will remain endemic or die out under parameters consistent with disease extinction is dependent both on $\mathcal{R}_0$ and on initial conditions.

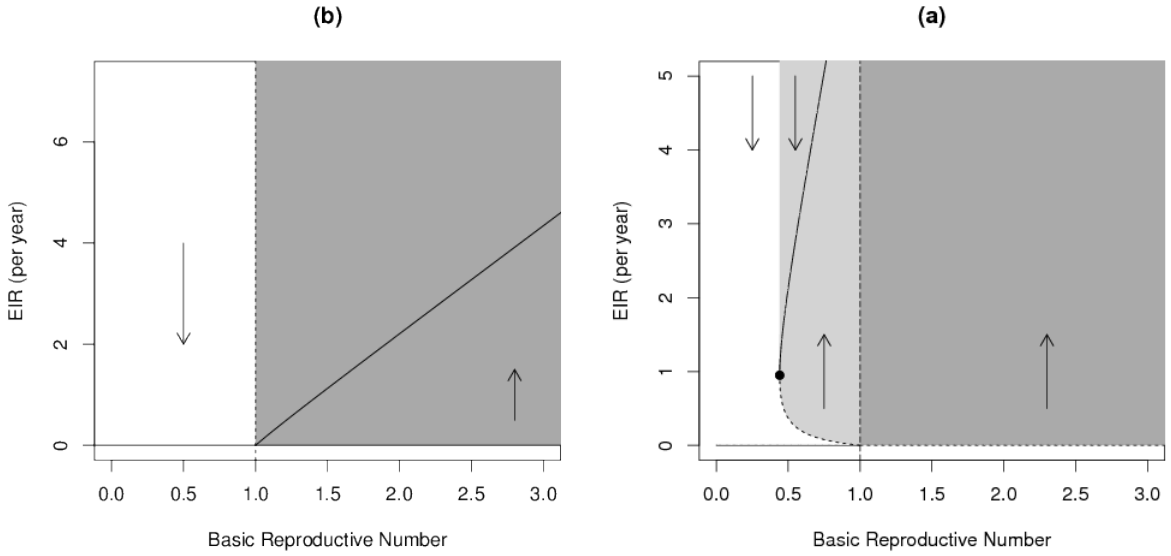

(a) Forward Bifurcation

(b) Backwards Bifurcation

Figure 4.4: **Bifurcation diagram for malaria.** The dashed line shows $\mathcal{R}_0 = 1$ and the arrows show the behavior of the system: in the white area, to the left of the manifold, the disease will die out while to the right of the manifold, in the shaded area, the disease will persist. The dark-shaded region represents the area in which malaria can invade and persist and the light-shaded area in which it persists, even though it would not invade. In these figures, all parameters are held constant except τ_N and τ_C. (a) A forward bifurcation occurs at $\mathcal{R}_0 = 1$. $\rho = 0.8$. (b) A backwards bifurcation occurs at $\mathcal{R}_0 = 1$. $\rho = 4$.

Fig. 4.4 gives a broader perspective on the two scenarios, using "bifurcation diagrams" showing how equilibrium incidence changes as $\mathcal{R}_0$ increases, while holding the relative

infectiousness of clinically immune individuals ($\rho \equiv \mathcal{R}_{CC}/\mathcal{R}_{NN}$) constant. Panel 4.4a illustrates the scenario where clinically immune individuals are relatively less effective at transmitting disease ($\rho < 1$). Here we see the simple, common, relationship between $\mathcal{R}_0$ and equilibrium incidence. As $\mathcal{R}_0$ increases past 1, the system moves smoothly from having a globally stable equilibrium at 0, to having a globally stable endemic equilibrium.

Panel 4.4b shows shows the scenario where clinically immune individuals are relatively more effective at transmitting disease ($\rho > 1$). In this case, we see a more complicated pattern, where both $\mathcal{R}_0$ and initial prevalence affect the final outcome. In particular, if we increase $\mathcal{R}_0$ smoothly past 1 in a population where the disease is absent, the equilibrium jumps abruptly; if the disease invades, and $\mathcal{R}_0$ is decreased back below 1 the disease does not necessarily go extinct. Similarly, if $\mathcal{R}_{\text{crit}} < \mathcal{R}_0 < 1$ (the light gray region of the plot), a temporary intervention that sharply reduces disease prevalence could succeed in eliminating the disease even without a long-term reduction in $\mathcal{R}_0$.

To be specific, we don't expect the disease to go extinct once established unless $\mathcal{R}_0$ is reduced beneath the minimum value for which the endemic equilibrium exists. We call this value $\mathcal{R}_{\text{crit}}$ and the force of infection Λ that corresponds to it Λ_{crit}. On the forward bifurcation diagram (Fig. 4.4a) $\mathcal{R}_{\text{crit}} = 1$ and on the backwards bifurcation diagram (Fig. 4.4b) $\mathcal{R}_{\text{crit}}$ is precisely the point where the stability of the endemic equilibrium (in a region of bistability) changes from unstable to stable (the black dot on Fig. 4.4b).

In text 4.A.1, we show that a backwards bifurcation will occur when the ratio $\rho = \mathcal{R}_{CC}/\mathcal{R}_{NN} > \rho^*$, where:

$$\rho^* = 1 + \frac{D}{\pi L} \tag{4.2}$$

Here $L = 1/(\alpha + \mu)$ is the duration of immunity, $D = 1/(\gamma_{NC} + \gamma_{NN})$ is the duration of naive infection, and $\pi = \frac{\gamma_{NC}}{\gamma_{NC}+\gamma_{NN}}$ is the proportion of people who become clinically

immune after a naive infection. This criterion determines for what parameters bistability can occur when $\mathcal{R}_0 < 1$. The value of ρ^* is always strictly greater than 1, meaning that bistability only occurs when $\mathcal{R}_{CC}$ exceeds $\mathcal{R}_{NN}$ by a sufficient amount. The amount of excess necessary is determined by how quickly immunity is lost (through death or waning) compared to the duration of infectiousness of the disease: when immunity lasts longer, bistability is more likely.

When $\rho > \rho*$, a backwards bifurcation occurs, resulting in a region of bistability where there exists a stable disease-free equilibrium and a stable endemic equilibrium for the same parameter values. Fig. 4.4b illustrates the backwards bifurcation and the region of bistability (light gray shaded region). Within the region of bistability, if malaria were to be eliminated, it would not be able to re-invade unless $\mathcal{R}_0$ were increased from below one back above one, making malaria elimination from these regions more sustainable. In order to eliminate malaria from a region of bistability, either the force of infection must be reduced below the unstable endemic equilibrium (dashed curve), or the reproductive number must be reduced below the critical value ($\mathcal{R}_{crit}$), or these in combination. In Fig. 4.4b, this is equivalent to leaving the light gray shaded region (without exceeding $\mathcal{R}_0 = 1$, the dashed line).

We explored how different model parameters affected the bifurcation (text 4.A.2), by varying each parameter individually. To vary $\mathcal{R}_0$, we changed τ_N and τ_C, while keeping their ratio constant. To vary ρ or to adjust ρ when necessary (e.g., when changing σ), we varied the ratio $\tau_N : \tau_C$.

We show that the region of bistability depends strongly on the ratio ρ. When ρ is large, bistability can occur even for large incidence rates, as shown in Fig. A1. Consequently, if malaria were to be eliminated then re-introduced, it would jump to being endemic at a higher level in the population than when ρ is small. When ρ is large, Λ_{crit} (the value of

Λ that corresponds to $\mathcal{R}_{crit}$) is also large. A large value of Λ_{crit} means that the force of infection needs to be reduced by less to move below the unstable endemic equilibrium and be eliminated.

We also found that even when ρ is held constant, the individual components of ρ (σ, π and γ_C) still affect the bifurcation, as shown in text 4.A.2. When we increased σ (text 4.A.2) while holding ρ constant, the region of bistability decreased. When σ is small (text 4.A.2) the proportion of infections that occur in clinically immune people increases, thus increasing the accumulation of clinical immunity and magnifying its effect on transmission.

We also explored the dynamics when varying the recovery rates (text 4.A.2), while holding ρ constant. When individuals recover quickly, the area of bistability is large, since there are more susceptible clinically immune individuals in the population. When γ_C is large, Λ_{crit} is also large; this means that the force of infection needs to be reduced by less to drop below the unstable endemic equilibrium for malaria to be eliminated. Also, when γ_C is large, the value of Λ when $\mathcal{R}_0 = 1$ is larger than when individuals recover slowly. So if malaria is eliminated then re-invades, it would jump to a high endemic level in the population. Resurgence of malaria has been found, in 75 resurgent events to jump from either eliminated or from a low-level in the population to a high endemic level [22]. We also change the proportion of naive infections, π. When π is large, so is $\mathcal{R}_{crit}$ and Λ_{crit} and as π is decreased, so is $\mathcal{R}_{crit}$ and Λ_{crit}, making the region of bistability larger.

4.5 Discussion

The question of whether there are places where malaria is endemic, but where it could remain stably eliminated *under current transmission and treatment conditions* (ie., places where malaria is bistable) is important to interpreting malaria data and planning control

measures. It has been suggested that treatment-seeking behavior can lead to bistability in the dynamics of malaria infections of humans [2].

In areas where malaria is bistable, an aggressive program that held malaria infection at low levels until clinical immunity wanes could result in the disease remaining absent even after the program is terminated. Malaria would not re-invade in this case because treatment seeking by non-immune infected individuals would lead to shorter duration of infectiousness and less overall transmission. This is a potentially risky strategy, however, because if malaria does re-invade such an area, the fact that clinical immunity has waned could lead to increased morbidity [134, 103, 102]. Mass drug administration (MDA) is a possible example of such an aggressive approach. Although MDA has so far proved unsuccessful in permanently interrupting malaria transmission, it is successful at reducing parasitemia and does temporarily reduce transmission [140]. Further investigation of factors underlying bistability could improve understanding of when and where MDA would be likely to lead to long-term elimination.

We analyzed a simple model, and found a simple criterion that determines whether bistability can occur. In particular, we found that the key quantity is the life-cycle “transmission effectiveness" of clinically immune individuals, relative to non-immune individuals. We encapsulate this relative infectiousness in a ratio, which we call ρ and show that bistability can occur when ρ exceeds $1 + D/(\pi L)$, where D is the duration of naive infection, π is the proportion of naive cases that recover to become clinically immune, and L is the length of immunity. We also show that, in addition to duration of infection and ability to transmit the disease, the relative *susceptibility* of clinically immune individuals to new infections is a key component of this ratio. Although the relative susceptibility is a key component to understanding bistability in malaria, little is known about the relative susceptibility of clinically immune individuals.

Chiyaka et al [21] discuss the importance of reducing the reproductive number under control efforts ($\mathcal{R}_C$) below one to eliminate malaria and to gage the size of an outbreak arising from an imported malaria case. They also point out that once malaria is eliminated, control efforts must be sustained to keep $\mathcal{R}_C < 1$ unless elimination of malaria permanently changed $\mathcal{R}_0$. Bistability of malaria, as we explore here, is one of the possible reasons why eliminating malaria could permanently alter $\mathcal{R}_0$. As eliminating malaria from a region of bistability will remain stably eliminated, even in the presence of imported malaria cases. Chiyaka et al [21] suggest that while evaluating control programs, countries should assess the stability of elimination. Determining if a country or region is experiencing bistability using our criterion, $\rho*$ is a cost-efficient, fast method to begin to assess the stability of malaria control of specific areas, where elimination can be maintained with little extra long-term effort.

The details of clinical immunity to malaria are more complex than those in our simple model: in particular, clinical immunity may continue to develop even in clinically immune individuals. Nonetheless, we expect our qualitative results to apply to more realistic situations. We expect the possibility of bistability when the relative life-cycle transmission effectiveness of clinically immune individuals is high. Thus, measuring the components of transmission effectiveness, both in clinically immune and non-immune individuals, is important for evaluating and planning malaria control efforts. Although certain aspects of malaria are well studied, it is surprisingly difficult to find information bearing directly on the components of transmission effectiveness, particularly in clinically immune individuals. Continued investigation of how these components determine transmission effectiveness will be important in understanding the population-level patterns of the spread and persistence of malaria.

Although duration of symptomatic infection is well studied [39, 89], little is known

about duration of asymptomatic infection [17]. This is a complicated question because malaria infections can be long and variable; failure to detect parasites may not mean an infectious event is over; and resurgence of parasites may be due to a new infectious event.

Transmission of infection to mosquitoes is another aspect of malaria biology that is not well understood. Although they are well studied individually, it is not clear how the components of transmission come together to affect the infectiousness per transmission event. These components include: gametocytemia [100, 124]; TBI [13, 31, 97], which increases with gametocytemia, and wanes with age and clinical immunity; and other human and mosquito-specific factors [32]. More information on how these components interact to affect transmission would help to unravel how clinical immunity affects population-level transmission.

As we've shown, susceptibility of clinically immune individuals to malaria is an important component of the ratio of life-cycle transmission effectiveness. Susceptibility to new infection is known to be complex [91] but not well understood; in the literature "susceptibility" is frequently used to refer to susceptibility to clinical disease [91, 32].

Our model neglects age structure, and oversimplifies the process of clinical immunity. In particular, the population is divided simply into those who are and are not clinically immune. Other omissions include seasonality, biting heterogeneity, and in fact, mosquitoes. For these reasons, the model is not expected to provide quantitatively accurate estimates of malaria dynamics.

The advantage of this simplistic approach, in our opinion, is that the model sheds light on the possible mechanisms and key quantities underlying bistability in malaria dynamics. In particular, we expect the importance of the quantity ρ – the ratio of life-cycle effectiveness of transmission between immune and non-immune individuals – to be robust to

including more model details. Similarly, we expect some analogue of the time scale ratio $D/(\pi L)$ – that is, the ratio between the time scales of infection and immunity – to be important in a detailed model.

4.6 Conclusions

It has been suggested that human malaria-transmission dynamics exhibit bistability, which would have important implications for control efforts. We have shown that bistability through treatment seeking by clinically immune individuals is plausible in human malaria transmission dynamics. Using a simple model, we have demonstrated how these dynamics might play out, and determined key parameters underlying when and whether bistability might occur in real populations.

We find that the key quantities underlying whether bistability is expected to occur are: the relative “effectiveness" of clinically immune individuals, compared to naive individuals, at transmission; and the time scale at which clinical immunity is lost, compared to the time scale of infectiousness. The model also shows that relative *susceptibility* to malaria infection should be considered part of transmission effectiveness, when making this comparison. We find that bistability can occur for plausible parameters, and suggest that more research into these two ratios may shed light on malaria dynamics, and guide future control efforts.

4.7 List of abbreviations

- TBI: Transmission-blocking Immunity

- MDA: Mass drug administration
- TNF: Tumor necrosis factor

4.8 Competing interests

There are no competing interests to be disclosed.

4.9 Author Contributions

LK and JD made and analyzed the model and drafted the manuscript. All authors have read and approved the manuscript.

4.10 Acknowledgments

The authors thank Jake Szamosi, Marta Wayne, Ben Bolker, Mark Loeb and David Earn for useful comments and suggestions. We also thank David Smith for helpful discussions about framing the research project.

4.A Additional Files

4.A.1 Additional File 1 – Backwards Bifurcation

To determine if bistability can occur, we analyze our model at the bifurcation point, $\mathcal{R}_0 = 1$, to determine the size of the ratio $\rho = \frac{\mathcal{R}_{NN}}{\mathcal{R}_{CC}}$ must be in order for a backwards bifurcation to

occur [33].

To analyze our model, we can disregard $\frac{dS_N}{dt}$ because the population remains constant. So we re-write $\frac{dI_N}{dt}$, $\frac{dS_C}{dt}$, and $\frac{dI_C}{dt}$ in terms of I_N, S_C, I_C and T. We define Y to be the vector (I_N, S_C, I_C). We take the Jacobian of Y, $H(Y)$.

We then find the eigenvectors of the matrix $H(Y)$ at equilibrium (when Y=0. The eigenvectors determine whether or not a backwards bifurcation will occur at $R_0 = 1$. This is determined by the sign of the dominant eigenvectors of the Jacobian matrix [34]. The dominant right eigenvector, which gives the direction of the initial spread of the disease, is V= $[1, \frac{\gamma_{NC}}{\tau_N - \gamma_{NN} - \gamma_{NC} - + \alpha}, 0]$ and the dominant left eigenvector which gives the contribution of each infected group to the overall spread is given by $W = [1, 0, \frac{\tau_C}{\tau_N - \gamma_{NN} - \gamma_{NC} + \gamma_C}]$.

To determine the criterion ρ^*, which gives the amount $\mathcal{R}_{CC}$ needs to be larger than $\mathcal{R}_{NN}$ in order for a backward bifurcation to occur, we look at the Jacobian matrix, H perturbed just a little from 0. Dushoff [34] showed that a backward bifurcation will occur if and only if

$$\rho* = W \cdot H_{\varepsilon}(0)V > 0 \tag{4.3}$$

For our model, we calculated ρ^* to be:

$$\rho* = 1 + \frac{\alpha + \mu}{\gamma_{NC}} \tag{4.4}$$

We take $\frac{1}{\alpha+\mu}$ to be the length of immunity (L), $\frac{1}{\gamma_{NN}+\gamma_{NC}}$ to be the duration of infection

(D), and $\frac{\gamma_{NC}}{\gamma_{NN}+\gamma_{NC}}$. We find that when $\mathcal{R}_0 = 1$, bistability will occur when:

$$\rho* = 1 + \frac{D}{\pi L} \tag{4.5}$$

4.A.2 Additional File 2 –Bifurcation Diagrams

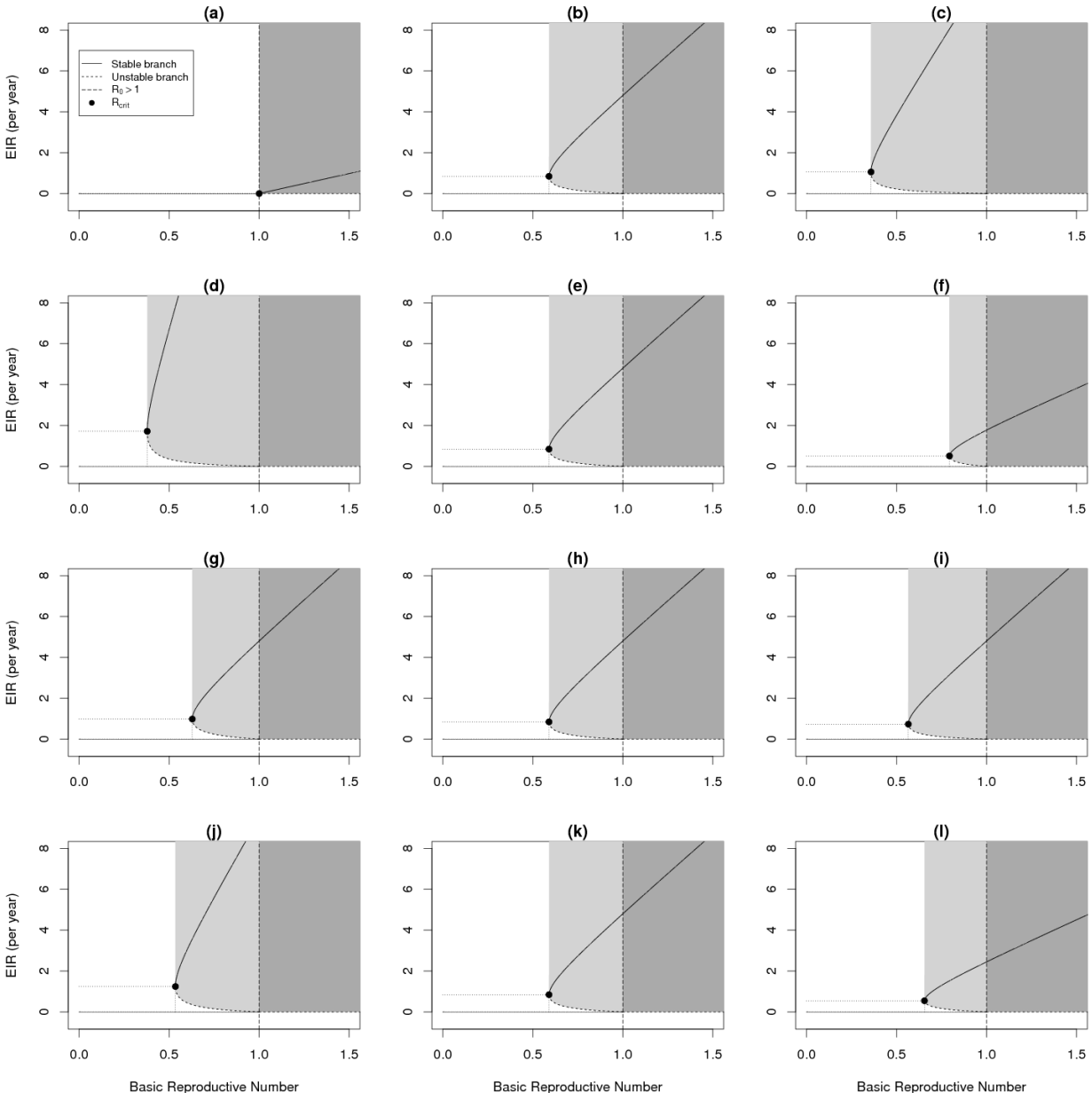

Figure A1: Bifurcation diagrams changing model parameters individually (ρ, σ, π, and γ_C) while keeping all other parameters constant at the base model values (Fig. 4.4b). The vertical dashed line shows $\mathcal{R}_0 = 1$; the solid curve represents the stable equilibrium and the dotted curve shows the unstable equilibrium; the point shows $(\mathcal{R}_{crit}, \Lambda_{crit})$; the light grey area shows the region of bistability– the area where malaria will persist, if endemic, but cannot invade; and the dark grey region shows where malaria can always invade and persist. In all of the bifurcation diagrams, $\mathcal{R}_0$ ranged from 0 to 1.5 and $\mathcal{R}_{CC}$ varied accordingly, changing only transmission rates (τ_N and τ_C). (a)-(c) vary ρ (a) The ratio $\mathcal{R}_{CC} : \mathcal{R}_{NN}$ is $1 : 2$ (b) The ratio $\mathcal{R}_{CC} : \mathcal{R}_{NN}$ is $2 : 1$ (c) The ratio $\mathcal{R}_{CC} : \mathcal{R}_{NN}$ is $4 : 1$. (d)-(f) vary σ (d) $\sigma = 0.5$, (e) $\sigma = 0.7$. (f) $\sigma = 1$. (g)-(i) vary π while keeping γ_{NC} constant (g) $\pi = 0.66$ (h) $\pi = 0.5$ (i)$\pi = 0.33$ (j)-(l) vary γ_C (j) clinically immune infections clear in 100 days (k) clinically immune infections clear in 200 days (l) clinically immune infections clear in 400 days.

Chapter 5

Modeling Clinical Immunity to Malaria in the East African Highlands

Keegan LT, Bolker BM, and Dushoff J

5.1 Introduction

Globally, 3.3 billion people are at risk of malaria infection each year [105]. The greatest burden of malaria lands on Africa, where it is estimated that 90% of all malaria deaths occur, primarily in children under the age of 5 [105]. Despite extensive efforts to eradicate it, malaria remains a significant global public health problem. One of the factors that complicates control is clinical immunity to malaria. Understanding the effects of clinical immunity on malaria transmission and control has long been of interest due to its complicated effects on malaria control.

Clinical immunity to malaria is the acquired immune response that provides protection against the clinical symptoms of malaria, despite the presence of parasites [125]. It is acquired with age and exposure, and can be lost without re-exposure [90, 47]. Because clin-

ical immunity can be lost, under certain circumstances a reduction in malaria transmission can result in an *increase* in morbidity and mortality [134, 103, 102]. Additionally, clinical immunity has been shown to be a mechanism for bistable malaria dynamics [2, 64]. That is, for some set of parameters, both an endemic equilibrium and a disease-free equilibrium are stable [35, 64, 2]. Bistability has important implications for control: if malaria could be eliminated until clinical immunity wanes, it would not be able to re-invade [2, 64]. Consequently, understanding the effects of clinical immunity on malaria transmission is critical for planning control. Keegan and Dushoff [64] identified important clinical immunity parameters that are still not well understood, including the duration of clinically immune infection and the relative susceptibility of clinically immune individuals. These parameters play a key role in determining if bistable-malaria can occur [64].

Although these are important clinical immunity parameters, relatively little is known about them. Some studies have attempted to estimate the duration of clinically immune infection [77, 17, 39], but the majority of studies rely on estimates of the duration of clinically immune infection from malariotherapy data [123].

Prior to the discovery of penicillin, malaria was a standard treatment for neurosyphilis; this type of treatment has come to be known as malariotherapy [123, 133]. Malariotherapy treatment involved infecting malaria-naive neurosyphilis patients with low-virulence strains of malaria [123]. These patients were monitored, but left untreated for up to one year [133]. They found the mean duration of infection to be 200 days [123]. In addition to malariotherapy, other studies have attempted to determine the duration of clinically immune infection [77, 17, 39, 15, 133]. Earle et al. [39] observed untreated malaria in children age 5-15 and found that they all cleared infection within a year. A more recent study in a highly endemic area found a similar mean duration of untreated infection to that of the malariotherapy data, but with a larger variance, as many infections were of shorter duration [15]. However, the

relationship between the duration of untreated naive and untreated clinically immune infection is not straightforward. Bruce et al. [17] measured "episodes" of parasitemia and showed that an episode lasted longer in children than in adults, which they suggested might be the result of clinical immunity. Additionally, using a similar model to the one used here, Laneri et al. [77] fit it to data from northwest India and found that for their model without including rainfall, the duration of clinically immune infection was 250 days, whereas when including rainfall into their model as a climate covariate, they found the duration of clinically immune infection to last 28 days.

The other key parameter that is not well understood is the relative susceptibility of clinically immune individuals to malaria. The susceptibility of naive individuals to clinical disease, parasitemia, and gametocytemia are well understood, but little is known about how susceptible clinically immune individuals are [91, 32]. There is evidence to suggest that clinically immune individuals are about as susceptible to malaria as naive individuals are [67]. However, individuals susceptibility to new infection is complex, and known to be influenced by genotype, parasite virulence, and specific immunity [91].

Here, we estimate these two key parameters, by fitting a modified version of the model in Keegan and Dushoff [64] to inpatient incidence data from the Kericho District in the East African Highlands, to better understand the role of clinical immunity in malaria transmission.

In much of sub-Saharan Africa, malaria is endemic, however, in some regions, such as the East African Highlands, conditions are less favorable and malaria transmission is considered epidemic. In epidemic areas, like the East African Highlands, malaria is imported from nearby endemic regions [127]. In areas with epidemic malaria, environmental factors such as temperature and rainfall have a large impact on malaria transmission. Variation in temperature has been shown to have a non-linear effect on malaria transmission by im-

pacting both the mosquito and the parasite [127, 24, 83, 95, 79]. The other climate factor that has a strong effect on malaria is rainfall. While rainfall is necessary for breeding sites for mosquitoes, the relationship between rainfall and malaria is more complex, partially because temperature and rainfall are inversely correlated [83].

We focus on malaria in the Kericho District, in the highland region of Kenya, near Lake Victoria, in the Great Rift Valley. Kericho is characterized by ample rainfall and fertile, well-drained soil, and hosts two tea plantations [53]. Historically, malaria in the Highland region has been largely imported. Prior to World War I, malaria did not exist. During World War I and World War II, soldiers were responsible for importing malaria. After World War II, intense, mass drug administration and indoor residual spraying campaigns successfully reduced malaria transmission [127]. Since then, malaria has largely been imported from the hyperendemic region around Lake Victoria. More recently, (1990 on Plantation 1 and as early as 1980 on Plantation 2) large, mid-year seasonal epidemics of malaria began. These explosive epidemics remained until 1999 on Plantation 1, at which point a rapid reduction of cases occurred [53, 127].

The resurgence of malaria in the highland region has received attention due to the possibility that climate change may be the underlying cause of the increase in malaria incidence (eg. [3, 104, 53]). The International Panel on Climate Change concluded that climate change would likely exacerbate malaria transmission, resulting in an extension in the distribution of malaria [53]. However, the role climate change has played in the resurgence of malaria in the East African Highlands is controversial and has been debated in the literature for over ten years [3, 104, 53, 54, 109, 52, 108, 145]. The two leading hypotheses to explain the increase in malaria incidence are climate change and drug resistance.

From 1986-1998, malaria cases on the Kericho tea plantations ballooned from 16 to 120 cases per 1,000 people. This, paired with the global temperature increase of $0.6°$C

over the last century has lead many to suspect that climate change was the driving force behind the increase in malaria transmission [53]. However, the original study [53] found no correlation between increased temperature and increased malaria in Kericho. Consequently they suggested drug resistance as the alternative hypothesis to the rapid increase in malaria cases. They postulated drug resistance as a potential cause, as chloroquine was used as a first-line malaria treatment until 1999 on Plantation 1, despite the emergence of widespread resistance. By 1999, fewer than 50% of cases were cleared by chloroquine [127, 53]. Additionally, they highlight the association between the shift from chloroquine to sulfadoxine-pyrimethamine (SP) in 1999, and a corresponding reduction in malaria incidence [53].

Using better meteorological data, more recent studies *have* found that the increase in temperature (estimated at 0.2°C and 0.3°C per decade, respectively [104, 3]) correlates with the increase in malaria transmission; suggesting a significant effect of warmer temperatures on the resurgence of malaria in the East African Highlands.

Here, we do not attempt to add to this debate. We incorporate temperature as a likely important factor in malaria transmission in Kericho, for the purpose of using this data to explore the effect clinical immunity on malaria transmission. In areas with low or intermittent transmission, like the East African Highlands, outbreaks tend to have higher morbidity and mortality due to low levels of immunity. Whereas in lowland regions with high levels of immunity, clinical immunity protects many of the adults from symptoms, concentrating morbidity and mortality largely in younger children [83].

Since there were relatively few malaria cases in Kericho prior to 1990, we expect relatively low levels of immunity during that period. However, after 1990, when epidemics become more intense, we expect transmission to be strong enough for clinical immunity to develop. Shanks et al. [127] found that around 1990, the ratio of adult (> 15 years old) to

child (< 15 years old) hospital confirmed cases drops, suggesting the development of clinical immunity in the population, making this data set potentially useful for understanding clinical immunity.

Here, we explore the model with transmission parameters that are either held constant (simple model), or vary (proportionally to each other) with the temperature (temperature model). Previous models have incorporated climate forcing functions using a variety of methods. Alonso et al. [3] incorporated temperature into their model by allowing it to affect mosquito development. Reiner et al. [119] incorporated temperature into a dengue model by using a non-parametric spline based approach. This approach is flexible and does not *a priori* assume periodicity, however, it does not allow for time-lagged effects. In a model of malaria in northwest India, Laneri et al. [77] used a spline based approach and incorporated rainfall as a linear function with an *a priori* threshold, below which no transmission can occur, above which, rainfall linearly increases transmission. Here we incorporate temperature as an exponential function with time lagged effects. The benefit of this approach is simplicity. It requires few parameters to be estimated but does not include seasonal effects independent of temperature.

In areas like Kericho, on the fringe of malaria transmission, temperature is an important factor for malaria transmission. Variation in temperature has been shown to have a non-linear effect on malaria transmission, impacting both the mosquito and the parasite [24, 79, 127]. Below 16°C, it is too cold for malaria transmission to occur; between 16°C and 22°C malaria transmission is unstable; and above 22°C is generally considered to be suitable for *stable* malaria transmission, as 15% of adult mosquitoes survive the 3 weeks sporogony takes at 22°C. It is possible for mosquitoes to escape the extreme cold temperatures by resting in more favorable micro-climates such as within occupied houses, where temperatures can be 3 - 5°C warmer than outdoors [127].

5.2 Methods

These data are a monthly time series of malaria cases from hospital records on tea Plantation 1 in the Kericho district of the Kenyan Highlands from 1970-2002 (Fig. 5.1a). We only consider data from 1970-1999 – we don't consider data after the hospital changed its first-line malaria treatment from Chloroquine to SP [53]. We use the temperature time series from Alonso et al. [3], which was generated by combining records from two meteorological stations adjacent to the tea plantation (Fig. 5.1b, see the appendix 5.A.1 for more details). The population size is generally considered to be fixed and estimates in the literature range from 50,000 to 100,000 [3, 127, 128] which includes both workers and their 3 to 4 dependents [127].

We fit our model (Fig. 5.2), using both a constant force of infection and a temperature-dependent force of infection (5.A.3). Unlike Alonso et al. [3], we model mosquitoes implicitly for ease of fitting. We thus allow temperature to affect the force of infection directly, rather than via mosquitoes. We subdivide the population into the following distinct classes: S_N, naive, susceptible to infection, these are individuals who have either never been infected with malaria, have been infected but have not developed clinical immunity, or who have lost all immunity; I_N, infected (infectious) with clinical malaria; S_C, susceptible with immunity to clinical symptoms; and I_C, infected (infectious) with clinical immunity. The total population size is N, which we assume to be fixed at $N = 50,000$. We are able to assume a closed population because we know the population on the tea plantation is fixed. Here we assume the birth/ death rate is analogous to the immigration/ emigration rate, μ. $N = S_N + I_N + S_C + I_C$. Naive and clinically immune individuals have different susceptibility (clinically immune individuals differ by a factor of σ). We incorporate clinical immunity but do not allow the development of full immunity to malaria. Our model allows

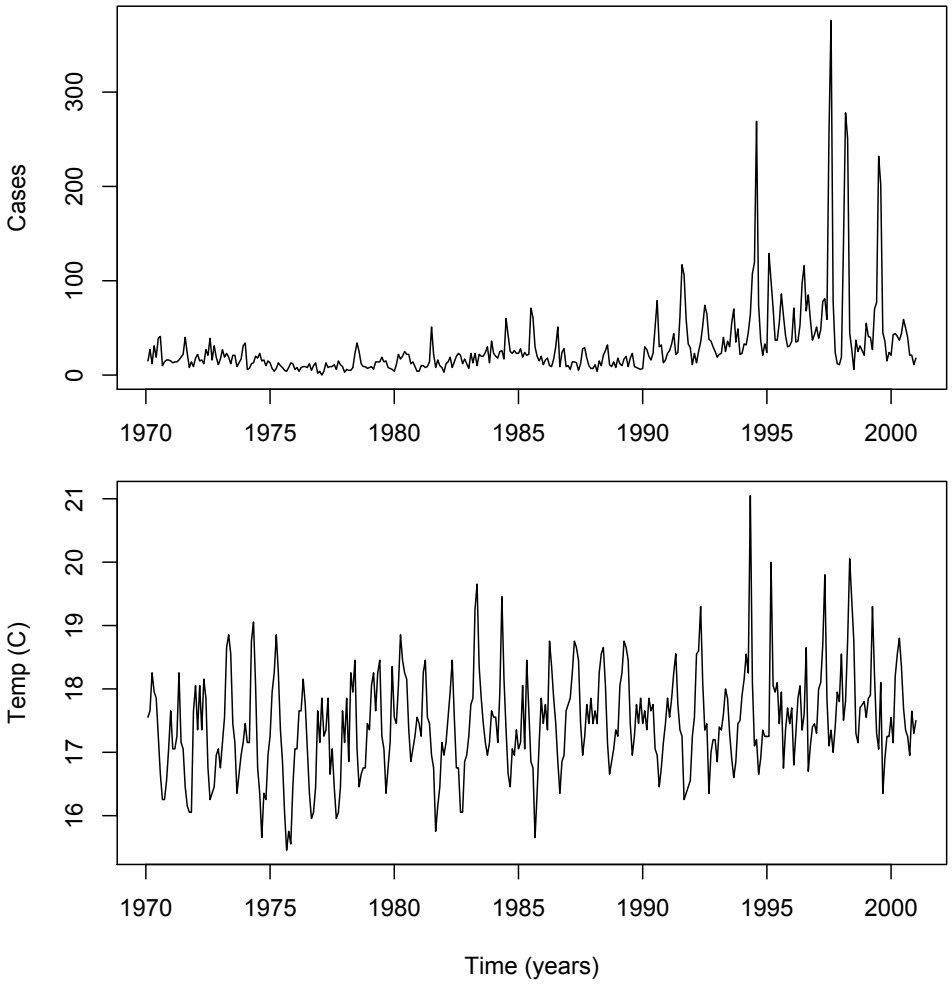

Figure 5.1: Monthly time series of (a) malaria cases and (b) mean temperature. The malaria incidence data are confirmed malaria cases from inpatients at the hospital serving a tea plantation from 1970-2002. The temperature data are from Alonso et al. [3] and were obtained by dovetailing records from two meteorological stations adjacent to the tea plantation (for more details see appendix section 5.A.1).

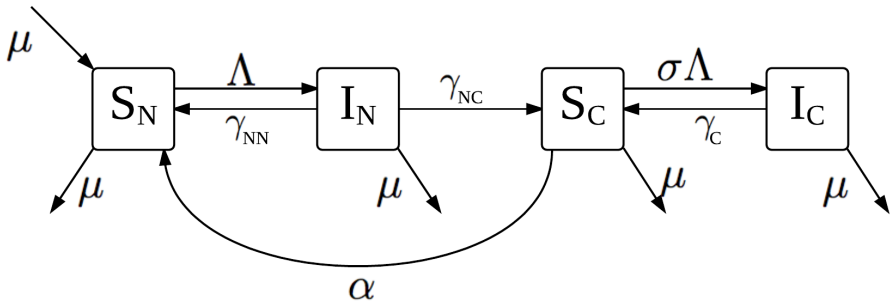

Figure 5.2: Flow diagram of our compartmental model of malaria transmission. Each compartment in the diagram represents a different epidemiological class, with susceptible and infected naive classes and susceptible and infected clinically immune classes.

individuals to either develop clinical immunity (by recovering from I_N to S_C at a rate γ_{NC}) or to remain naive (by recovering from I_N back to S_N at a rate γ_N) and clinical immunity can be lost (at rate α). This is meant to be a simple way to approximate that clinical immunity develops with exposure and is lost in the absence of re-exposure [90, 47]. The corresponding system of differential equations is given along with the details on climate and stochastic forcing in the appendix section 5.A.3.

An important aspect of developing clinical immunity is age. Clinical immunity develops with age and exposure and its onset is correlated with the onset of puberty [75, 49]. In appendix 5.A.4, we outline how we would incorporate age structure into this model, using data from Shanks et al. [127].

To estimate parameters we used a log-likelihood-based technique based on iterated filtering using the `mif` function of the R package `pomp` [70]. We describe this algorithm in the appendix 5.A.5. We will calculate profile likelihood confidence intervals for these estimates.

Parameter Name	γ_N	γ_{NC}	γ_C	σ
Start	0.136	0.262	0.45	0.88
Fit	0.969	0.802	0.048	0.73

Table 5.1: Table of starting values and key parameter estimates from the simple model fit to simulated data

5.3 Results

5.3.1 Simple model

We used the simple model of malaria from Keegan and Dushoff [64] (Fig. 5.2) with a constant force of infection and simulated data with realistic parameters to check our ability to fit the model. We then fit the simple model (with constant force of infection) to the actual data from Kericho.

Simulated Data– Using the `simulate` function in `pomp` with parameters taken from the literature, we simulated our model and fit the simple model (Fig. 5.2) with constant force of infection to the simulated data. The results are shown in Fig. 5.3, 5.4, and 5.5.

Fig. 5.3 shows the log cases of the simulated data and model fit; Fig. 5.4 shows a time plot of the average yearly cases; and Fig. 5.5 shows the cases aggregated by month for the simulated data and the model fit.

Kericho Data– We then fit our simple model with constant force of infection to the incidence data. The results are shown in Fig. 5.6, 5.7, and 5.8.

Fig. 5.6 shows the log cases of the simulated data and model fit; Fig. 5.7 shows a time plot of the average yearly cases; and Fig. 5.8 shows the cases aggregated by month for the simulated data and the model fit.

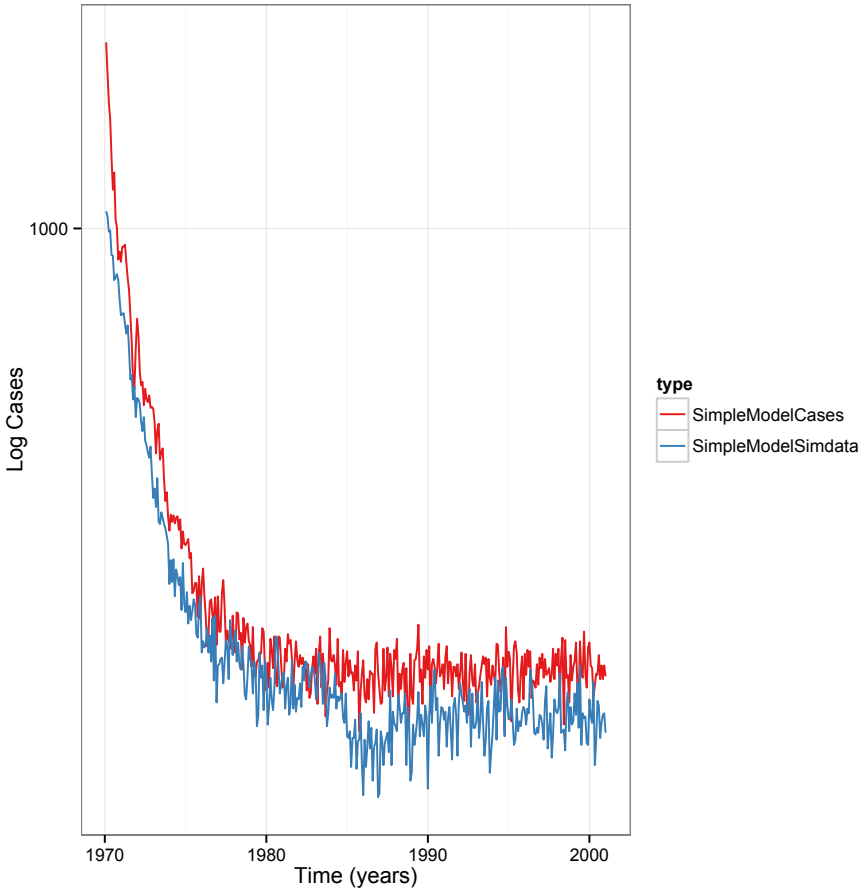

Figure 5.3: Time plot of log cases for the simple model fit to simulated data. The blue line is the simulated data and the red line is the fit.

Parameter Name	γ_N	γ_{NC}	γ_C	σ
Fit	0.0358	0.00294	0.00876	0.834

Table 5.2: Table of and key parameter estimates from the simple model fit to data

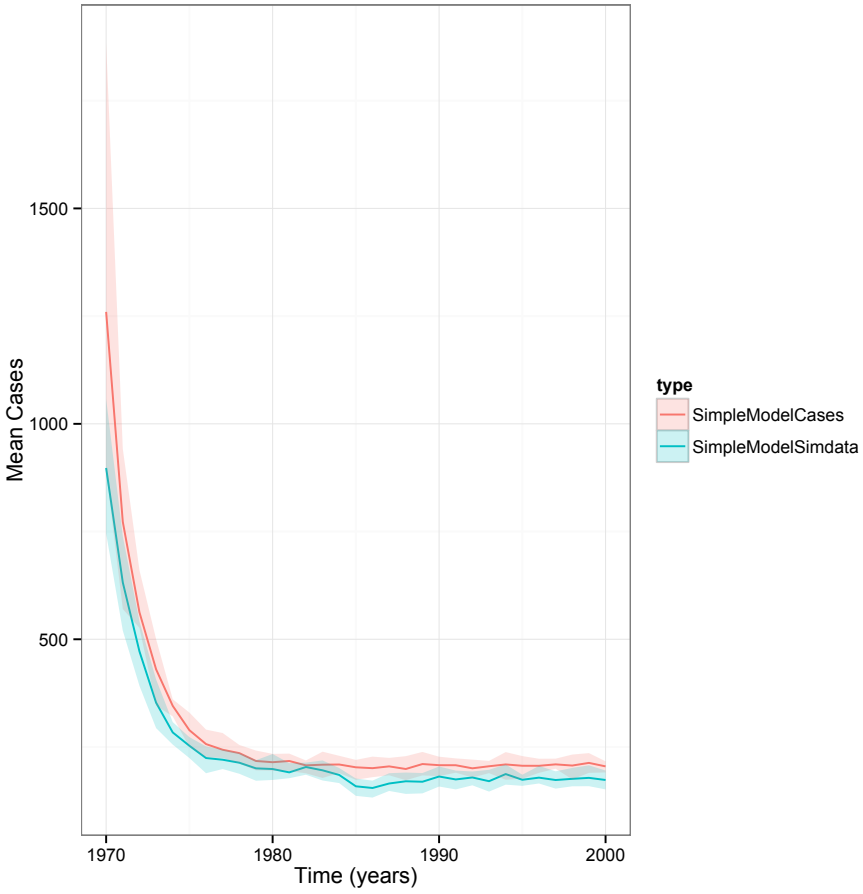

Figure 5.4: Time plot of the yearly mean cases for the simple model fit to simulated data. The blue line is the average number of cases from the simulated data that year. The red line is the average number of cases from the fitted model that year. The shaded regions represent the maximum and minimum cases during that year.

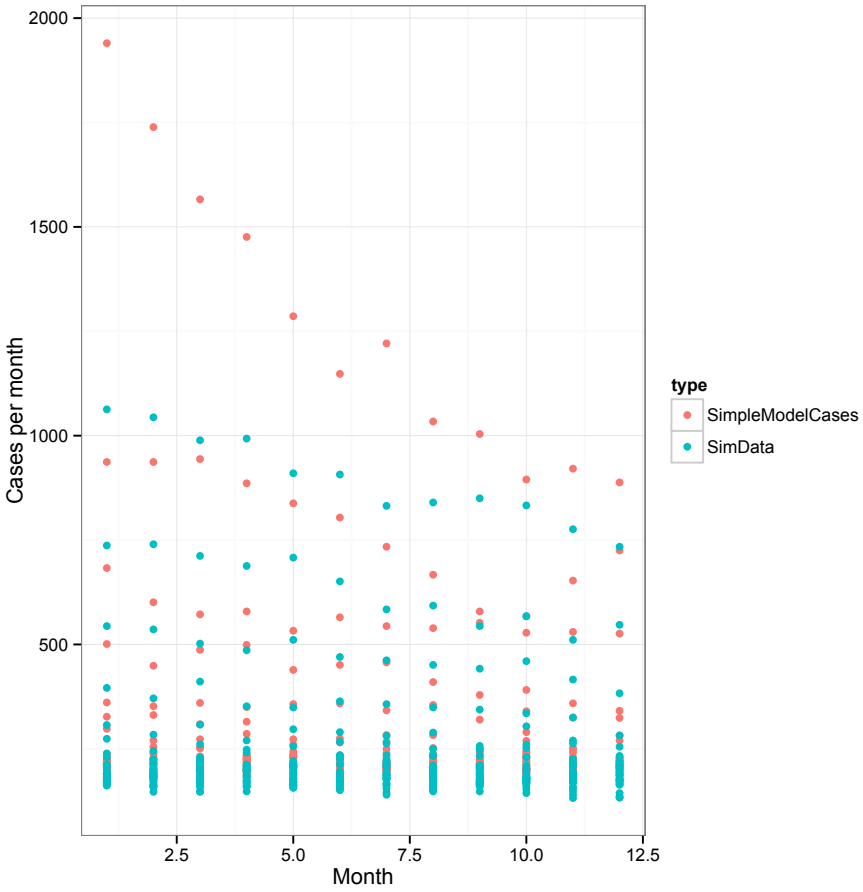

Figure 5.5: Plot of the number of cases each month for the simple model fit (red) to the simulated data (blue).

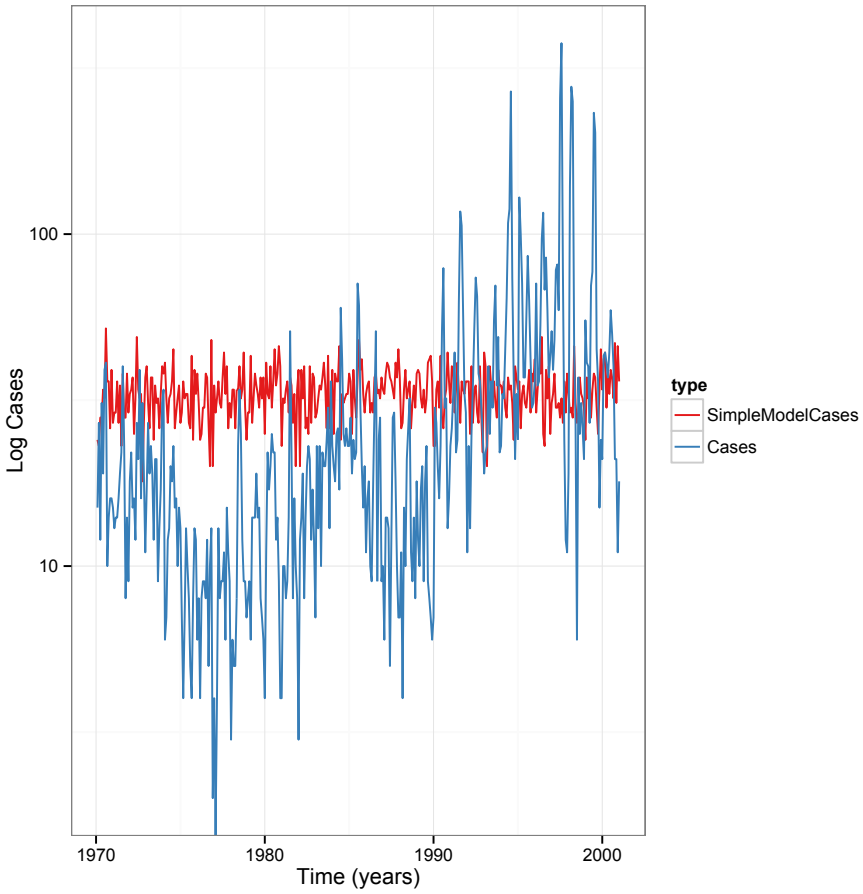

Figure 5.6: Time plot of log cases for the simple model fit to Kericho data. The blue line is the Kericho data and the red line is the fit.

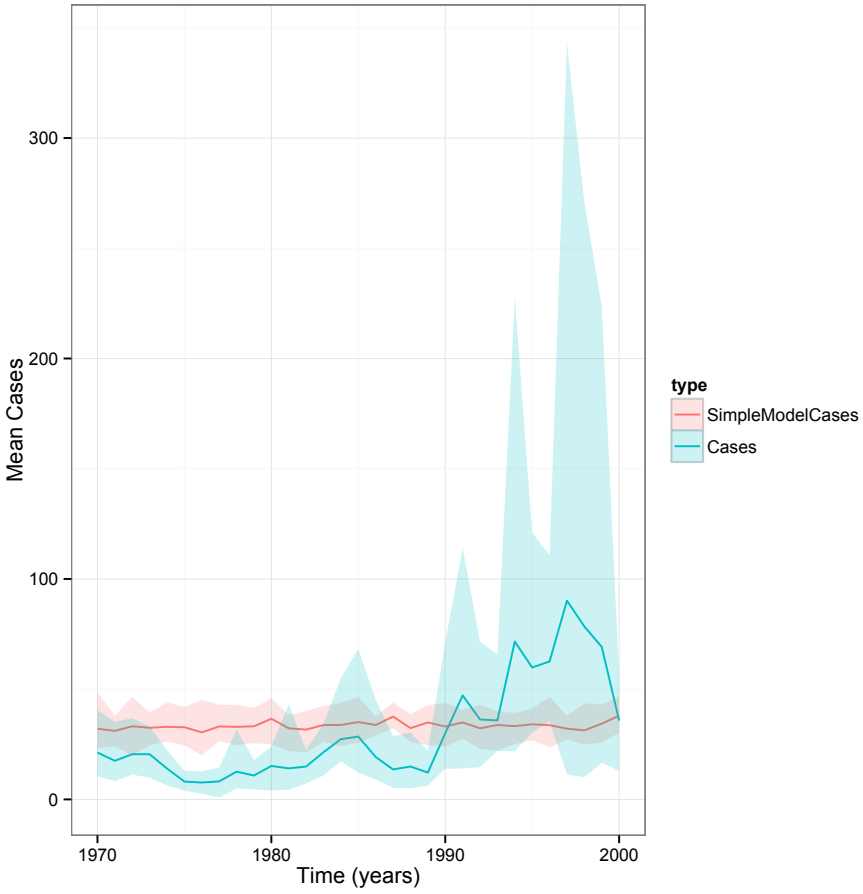

Figure 5.7: Time plot of the yearly mean cases for the simple model fit to Kericho data. The blue line is the average number of malaria cases from the Kericho that year. The red line is the average number of cases from the fitted model that year. The shaded regions represent the maximum and minimum cases during that year.

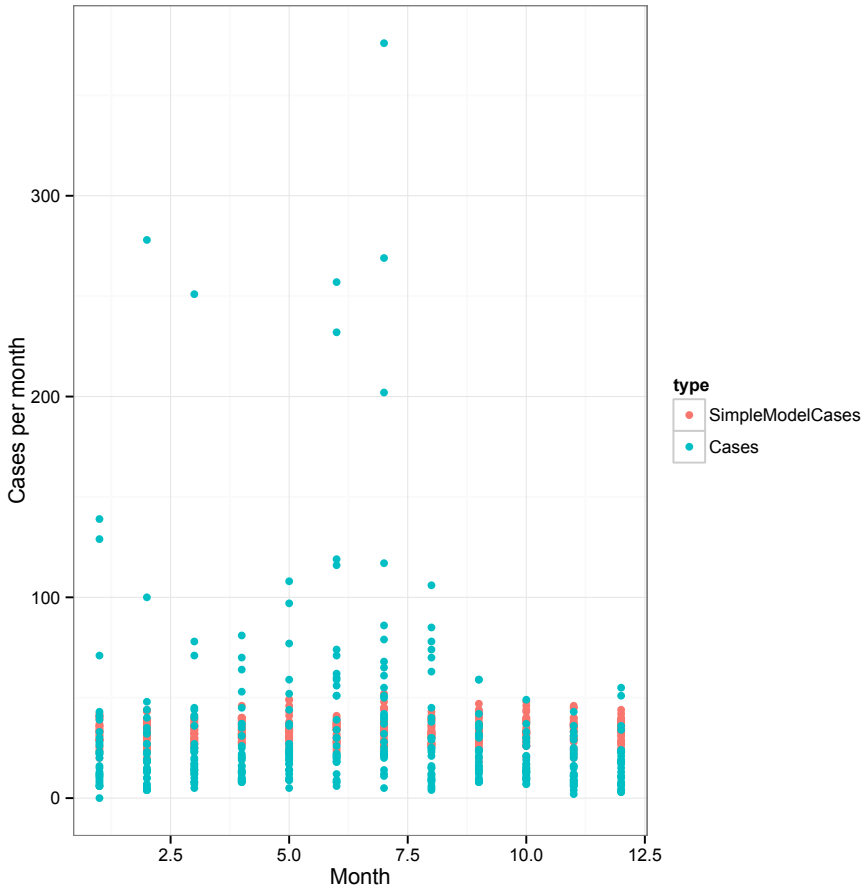

Figure 5.8: Time plot of the number of cases each month for the simple model fit to Kericho data. The blue line is the Kericho data and the red line is the fit.

Parameter Name	γ_N	γ_{NC}	γ_C	σ
Start	0.140	0.140	0.035	0.7
Fit	0.138	0.123	0.0242	0.657

Table 5.3: Table of starting values and key parameter estimates from the temperature model fit to simulated data

5.3.2 Temperature model

We then incorporated temperature into the model using

$$\beta = \exp(B_0 + B_t T + B_{t-1} T_{t-1}) \tag{5.1}$$

$$\Lambda = \iota + \frac{(\beta I_N + \beta I_C)}{N} \tag{5.2}$$

as the force of infection.

Simulated Data– As described in section 5.3.1, we simulated our temperature model and fit the model to the simulated data. The results are shown in Fig. 5.9, 5.10, and 5.11.

Fig. 5.9 shows the log cases of the simulated data and model fit; Fig. 5.10 shows a time plot of the average yearly cases; and Fig. 5.11 shows the cases aggregated by month for the simulated data and the model fit.

Further, we ran three fits with the same starting parameters and same seed to the simulated temperature data and present the results in 5.A.6.

Kericho Data– We then fit our temperature model with to the Kericho incidence data. The results are shown in Fig. 5.12, 5.13, and 5.14.

Fig. 5.12 shows the log cases of the data and model fit; Fig. 5.13 shows a time plot of the average yearly cases; and Fig. 5.14 shows the cases aggregated by month for the data and the model fit.

Parameter Name	γ_N	γ_{NC}	γ_C	σ
Fit	0.000263	0.000744	0.0682	0.62

Table 5.4: Table of and key parameter estimates from the temperature model fit to data

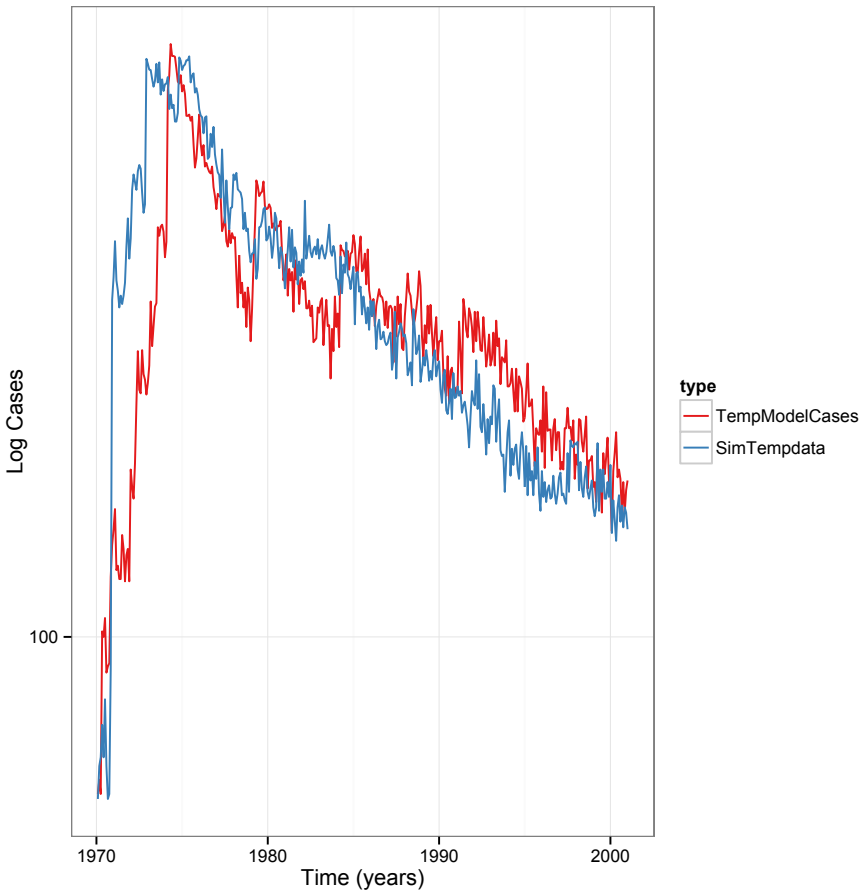

Figure 5.9: Time plot of log cases for the temperature model fit to simulated data. The blue line is the simulated data and the red line is the fit.

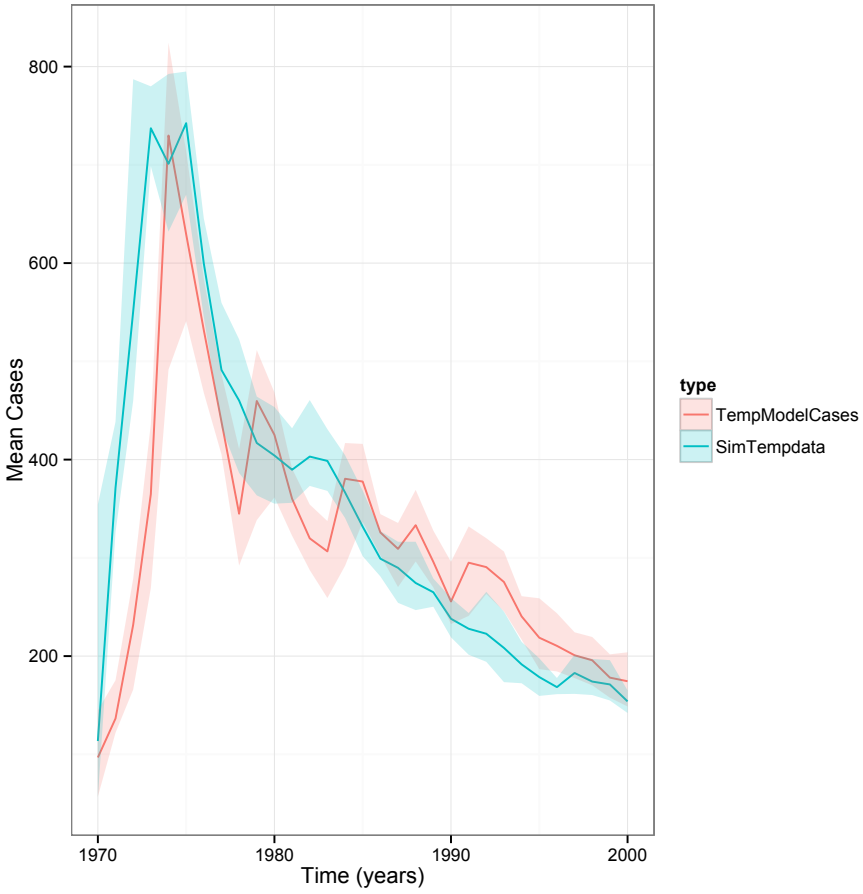

Figure 5.10: Time plot of the yearly mean cases for the temperature model fit to simulated data. The blue line is the average number of cases from the simulated data that year. The red line is the average number of cases from the fitted model that year. The shaded regions represent the maximum and minimum cases during that year.

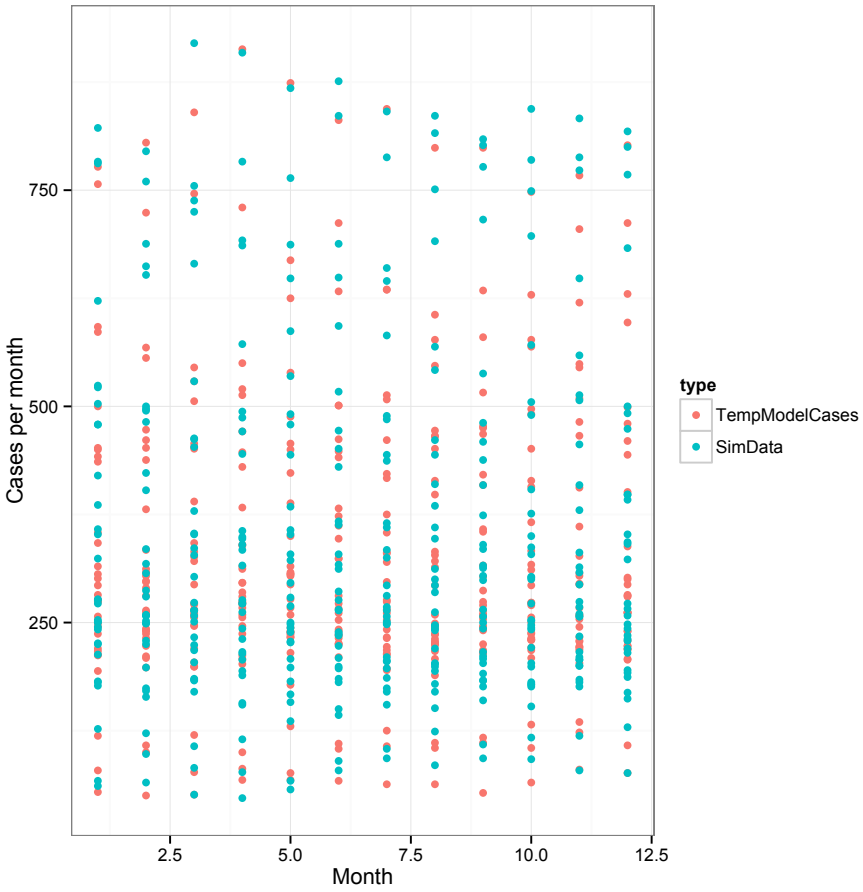

Figure 5.11: Plot of the number of cases each month for the temperature model fit (red) to the simulated data (blue).

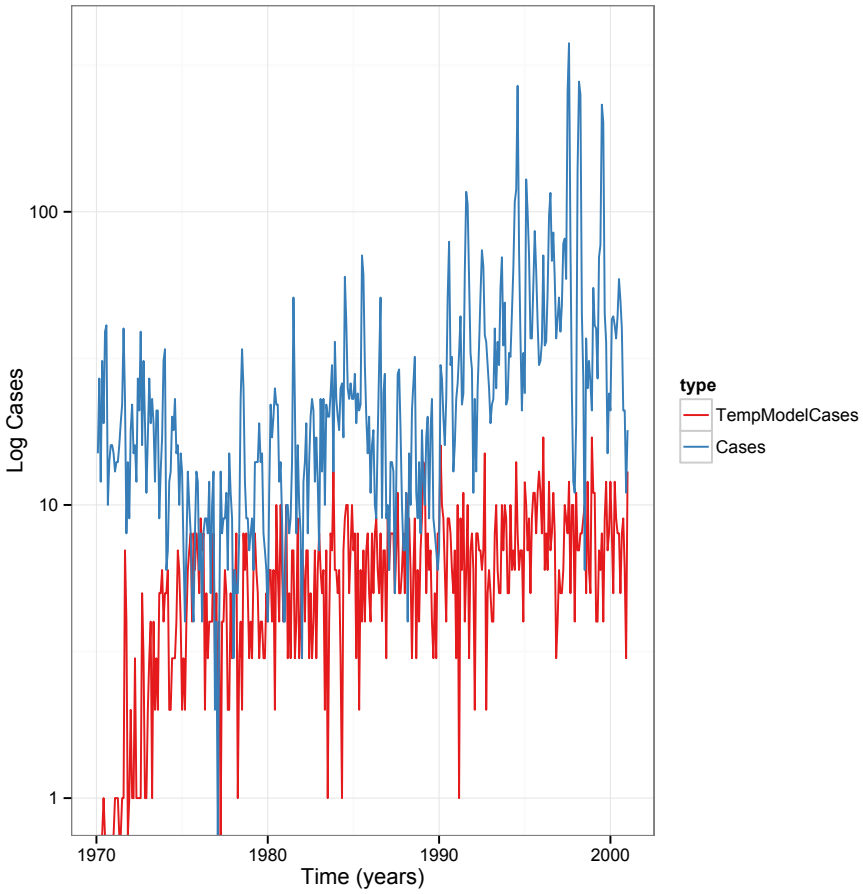

Figure 5.12: Time plot of log cases for the temperature model fit to data. The blue line is the data and the red line is the fit.

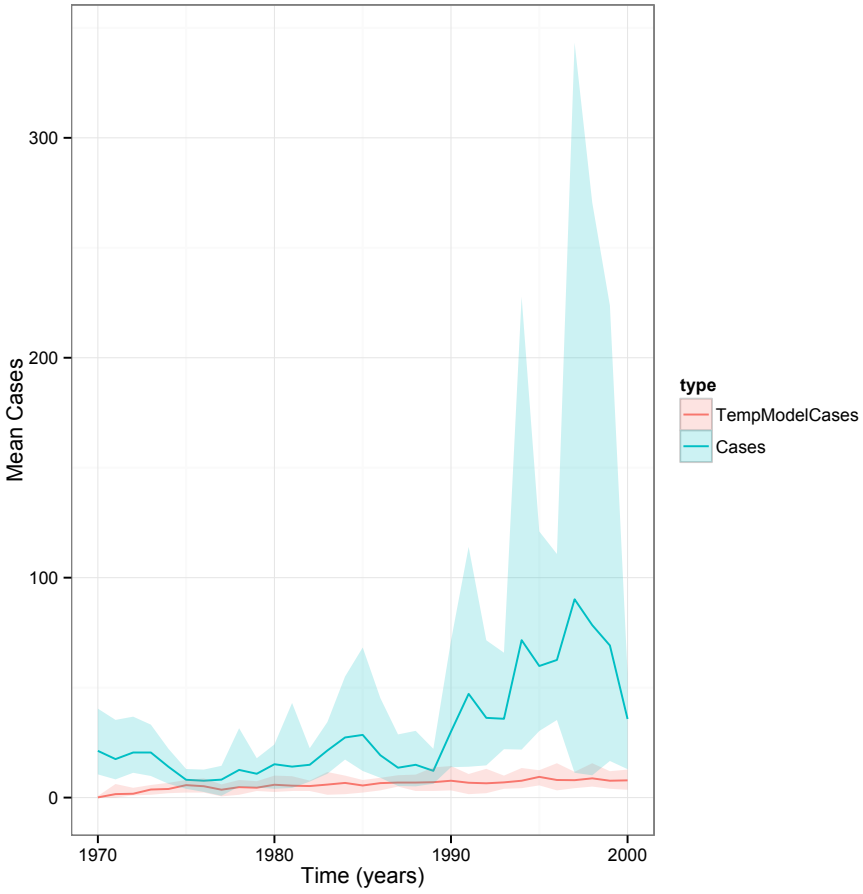

Figure 5.13: Time plot of the yearly mean cases for the temperature model fit to data. The blue line is the average number of cases from the data that year. The red line is the average number of cases from the fitted model that year. The shaded regions represent the maximum and minimum cases during that year.

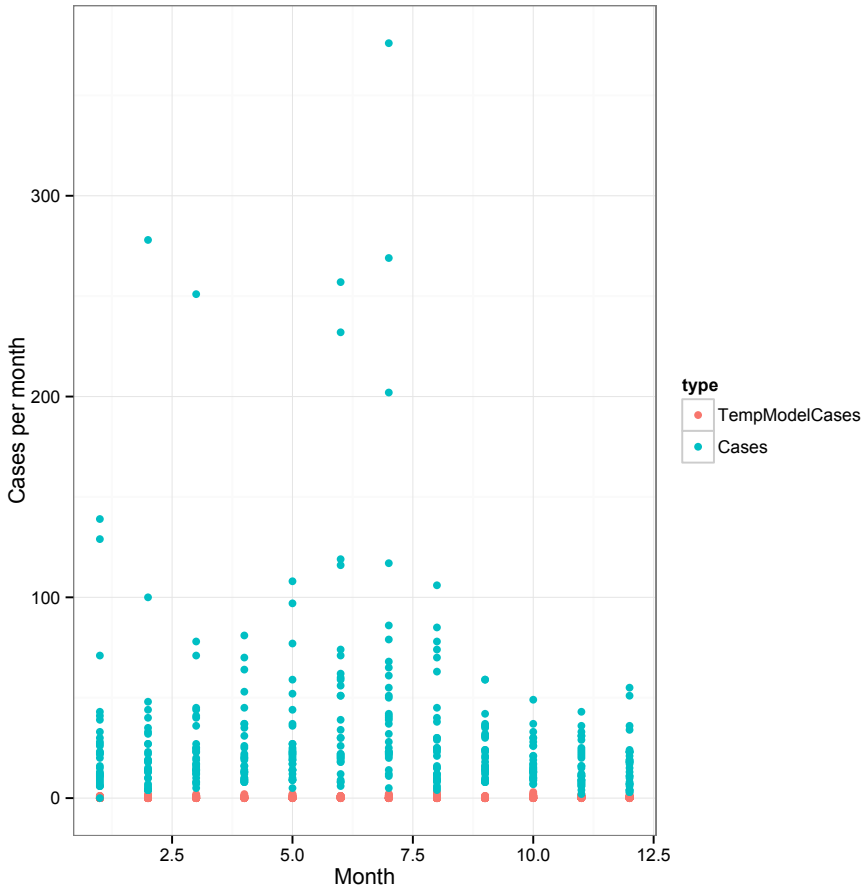

Figure 5.14: Plot of the number of cases each month for the temperature model fit (red) to the simulated data (blue).

5.4 Discussion

Although clinical immunity provides protection at the individual level, its effects at the population level are complex. Because clinical immunity can be lost, under certain circumstances, a reduction in transmission can lead to an increase in morbidity and mortality [49, 75]. Additionally, clinical immunity has been shown to be a mechanism for bistable malaria [64, 2]. Consequently, understanding how clinical immunity affects malaria transmission is an important component of malaria control. Here, we estimate key clinical immunity parameters, identified by Keegan and Dushoff [64] as being poorly understood. We fit a simple model of malaria, with and without temperature, to hospital confirmed data from Kericho, Kenya; to further elucidate the effects of clinical immunity on malaria transmission and to understand the key quantities underlying clinical immunity.

Our estimates of the duration of clinically immune infection are highly variable and depend on which model was used. From our simple model fit to actual data, we found the duration of clinically immune infection to be 111 days. Whereas from our temperature model fit to data, we found the duration of clinically immune infection to be 14 days. Laneri et al. [77] also found that the inclusion of climate data had a large effect on their estimates of the duration of clinically immune infection. From their model without rainfall, they found the duration of clinically immune infection was 250 days, which is similar to the estimates from malariotherapy data. However, for their model with rainfall, they found the duration of clinically immune infection to be 28 days.

Our estimates of the relative susceptibility of clinically immune individuals are 0.6 and 0.8 for the simple model and temperature model respectively. This is fairly consistent with the reported susceptibility of around 0.7 [64]. Although we have parameter estimates, we currently do not have confidence intervals on these estimates. Calculating pro-

file likelihood confidence intervals is a critical future direction that will be done using the `Profiledesign()` function in `POMP`.

To estimate these data, we made some simplifying assumptions about our model that could affect these estimates, including no age structure and that everyone enters the population into the susceptible naive class. Age is an important component of clinical immunity. Clinical immunity develops with age and exposure and the development of clinical immunity correlates with the onset of puberty [49, 75]. In 5.A.5, we outline how we would include age structure, using the data from Shanks et al. [127]. Additionally, we assume that everyone enters the population into the susceptible naive class. However, we know that prior to 1990, most malaria cases were imported from the holoendemic region around lake Victoria [127] (defined as having a parasite ratio consistently greater than 75% of infants [90]). Consequently, many people immigrating to Kericho have already developed clinical immunity.

Currently, our model only includes seasonality as a byproduct of temperature fluctuations. However, we plan to add seasonality independent of temperature as a future direction. Additionally, because of the large effect of adding temperature on the estimates of the duration of clinically immune infection, extending our model to include a variety of different temperature trends is an important future direction.

Finally, during the time working on this project, the authors of `POMP` proposed a new method with extra capabilities [59]. In 5.A.4, we outline the differences between an IF1, used here, and IF2. Updating our fitting methods to IF2 is a future direction of this project.

5.A Supplementary Methods

5.A.1 Temperature data

We used the temperature data from Alonso et al. [3] which they obtained by dovetailing the records from two meteorological stations within the tea estates, after adjusting for altitude. Data from the Tea Research Foundation Meteorological station (TRF) located at 2178 m was used up to 1992; after which a new meteorological station was established at 1977 m and data was used continuously from 1992 onwards, except for the period between December 1997 and March 1998 when data from TRF was used. Alonso et al. [3] compared the two datasets after adjusting for altitude and the comparison was consistent except for the period between 1994 and 1996, when TRF recorded much lower values of temperature.

5.A.2 Model

A diagram of our model and a description of the different classes can be found in Fig. 5.2. The corresponding system of differential equations is given by:

$$\frac{dS_N}{dt} = -\Lambda S_N + \alpha S_C - \mu S_N + \mu N + \gamma_{NN} I_N \tag{5.3a}$$

$$\frac{dI_N}{dt} = \Lambda S_N - (\gamma_N + \gamma_{NC}) I_N - \mu I_N \tag{5.3b}$$

$$\frac{dS_C}{dt} = -\sigma\Lambda S_C - \alpha S_C + \gamma_{NC} I_N + \gamma_C I_C - \mu S_C \tag{5.3c}$$

$$\frac{dI_C}{dt} = \sigma\Lambda S_C - \gamma_C I_C - \mu I_C \tag{5.3d}$$

We explored the model with two forces of infection, $\Lambda(t)$: a simple force of infection in

which the only variability was random noise, $\Lambda = \iota + \frac{\beta I_N + \beta I_C}{N}$; and a force of infection that included both random noise and a temperature covariate, $\Lambda = \iota + \frac{(\beta I_N + \beta I_C)}{N}$ (equation 5.2). In both cases, our force of infection allows both naive and clinically immune individuals to transmit infection. Additionally, our model couples the transmission dynamics within the tea estates to the surrounding areas through a constant, external force of infection. Environmental noise is included as Gamma white noise.

5.A.3 Specifying the POMP model

We fit our model using the `mif` function in `pomp`. In general, a POMP model consists of an unobserved stochastic process $\{X(t), t \geq t_0\}$ with observations $y_1, ..., y_N$ made at times $t_1, ..., t_N$.

To complete our model, we need to specify the relationship between the continuous time dynamical system and the monthly malaria case data, $y_1, y_2, \ldots, y_n$ at discrete times, $t_1, t_2, \ldots, t_n$. So the k-th observation, $y_k = C(t_{k-1}, t_k)$, is the observed number of cases from t_{k-1} to t_k. We model y_n as:

$$y_n \sim \text{Negbin}\left(\rho \Delta_{S \to I}(t_{n-1}, t_n), \theta\right) \tag{5.4}$$

We assume that the measurement error is negative-binomially distributed and ρ is the reporting rate, $\Delta_{S \to I}(t_{n-1}, t_n)$ is the accumulated number of cases on that interval, and θ measures over-dispersion in the reporting process.

5.A.4 Fitting the model by maximum likelihood

We estimated the parameters using iterated filtering, a Monte Carlo technique for estimating parameters and comparing models, first proposed by Ionides et al. [60]. This methodology has a "plug and play " property in that it does not require the explicit evaluation of the state transition densities, it only requires the ability to simulate the process portion of the model [60]. This has made likelihood-based inference possible for many situations where it was not previously so (eg. [77, 58]).

Iterated filtering algorithms search for the maximum likelihood of a function by repeatedly filtering to explore the likelihood surface at increasingly local scales. The algorithm takes an initial parameter vector, a noise intensity, and a "cooling" fraction. It then performs Monte Carlo filtering on the dynamical model with unknown parameters by performing a random walk with the given noise intensity. It then takes the weighted averages of all of the filtered estimates, with weights based on the uncertainty of the estimates. Finally, it returns the parameter estimates and the corresponding likelihood.

Ionides et al. [60] first proposed this method as a way to study stochastic differential equations, this method has made inference possible for systems which was previously not possible. Recently, Ionides et al. [59] proposed a new method with extra capabilities, which allows for further inference to be made about non-linear stochastic differential equations. The new method is called IF2 (making the original method IF1). Although IF1 and IF2 are both iterated particle filters used to find parameter estimates by maximizing the likelihood, they differ both in practical use and in theoretical justification.

In IF1, at each filtering iteration, a summary statistic is calculated based on the local mean and variance. This statistic is then used to update the parameter estimates for the next iteration. In IF2, rather than relying on the Fisher score function, it implements an iterated

Bayes map. That is, it introduces a stochastic perturbation, h, at every time step. IF1 relies on the stochasticity of the summary statistic to decrease, converging on the maximum likelihood estimate where as in IF2, the final set of J particles is what converges to the maximum likelihood estimate.

5.A.5 Incorporating age structure

An important aspect of the development of clinical immunity is that it develops with both age and exposure. Here, we outline how we would incorporate age structure into the model presented in the text (Fig. 5.2).

Shanks et al. [127] present data on the adult-to-child ratio of inpatient cases in Kericho from 1970 to 1990 with gaps from 1992-1993 and 1997. They categorize adults as older than 15 years old and children as younger than 15 years old. Because of this, we would model only two age classes, Adults (> 15 years old) and children (< 15 years old).

We model adults using the same model as presented in the text (Fig. 5.2). For children, we only allow them to be naive for simplicity of fitting, adding age structure complicates the fitting process and requires a lot of particles due to particle impoverishment.

An interesting question for incorporating age structure in Kericho is linking the adult and child populations in the model, or children “growing up". Since Each adult is allowed to have 3-4 dependents, we link μ_C (the child birth/ death rate) and μ_A (the adult birth/ death rate). Additionally, because we assume that the population is fixed and that the structure of the population is fixed, (ie 3-4 dependents for each worker) we do not allow children to

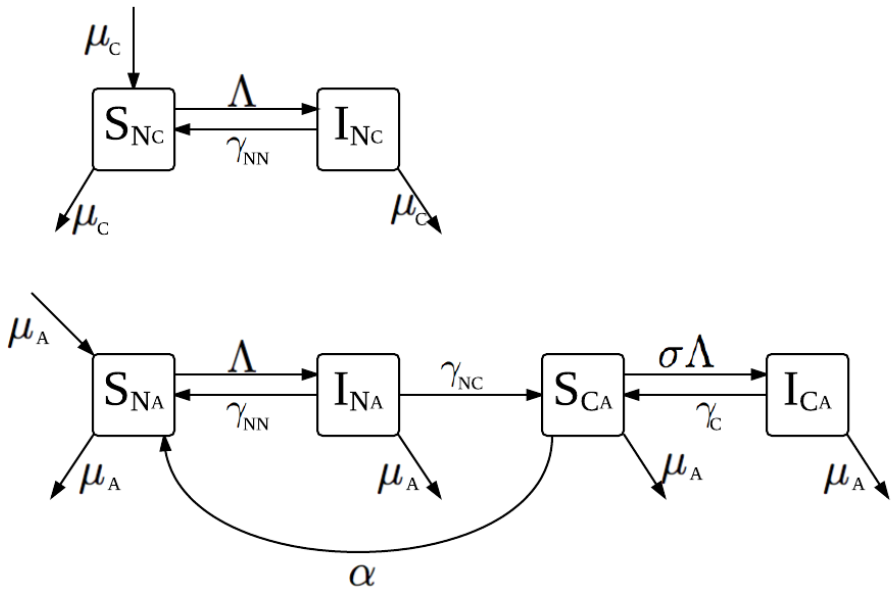

Figure A1: Flow diagram of our age-structured compartmental model of malaria transmission. Each compartment in the diagram represents a different epidemiological class, with susceptible and infected naive classes for children and susceptible and infected naive and clinically immune classes for adults.

“grow up" in the model.

$$\frac{dS_{N,C}}{dt} = -\Lambda S_{N,C} + \gamma_{NN} I_{N,C} + \mu(C - S_{N,C}) \tag{5.5a}$$
$$\frac{dI_{N,C}}{dt} = \Lambda S_{N,C} - \gamma_{NN} I_{N,C} + \mu I_{N,C} \tag{5.5b}$$
$$\frac{dS_{N,A}}{dt} = -\Lambda S_{N,A} + \alpha S_{C,A} - \mu S_{N,A} + \mu A + \gamma_{NN} I_{N,A} \tag{5.5c}$$
$$\frac{dI_{N,A}}{dt} = \Lambda S_{N,A} - (\gamma_N + \gamma_{NC}) I_{N,A} - \mu I_{N,A} \tag{5.5d}$$
$$\frac{dS_{C,A}}{dt} = -\sigma\Lambda S_{C,A} - \alpha S_{C,A} + \gamma_{NC} I_{N,A} + \gamma_C I_{C,A} - \mu S_{C,A} \tag{5.5e}$$
$$\frac{dI_{C,A}}{dt} = \sigma\Lambda S_{C,A} - \gamma_C I_C - \mu I_{C,A} \tag{5.5f}$$

5.A.6 Additional temperature model fits

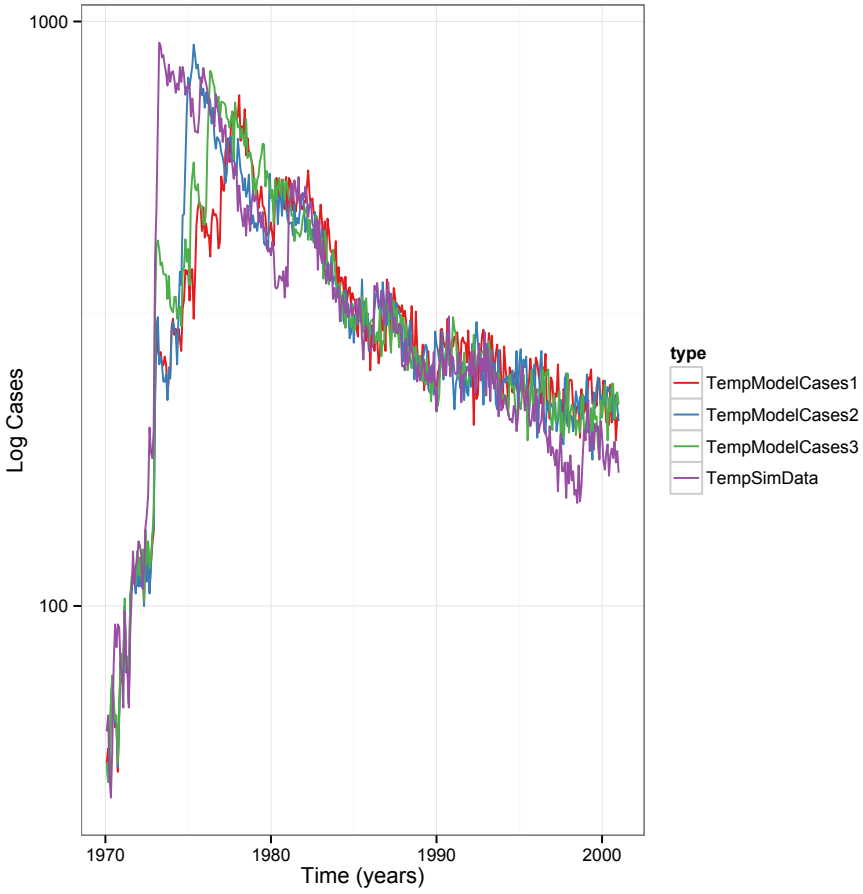

Figure A2: Time plot of log cases for the temperature model fit to simulated data for multiple fits using the same starting parameters and same seed. The purple line is the simulated data and the green, red, and blue lines are multiple fits with the same starting parameters and the same seed.

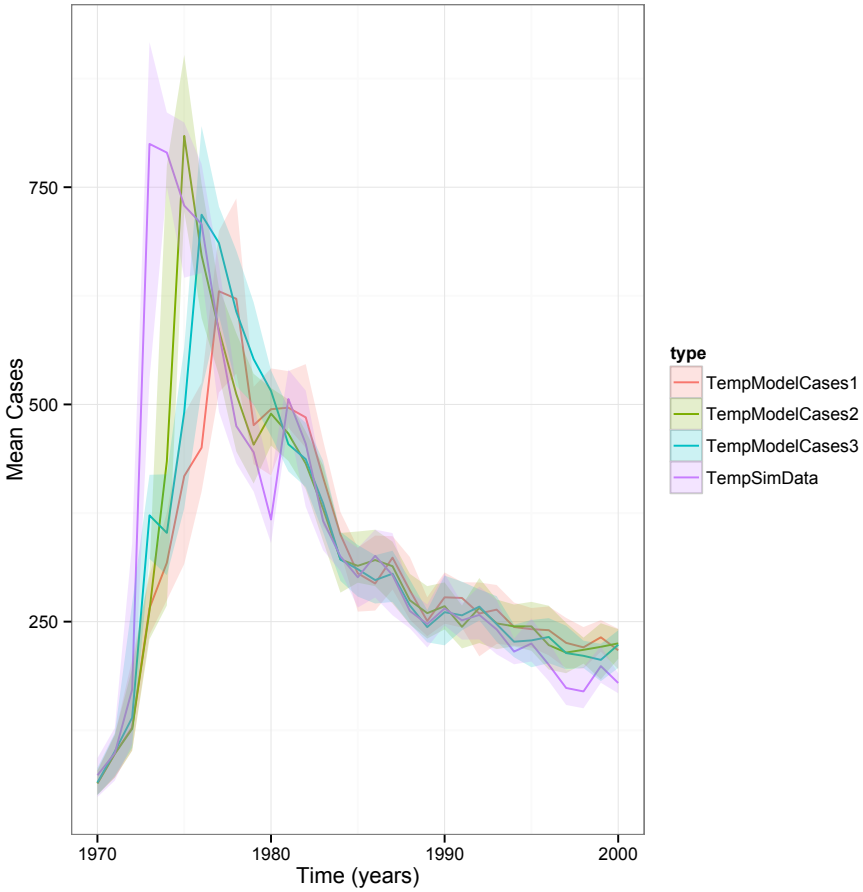

Figure A3: Time plot of the yearly mean cases for the temperature model fit to simulated data for multiple fits using the same starting parameters and same seed. The purple line is the average number of cases from the simulated data that year. The green, red, and blue lines are the average number of cases from multiple fits of the model with the same starting parameters and same seed, that year. The shaded regions represent the maximum and minimum cases during that year.

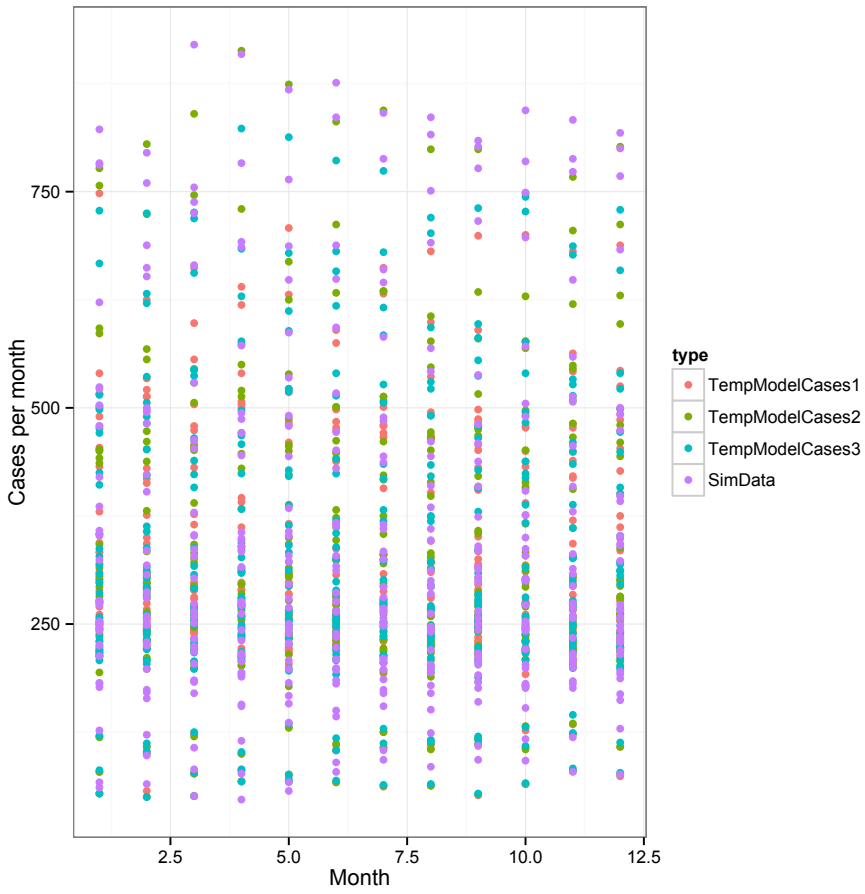

Figure A4: Plot of the number of cases each month for the temperature model fits to the simulated data for multiple fits using the same starting parameters and same seed. The purple dots are the simulated data and the green, red, and blue dots are the different fits of the model with the same starting parameters and the same seed.

Chapter 6

Conclusions

Mathematical models are an important tool that have been used for over a century to understand malaria dynamics and inform control [85, 122, 131, 73]. These models have been instrumental in identifying novel approaches to reduce malaria transmission. This thesis builds on previous work (including [132, 2, 77]) to address two aspects of malaria that have helped it to evade eradication. Our results provide insights into malaria dynamics that can help guide future control efforts.

The first aspect of malaria that we explore is the effect of finite population on the basic reproductive number. Accurate calculation of $\mathcal{R}_0$ is critical for understanding disease dynamics and planning control efforts. Classical calculations of $\mathcal{R}_0$ assume a disease spreading in an infinite population of susceptible hosts. However, recently it has been suggested that $\mathcal{R}_0$ be modified to account for the effects of finite population within a single disease-transmission generation. In chapter 2, we analytically calculated these finite-population reproductive numbers for both directly-transmitted and vector-borne diseases with homogeneous transmission. We found simple, generalizable formula for these finite-population reproductive numbers and showed that the finite-population reproductive numbers diverge

from $\mathcal{R}_0$ at around half of the size of the population. Additionally, we explore the effect of reducing the vector population in 2.A.

While homogeneous models of disease transmission have provided significant insights into disease dynamics, it is well known that most infectious diseases do not spread homogeneously through out the population. Although heterogeneity is well studied, careful, detailed discussion of the different types of heterogeneity in individual level parameters is limited [84, 35]. In chapter 4, we outline a framework for discussing the different types of heterogeneity in transmission. In particular, host heterogeneity has important implications for the basic reproductive number.

Previous models have shown that in an infinite population of susceptible hosts, heterogeneity in mixing increases $\mathcal{R}_0$. However, for diseases spreading in finite populations, Smith et al. [132] suggest that heterogeneity may actually *decrease* the reproductive number. In chapter 3, we calculated expressions for these finite-population reproductive numbers with different types of heterogeneity in transmission and showed that the effect of heterogeneity in a finite population is more complicated. We showed that for simple heterogeneity ($\mathcal{R}_{t_m}(N)$, $\mathcal{R}_{t_p}(N)$, $\mathcal{R}_{s_m}(N)$, and $\mathcal{R}_{s_p}(N)$), heterogeneity *decreases* the finite-population reproductive numbers; whereas heterogeneity in the intrinsic mixing rate *increases* the finite-population reproductive numbers when $\mathcal{R}_0$ is small relative to the size of the population and *decreases* the finite-population reproductive numbers when $\mathcal{R}_0$ is large relative to the size of the population. Although the effects of heterogeneity in a finite population are complex, the implications for control are straightforward: when $\mathcal{R}_0$ is large relative to the size of the population, heterogeneity decreases the finite-population reproductive numbers, making control or elimination easier than predicted by either $\mathcal{R}_0$ or $\mathcal{R}(N)$. Extending these results to include vector-borne diseases is an important future direction.

The other aspect of malaria that we address in this thesis is the effects of clinical immunity on malaria spread and control. Understanding the effects of clinical immunity on malaria dynamics has long been of interest to malaria modelers [93, 28, 6]. In particular, of the effects of clinical immunity on control efforts: because clinical immunity can be lost without re-exposure, under certain circumstances, a decrease in malaria transmission could result in an increase in morbidity and mortality [134, 103, 102]. Additionally, it has been suggested that clinical immunity could be a mechanism for bistable malaria dynamics [2]. This has important implications for control: if malaria could be eliminated from an area with bistability until clinical immunity waned, it would not be able to re-invade. In chapter 4, we built a simple model of malaria transmission and solved it to find a criteria for when we expect bistability to occur. We found a simple mechanism by which clinical immunity results in bistability and showed that bistability can occur for realistic parameter values. Additionally, we reviewed what is known about the underlying parameters of the model and highlighted key parameters that are not well understood. These results suggest that more research into these parameters may shed light on malaria dynamics and guide further control efforts.

In chapter 4, we highlighted key clinical immunity parameters that are not well understood. Building on this work, in chapter 5, we fit the simple model developed in chapter 4 to malaria incidence data to estimate these parameters. Because temperature is an important covariate in transmission of malaria in the fringe regions, we modify the constant force of infection from chapter 4 to allow the force of infection to vary by temperature. We estimated the parameters and found that these results are highly dependent on whether or not temperature was included in the model; this is consistent with what Laneri et al. [77] found.

We suggest extending the model to explore different temperature trends, due to the

impact of climate covariates on the parameter estimates. Additionally, extending the model to include age structure is an important future direction. Clinical immunity develops with age and exposure and its onset is correlated with puberty [75, 49]. Using the data on the adult-to-child ratio from Shanks et al. [127], we outline how we would include age structure in the model (in appendix 5.A.5) and suggest that this extension could lead to further insight into the key clinical immunity parameters and the effects of clinical immunity on malaria transmission.

Mathematical models have provided significant contributions to our understanding of malaria dynamics and have been instrumental in identifying novel approaches to reduce malaria transmission. In this thesis, we provide more accurate calculations of the reproductive number for disease spreading in small populations, and show that in small populations, control or elimination may be easier than predicted by $\mathcal{R}_0$. Additionally, we explored the effects of clinical immunity on the population-level dynamics of malaria. We found a simple criterion for when we expect bistability to occur and show that clinical immunity can act as a mechanism for bistability to occur for plausible parameter values. Further, we identified and estimated key clinical immunity parameters that are important in understanding how clinical immunity affects malaria transmission and prospects for control. These results should guide future malaria control efforts as they highlight potential opportunities for control.

Bibliography

[1] Laith J Abu-Raddad, Amalia S Magaret, Connie Celum, Anna Wald, Ira M Longini Jr, Steven G Self, and Lawrence Corey. Genital herpes has played a more important role than any other sexually transmitted infection in driving HIV prevalence in Africa. *PloS one*, 3(5):e2230, 2008.

[2] Ricardo Águas, Lisa J White, Robert W Snow, and M Gabriela M Gomes. Prospects for malaria eradication in sub-saharan africa. *PLoS One*, 3(3):e1767, 2008.

[3] David Alonso, Menno J Bouma, and Mercedes Pascual. Epidemic malaria and warmer temperatures in recent decades in an East African highland. *Proceedings of the Royal Society B: Biological Sciences*, 278(1712):1661–1669, 2011.

[4] Fabiana Alves, Rui Durlacher, Maria Menezes, Henrique Krieger, Luiz Silva, and Erney Camargo. High prevalence of asymptomatic *Plasmodium vivax* and *Plasmodium falciparum* infections in native Amazonian populations. *The American journal of tropical medicine and hygiene*, 66(6):641–648, 2002.

[5] J Ansell, KA Hamilton, M Pinder, GEL Walraven, and SW Lindsay. Short-range attractiveness of pregnant women to *Anopheles gambiae* mosquitoes. *Transactions of the Royal Society of Tropical Medicine and Hygiene*, 96(2):113–116, 2002.

[6] Joan L Aron. Dynamics of acquired immunity boosted by exposure to infection. *Mathematical Biosciences*, 64(2):249–259, 1983.

[7] V. Joseph Hotz Avner Ahituv and Tomas Philipson. The responsiveness of the demand for condoms to the local prevalence of AIDS. *The Journal of Human Resources*, 31(4):869–897, 1996.

[8] Norman Bailey. *The Biomathematics of Malaria*. Oxford University Press, 1982.

[9] Robert C Bailey, Stephen Moses, Corette B Parker, Kawango Agot, Ian Maclean, John N Krieger, Carolyn FM Williams, Richard T Campbell, and Jeckoniah O Ndinya-Achola. Male circumcision for HIV prevention in young men in Kisumu, Kenya: a randomised controlled trial. *The lancet*, 369(9562):643–656, 2007.

[10] M. T. Bassett and M. Mhloyi. Women and AIDS in Zimbabwe: the making of an epidemic. *Int J Health Serv*, 21(1):143–156, 1991.

[11] B. Bean, B. M. Moore, B. Sterner, L. R. Peterson, D. N. Gerding, and H. H. Balfour. Survival of influenza viruses on environmental surfaces. *Journal of Infectious Diseases*, 146(1):47–51, 1982.

[12] Emmanuel Bottius, Antonella Guanzirolli, Jean-François Trape, Christophe Rogier, L Konate, and Pierre Druilhe. Malaria: even more chronic in nature than previously thought; evidence for subpatent parasitaemia detectable by the polymerase chain reaction. *Transactions of the Royal Society of tropical Medicine and Hygiene*, 90(1):15–19, 1996.

[13] C Boudin, M Van Der Kolk, T Tchuinkam, C Gouanga, S Bonnet, I Safeukui, B Mulder, J Y Meunier, and J P Verhave. *Plasmodium Falciparum* transmission blocking immunity under conditions of low and high endemicity in Cameroon. *Parasite Immunology*, 26:105–110, Jun 2004.

[14] J Bousema, Louis Gouagna, Chris Drakeley, Annemiek Meutstege, Bernard Okech, Ikupa Akim, John Beier, John Githure, and Robert Sauerwein. *Plasmodium falciparum* gametocyte carriage in asymptomatic children in western Kenya. *Malaria journal*, 3(1):18, 2004.

[15] Michael Bretscher, Nicolas Maire, Nakul Chitnis, Ingrid Felger, Seth Owusu-Agyei, and Tom Smith. The distribution of *Plasmodium falciparum* infection durations. *Epidemics*, 3(2):109–118, 2011.

[16] Janet Brooks. The sad and tragic life of Typhoid Mary. *CMAJ: Canadian Medical Association Journal*, 154(6):915, 1996.

[17] MC Bruce, CA Donnelly, M Packer, M Lagog, N Gibson, A Narara, D Walliker, MP Alpers, and KP Day. Age-and species-specific duration of infection in asymptomatic malaria infections in papua new guinea. *Parasitology*, 121(03):247–256, 2000.

[18] Maria Domenica Cappellini and G Fiorelli. Glucose-6-phosphate dehydrogenase deficiency. *The lancet*, 371(9606):64–74, 2008.

[19] Margo Chase-Topping, David Gally, Chris Low, Louise Matthews, and Mark Woolhouse. Super-shedding and the link between human infection and livestock carriage of *Escherichia coli* O157. *Nature Reviews Microbiology*, 6(12):904–912, 2008.

[20] N. Z. Chimbindi, N. McGrath, K. Herbst, K. San Tint, and M. L. Newell. Sociodemographic determinants of condom use among sexually active young adults in rural KwaZulu-Natal, South Africa. *Open AIDS J*, 4:88–95, 2010.

[21] C Chiyaka, AJ Tatem, JM Cohen, PW Gething, G Johnston, R Gosling, R Laxminarayan, SI Hay, and DL Smith. The stability of malaria elimination. *Science*, 339(6122):909–910, 2013.

[22] Justin M Cohen, David L Smith, Chris Cotter, Abigail Ward, Gavin Yamey, Oliver J Sabot, and Bruno Moonen. Malaria resurgence: a systematic review and assessment of its causes. *Malaria Journal*, 11(1):1–1, Apr 2012.

[23] Francis EG Cox. History of the discovery of the malaria parasites and their vectors. *Parasit Vectors*, 3(1):5, 2010.

[24] MH Craig, RW Snow, and D Le Sueur. A climate-based distribution model of malaria transmission in sub-saharan africa. *Parasitology today*, 15(3):105–111, 1999.

[25] John de Benedictis, Esther Chow-Shaffer, Adriana Costero, Gary G Clark, John D Edman, and Thomas W Scott. Identification of the people from whom engorged *Aedes aegypti* took blood meals in Florida, Puerto Rico, using polymerase chain reaction-based DNA profiling. *The American journal of tropical medicine and hygiene*, 68(4):437–446, 2003.

[26] Odo Diekmann, JAP Heesterbeek, and Johan AJ Metz. On the definition and the computation of the basic reproduction ratio r 0 in models for infectious diseases in heterogeneous populations. *Journal of mathematical biology*, 28(4):365–382, 1990.

[27] K Dietz. The estimation of the basic reproduction number for infectious diseases. *Statistical Methods in Medical Research*, 2(1):23–41, 1993.

[28] K Dietz, L Molineaux, and A Thomas. A malaria model tested in the African savannah. *Bulletin of the World Health Organization*, 50(3-4):347, 1974.

[29] Klaus Dietz and JAP Heesterbeek. Daniel Bernoulli's epidemiological model revisited. *Mathematical biosciences*, 180(1):1–21, 2002.

[30] D. L Doolan, C Dobano, and J. K Baird. Acquired immunity to malaria. *Clinical Microbiology Reviews*, 22(1):13–36, Jan 2009.

[31] C J Drakeley, J T Bousema, N I J Akim, K Teelen, W Roeffen, A H Lensen, M Bolmer, and W Eling R W Sauerwein. Transmission-reducing immunity is inversely related to age in *Plasmodium falciparum* gametocyte carriers. *Parasite Immunology*, 28:185–190, Apr 2006.

[32] CC Draper. Observations on the infectiousness of gametocytes in hyperendemic malaria. *Transactions of the Royal Society of tropical Medicine and Hygiene*, 47(2):160–165, 1953.

[33] J Dushoff, W Huang, and C Castillo-Chavez. Backwards bifurcations and catastrophe in simple models of fatal diseases. *Journal of Mathematical Biology*, 36(3):227–248, 1998.

[34] Jonathan Dushoff. Incorporating immunological ideas in epidemiological models. *Journal of Theoretical Biology*, 180:181–187, Oct 1996.

[35] Jonathan Dushoff. Host heterogeneity and disease endemicity: a moment-based approach. *Theoretical population biology*, 56(3):325–335, 1999.

[36] Jonathan Dushoff, Audrey Patocs, and Chyun-Fung Shi. Modeling the population-level effects of male circumcision as an HIV-preventive measure: A gendered perspective. *PLoS ONE*, 6, 12 2011.

[37] C Dye and G Hasibeder. Population dynamics of mosquito-borne disease: effects of flies which bite some people more frequently than others. *Transactions of the Royal Society of Tropical Medicine and Hygiene*, 80(1):69–77, 1986.

[38] C Dye and G Hasibeder. Population dynamics of mosquito-borne disease: effects of flies which bite some people more frequently than others. *Transactions of the Royal Society of Tropical Medicine and Hygiene*, 80(1):69–77, 1986.

[39] WC Earle, Manuel Perez, Juan del Rio, and Carmen Arzola. Observations on the course of naturally acquired malaria in Puerto Rico. *The Puerto Rico Journal of Public Heath and Tropical Medicine*, 1939.

[40] David JD Earn, Paul W Andrews, and Benjamin M Bolker. Population-level effects of suppressing fever. *Proceedings of the Royal Society B: Biological Sciences*, 281(1778):20132570, 2014.

[41] Philip Eckhoff. *P. falciparum* infection durations and infectiousness are shaped by antigenic variation and innate and adaptive host immunity in a mathematical model. *PLoS ONE*, 7, 09 2012.

[42] João A. N Filipe, Eleanor M Riley, Christopher J Drakeley, Colin J Sutherland, and Azra C Ghani. Determination of the processes driving the acquisition of immunity to malaria using a mathematical transmission model. *PLoS Computational Biology*, 3(12):e255, Jan 2007.

[43] John P Fox, Lila Elveback, William Scott, Lael Gatewood, and Eugene Ackerman. Herd immunity: basic concept and relevance to public health immunization practices. *American journal of epidemiology*, 141(3):187–197, 1995.

[44] S. Funk, E. Gilad, C. Watkins, and V. A. Jansen. The spread of awareness and its impact on epidemic outbreaks. *Proc. Natl. Acad. Sci. U.S.A.*, 106(16):6872–6877, Apr 2009.

[45] Alison P Galvani and Robert M May. Epidemiology: dimensions of superspreading. *Nature*, 438(7066):293–295, 2005.

[46] Shannon R Galvin and Myron S Cohen. The role of sexually transmitted diseases in HIV transmission. *Nature Reviews Microbiology*, 2(1):33–42, 2004.

[47] Michelle L Gatton and Qin Cheng. Modeling the development of acquired clinical immunity to *Plasmodium falciparum* malaria. *Infection and immunity*, 72(11):6538–6545, 2004.

[48] Judith R Glynn, Michel Caraël, Betran Auvert, Maina Kahindo, Jane Chege, Rosemary Musonda, Frederick Kaona, Anne Buvé, Study Group on the Heterogeneity of HIV Epidemics in African Cities, et al. Why do young women have a much higher prevalence of HIV than young men? a study in Kisumu, Kenya and ndola, zambia. *Aids*, 15:S51–S60, 2001.

[49] S Gupta, RW Snow, CA Donnelly, K Marsh, and C Newbold. Immunity to non-cerebral severe malaria is acquired after one or two infections. *Nature Medicine*, 5(3):340–343, 1999.

[50] Caroline Breese Hall. The spread of influenza and other respiratory viruses: complexities and conjectures. *Clinical Infectious Diseases*, 45(3):353–359, 2007.

[51] Kristin Harper and George Armelagos. The changing disease-scape in the third epidemiological transition. *International journal of environmental research and public health*, 7(2):675–697, 2010.

[52] Simon I Hay, David J Rogers, Sarah E Randolph, David I Stern, Jonathan Cox, G Dennis Shanks, and Robert W Snow. Hot topic or hot air? climate change and malaria resurgence in east african highlands. *Trends in parasitology*, 18(12):530–534, 2002.

[53] Simon I Hay, David J Rogers, G Dennis Shanks, Monica F Myers, and Robert W Snow. Malaria early warning in kenya. *Trends in parasitology*, 17(2):95–99, 2001.

[54] Simon I Hay, Eric C Were, Melanie Renshaw, Abdisalan M Noor, Sam A Ochola, Iyabode Olusanmi, Nicholas Alipui, and Robert W Snow. Forecasting, warning, and detection of malaria epidemics: a case study. *The Lancet*, 361(9370):1705–1706, 2003.

[55] JM Heffernan, RJ Smith, and LM Wahl. Perspectives on the basic reproductive ratio. *Journal of the Royal Society Interface*, 2(4):281–293, 2005.

[56] Herbert W Hethcote, James A Yorke, and Annett Nold. Gonorrhea modeling: a comparison of control methods. *Mathematical Biosciences*, 58(1):93–109, 1982.

[57] K. Ijumba, R. Gamieldien, L. Myer, and C. Morroni. Sexual risk behaviours are influenced by knowing someone with HIV/AIDS. *S. Afr. Med. J.*, 94(7):522–523, Jul 2004.

[58] Edward L Ionides, Anindya Bhadra, Yves Atchadé, Aaron King, et al. Iterated filtering. *The Annals of Statistics*, 39(3):1776–1802, 2011.

[59] Edward L Ionides, Dao Nguyen, Yves Atchadé, Stilian Stoev, and Aaron A King. Inference for dynamic and latent variable models via iterated, perturbed bayes maps. *Proceedings of the National Academy of Sciences*, 112(3):719–724, 2015.

[60] EL Ionides, C Bretó, and AA King. Inference for nonlinear dynamical systems. *Proceedings of the National Academy of Sciences*, 103(49):18438–18443, 2006.

[61] PH Kao and Ruey-Jen Yang. Virus diffusion in isolation rooms. *Journal of Hospital infection*, 62(3):338–345, 2006.

[62] Yasmin G Karim, M Khalid Ijaz, Syed A Sattar, and C Margaret Johnson-Lussenburg. Effect of relative humidity on the airborne survival of rhinovirus-14. *Canadian journal of microbiology*, 31(11):1058–1061, 1985.

[63] Lindsay Keegan and Jonathan Dushoff. Analytic calculation of finite-population reproductive numbers for direct- and vector-transmitted diseases with homogeneous mixing. *Bull. Math. Biol.*, pages 1–12, Apr 2014.

[64] Lindsay T Keegan and Jonathan Dushoff. Population-level effects of clinical immunity to malaria. *BMC infectious diseases*, 13(1):428, 2013.

[65] Matt Keeling and Bryan Grenfell. Individual-based perspectives on R_0. *Journal of Theoretical Biology*, 203(1):51–61, 2000.

[66] W O Kermack and A G McKendrick. A contribution to the mathematical theory of epidemics. *Proceedings of the Royal Society of London: Series A*, 115(772):700–721, 1927.

[67] Gerry Killeen, Amanda Ross, and Thomas Smith. Infectiousness of malaria-endemic human populations to vectors. *The American journal of tropical medicine and hygiene*, 75(2 suppl):38–45, 2006.

[68] Gerry Killeen, Amanda Ross, and Thomas Smith. Infectiousness of malaria-endemic human populations to vectors. *The American journal of tropical medicine and hygiene*, 75(2 suppl):38–45, 2006.

[69] A Marm Kilpatrick, Peter Daszak, Matthew J Jones, Peter P Marra, and Laura D Kramer. Host heterogeneity dominates West Nile virus transmission. *Proceedings of the Royal Society B: Biological Sciences*, 273(1599):2327–2333, 2006.

[70] Aaron A. King, Edward L. Ionides, Carles Martinez Bretó, Stephen P. Ellner, Matthew J. Ferrari, Bruce E. Kendall, Michael Lavine, Dao Nguyen, Daniel C. Reuman, Helen Wearing, and Simon N. Wood. *pomp: Statistical inference for partially observed Markov processes (R package)*, 2014.

[71] Susan E. Kline, Linda L. Hedemark, and Scott F. Davies. Outbreak of tuberculosis among regular patrons of a neighborhood bar. *New England Journal of Medicine*, 333(4):222–227, 1995. PMID: 7791838.

[72] B. G. Knols, R. de Jong, and W. Takken. Differential attractiveness of isolated humans to mosquitoes in Tanzania. *Trans R Soc Trop Med Hyg*, 89:604–6, 1995 Nov-Dec.

[73] Jacob C Koella. On the use of mathematical models of malaria transmission. *Acta tropica*, 49(1):1–25, 1991.

[74] Jacob C Koella. On the use of mathematical models of malaria transmission. *Acta tropica*, 49(1):1–25, 1991.

[75] J.D Kurtis, R Mtalib, F.K Onyango, and P.E Duffy. Human resistance to *Plasmodium falciparum* increases during puberty and is predicted by dehydroepiandrosterone sulfate levels. *Infection and Immunity*, 69(1):123, 2001.

[76] Dolie D Laishram, Patrick L Sutton, Nutan Nanda, Vijay L Sharma, Ranbir C Sobti, Jane M Carlton, and Hema Joshi. The complexities of malaria disease manifestations with a focus on asymptomatic malaria. *Malaria Journal*, 11(1):29, Jan 2012.

[77] Karina Laneri, Anindya Bhadra, Edward L Ionides, Menno Bouma, Ramesh C Dhiman, Rajpal S Yadav, and Mercedes Pascual. Forcing versus feedback: epidemic malaria and monsoon rains in northwest India. *PLoS computational biology*, 6(9):e1000898, 2010.

[78] Charles Louis Alphonse Laveran, BH Kean, Kenneth E Mott, and Adair J Russell. A newly discovered parasite in the blood of patients suffering from malaria. parasitic etiology of attacks of malaria. *Reviews of infectious diseases*, pages 908–911, 1982.

[79] HS Leeson. Longevity of anopheles maculipennis race atroparvus, van thiel, at controlled temperature and humidity after one blood meal. *Bulletin of entomological research*, 30(03):295–301, 1939.

[80] Thierry Lefèvre, Louis-Clément Gouagna, Kounbobr Roch Dabiré, Eric Elguero, Didier Fontenille, François Renaud, Carlo Costantini, and Frédéric Thomas. Beer consumption increases human attractiveness to malaria mosquitoes. *PLoS One*, 5(3):e9546, 2010.

[81] Christian Lengeler et al. Insecticide-treated bed nets and curtains for preventing malaria. *Cochrane Database Syst Rev*, 2(2), 2004.

[82] Steve Lindsay, Juliet Ansell, Colin Selman, Val Cox, Katie Hamilton, and Gijs Walraven. Effect of pregnancy on exposure to malaria mosquitoes. *The Lancet*, 355(9219):1972, 2000.

[83] SW Lindsay and WJ Martens. Malaria in the african highlands: past, present and future. *Bulletin of the World Health Organization*, 76(1):33, 1998.

[84] JO Lloyd-Smith, SJ Schreiber, PE Kopp, and WM Getz. Superspreading and the effect of individual variation on disease emergence. *Nature*, 438(7066):355–359, 2005.

[85] George Macdonald et al. The epidemiology and control of malaria. *The Epidemiology and Control of Malaria.*, 1957.

[86] C. MacPhail, F. Terris-Prestholt, L. Kumaranayake, P. Ngoako, C. Watts, and H. Rees. Managing men: women's dilemmas about overt and covert use of barrier methods for HIV prevention. *Cult Health Sex*, 11(5):485–497, Jun 2009.

[87] Alphaxard Manjurano, Nuno Sepulveda, Behzad Nadjm, George Mtove, Hannah Wangai, Caroline Maxwell, Raimos Olomi, Hugh Reyburn, Eleanor M Riley, Christopher J Drakeley, et al. African glucose-6-phosphate dehydrogenase alleles associated with protection from severe malaria in heterozygous females in tanzania. *PLoS Genet*, 11(2):e1004960, 2015.

[88] Robert M May and Roy M Anderson. Spatial heterogeneity and the design of immunization programs. *Mathematical Biosciences*, 72(1):83–111, 1984.

[89] S.C McCombie. Treatment seeking for malaria: a review of recent research. *Social Science and Medicine*, 43(6):933–945, Jan 1996.

[90] D Metselaar and PH Van Thiel. *Classification of malaria*. 1959.

[91] F Migot-Nabias, AJ Luty, P Ringwald, M Vaillant, B Dubois, A Renaut, RJ Mayombo, TN Minh, N Fievet, and JR Mbessi. Immune responses against *Plasmodium falciparum* asexual blood-stage antigens and disease susceptibility in Gabonese and Cameroonian children. *The American journal of tropical medicine and hygiene*, 61(3):488–494, 1999.

[92] William S Miller and Malcolm S Artenstein. Aerosol stability of three acute respiratory disease viruses. *Experimental Biology and Medicine*, 125(1):222–227, 1967.

[93] L Molineaux. The pros and cons of modelling malaria transmission. *Transactions of the Royal Society of Tropical Medicine and Hygiene*, 79(6):743–747, 1985.

[94] L Molineaux, HH Diebner, M Eichner, WE Collins, GM Jeffery, and K Dietz. *Plasmodium falciparum* parasitaemia described by a new mathematical model. *Parasitology*, 122(04):379–391, 2001.

[95] Louis Molineaux, WH Wernsdorfer, I McGregor, et al. The epidemiology of human malaria as an explanation of its distribution, including some implications for its control. *Malaria: principles and practice of malariology. Volume 2.*, pages 913–998, 1988.

[96] W. R. Mukabana, W. Takken, R. Coe, and B. G. J. Knols. Host-specific cues cause differential attractiveness of Kenyan men to the African malaria vector *Anopheles gambiae*. *Malar J*, 1:17, 2002 Dec 6.

[97] B Mulder, T Tchuinkam, K Dechering, JP Verhave, P Carnevale, Meuwissen JHET, and V Robert. Malaria transmission-blocking activity in experimental infections of *Anopheles gambiae* from naturally infected *Plasmodium falciparum* gametocyte carriers. *Transactions of the Royal Society of Tropical Medicine and Hygiene*, 88(1):121–125, JAN-FEB 1994.

[98] José A Nájera, Matiana González-Silva, and Pedro L Alonso. Some lessons for the future from the global malaria eradication programme (1955–1969). *PLoS medicine*, 8(1):e1000412, 2011.

[99] T Naotunne, Nadira Karunaweera, G Del Giudice, MU Kularatne, GE Grau, R Carter, and KN Mendis. Cytokines kill malaria parasites during infection crisis: extracellular complementary factors are essential. *The Journal of experimental medicine*, 173(3):523–529, 1991.

[100] B.H Noden, P.S Beadle, J.A Vaughan, C.B Pumpuni, M.D Kent, and J.C Beier. *Plasmodium falciparum*: the population structure of mature gametocyte cultures has little effect on their innate fertility. *Acta Tropica*, 58(1):13–19, 1994.

[101] Annett Nold. Heterogeneity in disease-transmission modeling. *Mathematical Biosciences*, 52(3):227–240, 1980.

[102] Wendy P O'Meara, Phillip Bejon, Tabitha W Mwangi, Emelda A Okiro, Norbert Peshu, Robert W Snow, Charles RJC Newton, and Kevin Marsh. Effect of a fall in malaria transmission on morbidity and mortality in kilifi, kenya. *The Lancet*, 372(9649):1555–1562, Oct 2008.

[103] Wendy P OMeara, Tabitha W Mwangi, Thomas N Williams, F Ellis McKenzie, Robert W Snow, and Kevin Marsh. Relationship between exposure, clinical malaria, and age in an area of changing transmission intensity. *Am. J. Trop. Med. Hyg*, 79(2):185–191, 2008.

[104] Judith A Omumbo, Bradfield Lyon, Samuel M Waweru, Stephen J Connor, and Madeleine C Thomson. Raised temperatures over the Kericho tea estates: revisiting the climate in the East African Highlands malaria debate. *Malar J*, 10(1):12, 2011.

[105] Global Malaria Programme World Health Organization. World malaria report. 2014.

[106] World Health Organization. World malaria report. 2012.

[107] S Owusu-Agyei, KA Koram, JK Baird, GC Utz, FN Binka, FK Nkrumah, DJ Fryauff, and SL Hoffman. Incidence of symptomatic and asymptomatic *Plasmodium falciparum* infection following curative therapy in adult residents of northern Ghana. *The American journal of tropical medicine and hygiene*, 65(3):197–203, 2001.

[108] Krijn P Paaijmans, Andrew F Read, and Matthew B Thomas. Understanding the link between malaria risk and climate. *Proceedings of the National Academy of Sciences*, 106(33):13844–13849, 2009.

[109] Jonathan A Patz, Mike Hulme, Cynthia Rosenzweig, Timothy D Mitchell, Richard A Goldberg, Andrew K Githeko, Subhash Lele, Anthony J McMichael, and David Le Sueur. Climate change (communication arising): Regional warming and malaria resurgence. *Nature*, 420(6916):627–628, 2002.

[110] T Alex Perkins, Thomas W Scott, Arnaud Le Menach, and David L Smith. Heterogeneity, mixing, and the spatial scales of mosquito-borne pathogen transmission. *PLoS computational biology*, 9(12):e1003327, 2013.

[111] Aree Pethleart, Somsak Prajakwong, Wannapa Suwonkerd, Boontawee Corthong, Roger Webber, and Christopher Curtis. Infectious reservoir of *Plasmodium* infection in Mae Hong Son province, north-west Thailand. *Malaria Journal*, 3(1):34, 2004.

[112] A. E. Pettifor, D. M. Measham, H. V. Rees, and N. S. Padian. Sexual power and HIV risk, South Africa. *Emerging Infect. Dis.*, 10(11):1996–2004, Nov 2004.

[113] Virginia E Pitzer, Cayley C Bowles, Stephen Baker, Gagandeep Kang, Veeraraghavan Balaji, Jeremy J Farrar, and Bryan T Grenfell. Predicting the impact of vaccination on the transmission dynamics of typhoid in south Asia: a mathematical modeling study. *PLoS neglected tropical diseases*, 8(1):e2642, 2014.

[114] Agnes Le Port, Michel Cot, Jean-Francois Etard, Oumar Gaye, Florence Migot-Nabias, and Andre Garcia. Relation between *Plasmodium falciparum* asymptomatic infection and malaria attacks in a cohort of Senegalese children. *Malar J*, 7(1):193, Jan 2008.

[115] GR Port, PFL Boreham, and Joan H Bryan. The relationship of host size to feeding by mosquitoes of the *Anopheles gambiae* Giles complex (Diptera: Culicidae). *Bulletin of Entomological Research*, 70(01):133–144, 1980.

[116] Thomas C Quinn and Julie Overbaugh. HIV/AIDS in women: an expanding epidemic. *Science*, 308(5728):1582–1583, 2005.

[117] R Core Team. *R: A Language and Environment for Statistical Computing*. R Foundation for Statistical Computing, Vienna, Austria, 2012.

[118] David C Rees, Thomas N Williams, and Mark T Gladwin. Sickle-cell disease. *The Lancet*, 376(9757):2018–2031, 2010.

[119] Robert C Reiner, Steven T Stoddard, Brett M Forshey, Aaron A King, Alicia M Ellis, Alun L Lloyd, Kanya C Long, Claudio Rocha, Stalin Vilcarromero, Helvio Astete, et al. Time-varying, serotype-specific force of infection of dengue virus. *Proceedings of the National Academy of Sciences*, 111(26):E2694–E2702, 2014.

[120] Amanda Ross, Gerry Killeen, and Thomas Smith. Relationships between host infectivity to mosquitoes and asexual parasite density in *Plasmodium falciparum*. *The American journal of tropical medicine and hygiene*, 75(2 suppl):32–37, 2006.

[121] Joshua Ross. Invasion of infectious diseases in finite homogeneous populations. *Journal of Theoretical Biology*, 289:83–89, 2011.

[122] Ronald Ross. *The Prevention of Malaria*. John Murray, 1910.

[123] W Sama, G Killeen, and T SMITH. Estimating the duration of *Plasmodium falciparum* infection from trials of indoor residual spraying. *The American Journal of Tropical Medicine and Hygiene*, 70(6):625, 2004.

[124] JJ Schall. Transmission success of the malaria parasite *Plasmodium mexicanum* into its vector: role of gametocyte density and sex ratio. *Parasitology*, 121(06):575–580, 2000.

[125] Louis Schofield and Ivo Mueller. Clinical immunity to malaria. *Current molecular medicine*, 6(2):205–221, 2006.

[126] Thomas W Scott, Andrew K Githeko, Andrew Fleisher, Laura C Harrington, and Guiyun Yan. Dna profiling of human blood in anophelines from lowland and highland sites in western Kenya. *The American journal of tropical medicine and hygiene*, 75(2):231–237, 2006.

[127] G Dennis Shanks, Simon I Hay, Judy A Omumbo, and Robert W Snow. Malaria in Kenya's western highlands. *Emerging infectious diseases*, 11(9):1425, 2005.

[128] G Dennis Shanks, Simon I Hay, David I Stern, Kimutai Biomndo, and Robert W Snow. Meteorologic influences on *Plasmodium falciparum* malaria in the highland tea estates of Kericho, western Kenya. *Emerg Infect Dis*, 8(12):1404–1408, 2002.

[129] O Shirai, Takao Tsuda, Shinya Kitagawa, Ken Naitoh, Taisuke Seki, Kiyoshi Kamimura, and Masaaki Morohashi. Alcohol ingestion stimulates mosquito attraction. *Journal of the American Mosquito Control Association*, 18(2):91–96, 2002.

[130] Yoshikazu Shirai, Hisashi Funada, Hisao Takizawa, Taisuke Seki, Masaaki Morohashi, and Kiyoshi Kamimura. Landing preference of *Aedes albopictus* (Diptera: Culicidae) on human skin among ABO blood groups, secretors or nonsecretors, and ABH antigens. *Journal of medical entomology*, 41(4):796–799, 2004.

[131] David L Smith, Katherine E Battle, Simon I Hay, Christopher M Barker, Thomas W Scott, and F Ellis McKenzie. Ross, macdonald, and a theory for the dynamics and control of mosquito-transmitted pathogens. *PLoS pathogens*, 8(4):e1002588, 2012.

[132] David L Smith, F Ellis McKenzie, Robert W Snow, and Simon I Hay. Revisiting the basic reproductive number for malaria and its implications for malaria control. *PLOS Biology*, 5(3):531–542, Feb 2007.

[133] Georges Snounou and Jean-Louis Pérignon. Malariotherapy: insanity at the service of malariology. *Adv Parasitol*, 81(6):223–55, 2013.

[134] R.W. Snow and K. Marsh. Will reducing plasmodium falciparum transmission alter malaria mortality among african children? *Parasitology Today*, 11(5):188 – 190, 1995.

[135] Richard A Stein. Super-spreaders in infectious diseases. *International Journal of Infectious Diseases*, 15(8):e510–e513, Aug 2011.

[136] TP Stephens, TA McAllister, and K Stanford. Perineal swabs reveal effect of super shedders on the transmission of O157: H7 in commercial feedlots. *Journal of animal science*, 87(12):4151–4160, 2009.

[137] Marie J Stuart and Ronald L Nagel. Sickle-cell disease. *The Lancet*, 364(9442):1343–1360, 2004.

[138] Paul E Szmitko, Magdie L Kohn, and Andrew E Simor. *Plasmodium falciparum* malaria occurring 8 years after leaving an endemic area. *Diagnostic Microbiology and Infectious Disease*, 63(1):105–107, Dec 2008.

[139] Malaria atlas project UCSF Global Health Group. Atlas of malaria eliminating countries. 2011.

[140] L von Seidlein and B.M Greenwood. Mass administrations of antimalarial drugs. *Trends in parasitology*, 19(10):452–460, 2003.

[141] Maria J Wawer, Ronald H Gray, Nelson K Sewankambo, David Serwadda, Xianbin Li, Oliver Laeyendecker, Noah Kiwanuka, Godfrey Kigozi, Mohammed Kiddugavu, Thomas Lutalo, et al. Rates of HIV-1 transmission per coital act, by stage of HIV-1 infection, in Rakai, Uganda. *Journal of Infectious Diseases*, 191(9):1403–1409, 2005.

[142] Brian G Williams, James O Lloyd-Smith, Eleanor Gouws, Catherine Hankins, Wayne M Getz, John Hargrove, Isabelle De Zoysa, Christopher Dye, and Bertran Auvert. The potential impact of male circumcision on HIV in sub-Saharan Africa. *PLoS medicine*, 3(7):e262, 2006.

[143] M.E.J Woolhouse, C Dye, J.F Etard, T Smith, JD Charlwood, GP Garnett, P Hagan, JLK Hii, PD Ndhlovu, and RJ Quinnell. Heterogeneities in the transmission of infectious agents: implications for the design of control programs. *Proceedings of the National Academy of Sciences*, 94(1):338, 1997.

[144] M.E.J Woolhouse, C Dye, J.F Etard, T Smith, JD Charlwood, GP Garnett, P Hagan, JLK Hii, PD Ndhlovu, and RJ Quinnell. Heterogeneities in the transmission of infectious agents: implications for the design of control programs. *Proceedings of the National Academy of Sciences*, 94(1):338, 1997.

[145] Guofa Zhou, Noboru Minakawa, Andrew K Githeko, and Guiyun Yan. Association between climate variability and malaria epidemics in the east african highlands. *Proceedings of the National Academy of Sciences of the United States of America*, 101(8):2375–2380, 2004.